IMPROVING THE DROUGHT RISK ASSESSMENT AND PREPAREDNESS FOR WINTER WHEAT FARMING IN OKLAHOMA

By

ALI AJAZ

Bachelor of Science in Agricultural Engineering
Bahauddin Zakariya University
Multan, Pakistan
2009

Master of Science in Water Science and Engineering
UNESCO-IHE, Institute for Water Education
Delft, The Netherlands
2016

Submitted to the Faculty of the
Graduate College of the
Oklahoma State University
in partial fulfillment of
the requirements for
the Degree of
DOCTOR OF PHILOSOPHY
July, 2020

IMPROVING THE DROUGHT RISK ASSESSMENT AND PREPAREDNESS FOR WINTER WHEAT FARMING IN OKLAHOMA

Dissertation Approved:

Dr. Saleh Taghvaeian

Dissertation Adviser

Dr. Paul Weckler

Dr. Phillip Alderman

Dr. Prasanna H. Gowda

ACKNOWLEDGEMENTS

After praising the Almighty, first and foremost I extend gratitude to Dr. Saleh Taghvaein, my Ph.D. advisor, who has always been a true mentor. Throughout my doctoral program, he helped me to sharpen my research and writing skills. The trust he showed in my abilities not only allowed me to work independently but also developed a great sense of responsibility in me to produce quality research. No doubt, without his kind support, the goal of earning a doctoral degree would not have been possible. I am also grateful to my committee members who extended their help whenever needed and always provided great suggestions.

The role and support of my wife Hadia have been unprecedented through my degree program at Oklahoma State University. She took care of our home along with her graduate studies as well as she took me to fishing trips whenever needed to kill the stress. I always appreciate her gifted insight into the complexities around us, and the way she helped me untangling the knots was remarkable.

My late father always wanted me to achieve a terminal degree in Science and Engineering, and I feel proud that I fulfilled his dreams. My mother's prayers have always been with me and showed me the light of hope whenever the odds were not in my favor. Thanks to my aunt for sending prayers to us. The presence of my brothers in my life is a continuous source of happiness and strength for me that provided me the energy to complete this Ph.D. Also, the smiles of the newest addition to our family, Ibrahim, kept me going.

I am also indebted to my research colleagues, our support staff, and all those people who supported me with their encouraging words.

Name: ALI AJAZ

Date of Degree: JULY, 2020

Title of Study: IMPROVING THE DROUGHT RISK ASSESSMENT AND PREPAREDNESS FOR WINTER WHEAT FARMING IN OKLAHOMA

Major Field: BIOSYSTEMS AND AGRICULTURAL ENGINEERING

Abstract: Droughts pose a persistent threat to agriculture in the Southern Great Plains (SGP). Oklahoma is a major contributor to dryland winter wheat farming in the SGP, a crop that is highly susceptible to drought episodes. Modern tools of environmental monitoring and crop simulations provide great opportunity to improve agricultural drought risk assessment and preparedness. However, in the wheat belt of Oklahoma, these modern technologies have been less utilized to understand the dynamics of drought and its effects on winter wheat growth. There is an immediate need to investigate the prospective of advanced environmental monitoring networks and practitioner-oriented crop models to mitigate the impacts of dry periods on crop yield. The objectives of this study were to: 1) develop a new drought index using soil moisture and weather data for improved drought monitoring of winter wheat; 2) calibrate and validate a crop model and employ it to study the impacts of planting date and water availability at planting on the yield of dryland and irrigated winter wheat; and 3) apply the calibrated crop model across the winter wheat belt in Oklahoma to investigate the spatial variation in yield and its drought sensitivity. The development of a new drought index showed that soil moisture information in conjunction with reference evapotranspiration can improve the estimation of drought magnitude. Also, the new drought index correlated well with the winter wheat yield, showing its potential for agricultural drought monitoring for Oklahoma. Long-term crop modeling study for winter wheat in Oklahoma revealed that October planting dates usually provide better yields in comparison to September sowing. Moreover, the considerable impact of soil moisture at the time of sowing was noted on overall wheat yields, and the irrigation had noticeable positive effect on yield, especially in drought years. Gridded crop modeling helped understanding the spatial variation in potential dryland yields in wheat belt of Oklahoma. Furthermore, it was found that the winter wheat yield was highly correlated to drought in the months of March to May, and West Central climate division was highly sensitive to dry periods in Oklahoma.

TABLE OF CONTENTS

Chapter Page

LIST OF TABLES

LIST OF FIGURES

Figure Page

Figure Page

Figure Page

CHAPTER I

INTRODUCTION

1.1. Background

Agriculture is considered the backbone of the economy of the Great Plains of the United States and wheat (Triticum aestivum) is among the major crops that are grown in the region (Stewart et al., 2018). The total area that comes under wheat in the Great Plains states is approximately 15 million ha (Mha) – about 30% of the total area under crops – and the economic contribution of this crop is about $7 billion. Almost 80% of the wheat grown in the Great Plains is rainfed (USGS, 2012), which makes precipitation the sole source of water to replenish the soil moisture necessary to fulfill crop water requirements.

The precipitation gradient is from east to west in Great Plains where eastern parts of Oklahoma and Texas receive more than 1270 mm of annual precipitation, whereas areas in Montana, Wyoming, western regions of Oklahoma and Texas receive less than 380 mm of average annual precipitation (Shafer et al., 2014). Climate change studies have predicted that the future precipitation patterns will vary at regional and sub-regional levels. Prolonged wet seasons have been projected for the northern Great Plains, while the central Great Plains is expected to experience a decrease in the amount of summer precipitation. Furthermore, Oklahoma and Texas will face longer dry periods (Shafer et al., 2014; Walsh et al., 2014). Higher temperatures have also been predicted amid future climate change in the Great Plains, giving rise to evaporative demand and consequently increased extraction of both surface and groundwater resources. The

documented history of droughts and their impact on agriculture goes back to the 1930s (the era of dust bowls). Out of 10 major drought events that were recorded between 1980 and 2003 in the U.S., six occurred in the Great Plains and caused a total loss of $131.7 billion, which was estimated as 91% of total monetary losses due to drought in the U.S. (Basara et al., 2013). The recent drought period between years 2010 and 2012 was another reminder of the vulnerability of farming sector to natural calamities. The 2010-12 drought mostly loomed over the states comprising Great Plains and the economic damages associated with agriculture were accounted for $30 billion (Rippey, 2015). The winter wheat planted area in these states was reduced by 15% (approximately 5 Mha in comparison to the past 10 years) due to unavailability of much required water during sowing period, and the harvest of 2011 was reduced by 18%.

Depending on the variables used for defining drought, this phenomenon can be categorized into four classes of 1) meteorological drought; 2) hydrological drought; 3) agricultural drought; and, 4) socio-economic drought (Mishra & Singh, 2010). These categories follow the chronological order with respect to their time of incidence. Meteorological drought occurs when there is an irregularity in the natural precipitation cycle of the watershed. This results in the hydrological drought as lack of precipitation causes reduction in stream flows and soil moisture (Keyantash & Dracup, 2002). Due to unavailability of water, agricultural production suffers, causing an agricultural drought. Ultimately, it builds the ground for economic drought as the financial stability of the society gets disturbed, leading to unstable economies and mass migrations in extreme cases (Mcleman & Hunter, 2010). Since droughts cannot be avoided, mitigation and preparedness become the best response strategies for reducing their impacts. In order to develop comprehensive drought contingency plans, scaling the severity of the drought becomes inevitable. A thorough understanding of the magnitude of a drought episode could not only help decision makers to initialize the relief activities but it would also allow the growers to optimize their farm investments (Svoboda et al, 2015).

Drought severity is the product of average magnitude and duration of drought (Keyantash & Dracup, 2002). It is important to mention here that scaling the magnitude of drought could be subjective as it mainly depends on the category of drought (Moorhead et al., 2015). For measuring the magnitude of agricultural drought, information of soil moisture (SM) and evapotranspiration (ET) is desirable. Ideally, such information should be obtained from in-situ sensors at farms; however, public weather networks e.g., Oklahoma Mesonet, etc. are also good source of soil moisture and ET data (Ajaz et al., 2019). The aforementioned environmental variables are usually synthesized using equations designed for modeling the magnitude of the drought that are called drought indices. Since most of these indices are based on the assimilated and historical data, they also have great potential to be used for simulating the yield of dryland crops. Narasimhan & Srinivasan (2005) and Yu et al (2018) compared the drought indices with the winter wheat yield and found them highly correlated. In the Great Plains, where winter wheat is used for dual purposes of grazing and grain production, such information could be crucial for wheat growers to decide about their investment (e.g., fertilizers, herbicides, etc.) with an estimate of probable yield at the time of harvest (Edwards et al., 2011).

Simulation models have been listed as one of the research areas that would be extensively explored in near-future (Douglas-Mankin, 2018) since field-based agricultural research is facing increasing uncertainty in public funding (Schimmelpfennig & Heisey, 2009). Though field experiments have their own importance, modeling crop growth and performance under certain scenarios and parameters (e.g. varying past and future climates) has several advantages. For instance, field experiments are mostly valid for a certain climatic zone or geographical boundary. This makes the results of experimental studies comparatively less applicable to regions with different climate and water resources availability. Also, field studies are labor intensive and require certain set of skills to run the trials in compliance with scientific standards. On the other

hand, crop simulation models can be extensively used as a tool to assess the performance of crops in new environments and to make decisions regarding land-use (van Keulen & Asseng, 2019).

AquaCrop is a crop growth simulation model developed by Food and Agriculture Organization (FAO) and is known to maintain the balance of accuracy and complexity, a key factor in selection and utilization of models by end-users. AquaCrop primarily estimates the crop canopy and simulates the attainable crop biomass and yield at harvest in response to water availability. AquaCrop's focus is on simulating crops' response to water availability, which makes it an ideal model for studying the effects of droughts and heatwaves on crop productions. Some of the practical benefits that AquaCrop offers are that it requires relatively low input data, the user interface is less complex than other crop models, and the well-structured calculation scheme gives its user confidence while interpreting the results. Additionally, AquaCrop's open-source (OS) version allows researchers to adapt the code according to their research needs. In a recent study, Nouri et al. (2018) employed the open-source version of AquaCrop and found it effective to analyze the effects of water conservation techniques (mulching and drip irrigation) at basin level. Since the AquaCrop-OS allows to run multiple parallel simulations within a fairly shorter duration of time, it is possible to assess the impact of climate anomalies on important grain crops such as wheat at a large spatial scale. This leads towards the opportunity of developing yield maps at state or national levels using gridded datasets of environmental variables and soil types.

There could be multiple applications of such spatial crop modeling. For example, gridded drought indices can be correlated with crop yield maps and areas susceptible to higher crop damages can be marked for better drought mitigation in future and sub-regional crop advisories (Yu et al., 2018). In addition, the overall yield potential of a particular region can be thoroughly studied and reasons for significant yield variations can be explored. Better decisions related to planting dates can be also made across a region based on long-term climate variations in the past and future. Most of the previous studies have focused on crop model applications at a few locations across a

region, mainly due to computational constraints. Very few studies have focused on the application of crop models to study the impacts of drought on a large spatial scale in the Great Plains.

1.2. Objectives

The main goal of this research is to improve the drought preparedness for winter wheat farming in Oklahoma using a combination of drought monitoring tools and crop growth simulation model. The specific objectives are:

1. To develop a new drought index using soil moisture and weather data for improved drought monitoring of winter wheat;

2. To calibrate and validate a crop model and employ it to study the impacts of planting date and water availability on winter wheat yield; and,

3. To apply the calibrated crop model across the winter wheat belt in Oklahoma to investigate the spatial variation in yield and study drought sensitivity.

CHAPTER II

DEVELOPMENT AND EVALUATION OF AN AGRICULTURAL DROUGHT INDEX BY HARNESSING SOIL MOISTURE AND WEATHER DATA

2.1. Introduction

Drought events occur frequently in the Southern Great Plains of the United States, negatively impacting agricultural production and sustainability. This is mainly due to scarce surface water resources in this region. Groundwater resources, such as the Ogallala aquifer, help producers mitigate drought impacts (Taghvaeian et al., 2015). However, these resources are being depleted at an unsustainable rate, especially during dry periods (Khand et al., 2017). In Oklahoma, recorded drought history dates to the start of the 20th century, when major droughts were experienced in the decadal spans of 1910, 1930, 1950, 1960, and 1970. The beginning of the 21st century brought severe drought-related losses to Oklahoma's agriculture. For instance, the drought episode of 2001–2002 cost $210 million to the state's economy due to significant yield loss of winter wheat, alfalfa, and hay (Khand et al., 2017).

A more recent period of extreme and exceptional drought in Oklahoma was between 2011 and 2015, with devastating impacts on irrigated agriculture. As a result of this episode and consequent declines in reservoir water levels, the Luger-Altus Irrigation District in southwest Oklahoma could not deliver irrigation water during the 2011–2014 period (Khand et al., 2017). In addition, groundwater resources experienced greater-than-usual depletions. The Ogallala aquifer underlying the Oklahoma Panhandle recorded a rate of decline that was 2.75 times larger than

non-drought years. Recurrent dry periods along with low precipitation and consequent low agricultural production have been projected for the Southern Great Plains region under a changing climate (Reilly et al., 2003; Rosenzweig et al., 1993; Shrestha et al., 2020). Considering these existing and future challenges, managing and planning of limited agricultural water resources for sustainable agricultural production in the region should consider innovative approaches to improve drought monitoring and assessment.

Drought assessment is key to water resources management and planning (Mishra and Singh, 2010). Optimal selection of drought monitoring tools, such as drought indicators and indices, can elevate the drought mitigation measures (Hayes et al., 2011; Moorhead et al., 2017). Drought indices are the assimilation of single or multiple weather and/or hydrologic variables and are considered more pertinent for drought monitoring compared to standalone indicators (e.g., temperature, precipitation, etc.) (Zargar et al., 2011). Soil moisture is one of the variables used in drought monitoring and assessment, especially in the case of agricultural drought. This is mainly because soil moisture availability governs physiological processes in plants, and any paucity of water content in the crop root-zone can impede productivity (Wang et al., 2011; Mannocchi et al., 2004). A drought index using soil moisture would be directly related to crop growth potential and could provide a decision support tool.

There are typically four common approaches to development of drought indices that use measured or modeled soil moisture data. One approach compares the soil moisture with thresholds such as field capacity and wilting point (Martínez-Fernández et al., 2015; Sridhar et al., 2007; Hunt et al., 2008). The second approach applies statistical analysis (e.g., probability, probability density function, normalization, etc.) on soil moisture data and then quantifies drought intensity based on the attributes of the computed statistics (Carrão et al., 2016; Li et al., 2016; Dutra et al., 2008; Narasimhan and Srinivasan, 2004). The third approach combines the first two approaches (Torres et al., 2013; Cammalleri et al., 2016), while the fourth one adds additional

variables such as evapotranspiration (ET) to improve the sensitivity of the estimated drought index (Sohrabi et al., 2015; Woli et al., 2012).

Regardless of the approach used, soil moisture (SM) based indices have had similar or improved performance compared to other indices. In addition, SM indices have been found to be highly correlated with crop yield (Mannocchi et al., 2004; Carrão et al., 2016) and in good agreement with the net difference between precipitation and potential ET at different time scales and lags (Martínez-Fernández et al., 2015; Hunt et al., 2008; Cammalleri et al., 2016). Previously developed indices such as Z-Index (Palmer, 1965) and Agriculture Reference Index for Drought (ARID) (Woli et al., 2012) have shown that calculations involving both SM and ET outperform conventional indices in tracking agricultural drought by approximating the water deficit and characterizing the moisture dynamics during transition between wet and dry conditions. Nonetheless, these indices have been identified with adaptability issues. For example, Keyantash and Dracup (2002) ranked Z-Index low in terms of "tractability" and "transparency" due to its complicated formulation and computations. ARID was assigned the lowest rank in "ease of use" classifications of the World Meteorological Organization (WMO) and the Global Water Partnership (GWP) (2016), as it requires advanced modeling efforts for site specific simulations (Woli et al., 2013). The aforementioned limitations in drought indices reduce their acceptability among producers and reduce the effectiveness of outreach efforts to convey drought conditions to a larger audience (Keyantash and Dracup, 2002).

In addition, the ability of a drought index to capture the impact of climate anomalies on the crop productivity is of crucial importance. Though the relationship of crop production and climate is non-linear and complex due to seasonal variability (Mladenova et al., 2017), a drought index capable of explaining a large part of variability in the anticipated crop yield would be potentially preferred by the farmers—especially in regions such as Oklahoma where agricultural economy depends significantly on a crop (dryland winter wheat) that is highly susceptible to drought

(Arndt, 2002). Such an index could have a considerable economic impact, as the winter wheat growers have to make decisions about grazing in early crop stages based on expected yields and the dynamics of the market (Doye and Sahs, 2018). Testing the index's performance against the crop production under rain-fed conditions could help with evaluating the efficacy of the index (Martínez-Fernández et al., 2015; Carrão et al., 2016), and the dryland yield could be used as a benchmark to determine the suitability of agricultural drought index (Woli et al., 2012). Consequently, there is a need for an agricultural drought index that not only harnesses the efficacy of high quality SM and ET databases but also holds the simplicity in design and computation, providing a decision making tool to end-users. The main goal of this study was to develop and evaluate a new agricultural drought index by utilizing daily SM and ET datasets in Oklahoma. More specific objectives were: i) to investigate the relationships between the new index and several previously developed SM-based and meteorological indices; ii) to study the spatial and the temporal variations in the new index across Oklahoma; and iii) to explore the response of winter wheat production to drought magnitude estimated by new and existing drought indices. The Oklahoma Mesonet (McPherson et al., 2007), containing soil moisture and weather data across a range of climates, provided a unique opportunity to develop and evaluate the proposed new index.

2.2. Materials and methods

2.2.1. Study sties

This study was conducted using data collected during a 17-year period from 2000 to 2016 at five Mesonet weather stations (McPherson et al., 2007; Brock and Crawford, 1995) under natural grassland across Oklahoma. These sites are located near the cities of Goodwell, Hollis, El Reno, Pawnee, and Wister, representing Panhandle, Southwest, Central, Northeast, and Southeast Oklahoma, respectively. The selected sites were spread across the precipitation gradient in Oklahoma, which increases approximately 250 mm for every 1° longitude from the Panhandle to

southeast Oklahoma (Figure 2.1). Table 2.1 presents annual temperature, precipitation, and reference evapotranspiration data for each study site.

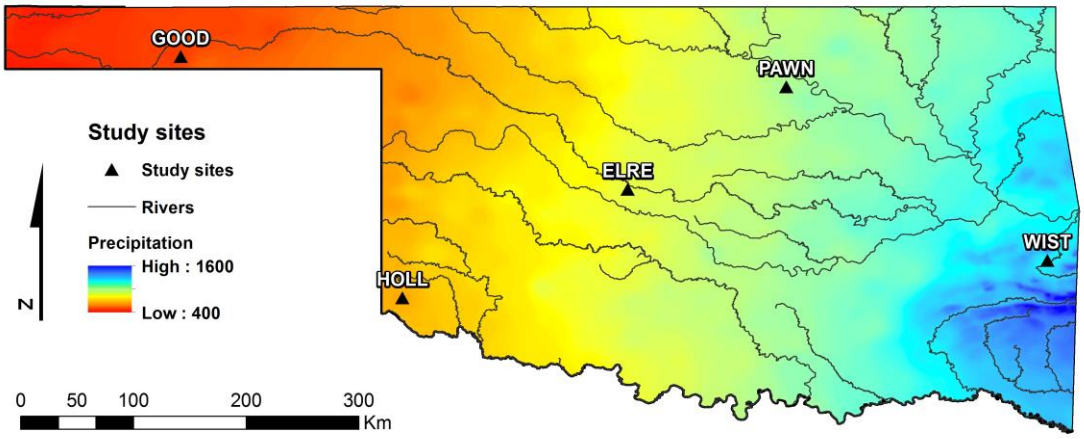

Figure 2.1. Normal annual precipitation in Oklahoma (1981–2010). Source: PRISM raster map. The locations of study sites and major rivers are also demonstrated.

Table 2.1. Annual average daily air temperature, total precipitation, and total reference evapotranspiration (ET_r) measured at each study site over the study period (2000–2016).

SITE	Abbreviation	Region	Temperature (˚C)	Precipitation (mm)	ET_r (mm)
Goodwell	GOOD	Panhandle	13.42	435	2675
Hollis	HOLL	Southwest	16.32	660	2355
El Reno	ELRE	Central	15.66	871	1997
Pawnee	PAWN	Northeast	15.44	1010	1871
Wister	WIST	Southeast	16.42	1252	1542

2.2.2. Input data

Each Mesonet station was equipped with automated sensors to record precipitation, air temperature, relative humidity, wind speed, solar radiation, and soil moisture. Soil moisture was estimated using heat dissipation sensors (model 229-L, Campbell Scientific, Inc., Logan, UT,

USA; accuracy < ± 0.5 °C) installed at three depths of 5, 25, and 60 cm below the soil surface (Illston et al., 2008). Each sensor was calibrated before installation to obtain an accurate relationship between heat dissipation and soil matric potential, which was then converted to volumetric water content (VWC) based on the van Genuchten (1980) method. Measurements from undisturbed soil cores at each site were used for determining water contents at field capacity (FC) and wilting point (WP) as well as the van Genuchten parameters (Scott et al., 2013). Using accurate estimates of soil parameters based on in-situ measurements is a major requirement in obtaining reliable SM based drought indices, a point that was highlighted in previous studies (Martínez-Fernández et al., 2015; Sridhar et al., 2007; Hunt et al., 2008; Cammalleri et al., 2016). Table 2.2 presents the soil texture and the VWC at FC and WP for the three sensor installation depths at each site.

Table 2.2 Soil texture and volumetric water content (VWC) (m^3 m^{-3}) at field capacity (FC) and wilting point (WP) thresholds for the three sensor installation depths of 5, 25, and 60 cm at each study site.

SITE	**Texture**			**VWC at FC** (m^3 m^{-3})			**VWC at WP** (m^3 m^{-3})		
	5 cm	**25 cm**	**60 cm**	**5**	**25**	**60**	**5**	**25**	**60**
GOOD	Clay loam	Clay loam	Clay loam	0.25	0.29	0.21	0.13	0.17	0.14
HOLL	Clay	Clay	Clay	0.33	0.35	0.35	0.21	0.25	0.25
ELRE	Silty loam	Silty clay loam	Silty clay	0.41	0.29	0.33	0.11	0.12	0.21
PAWN	Silty clay loam	Silty clay	Clay	0.39	0.43	0.42	0.23	0.27	0.27
WIST	Silty loam	Silty clay loam	Clay	0.32	0.27	0.42	0.12	0.13	0.28

Daily VWC data for the study period (2000–2016) collected at each of the three depths from the five sites were used in the analysis. The Mesonet soil moisture database had some missing values, but they accounted for only 3% of all collected data at each site on average. In addition, more

than half of missing values occurred during periods with no measured precipitation. Thus, the gaps were filled using a linear interpolation technique. Meteorological data such as precipitation, air temperature, relative humidity, wind speed, and solar radiation were also measured by the Mesonet station at each site and were retrieved for the study period (2000–2016).

To investigate the impact of drought on crop yield, the relationship between drought indices and winter wheat production—a major crop in Oklahoma—was analyzed. County wise data on winter wheat production were downloaded from the website of the U.S. Department of Agriculture, National Agriculture Statistics Service (https://quickstats.nass.usda.gov/). The reported values represented both irrigated and non-irrigated winter wheat in Oklahoma. Segregated datasets of non-irrigated and irrigated winter wheat were not available for the complete study period. Furthermore, almost 96% of the winter wheat harvested area was non-irrigated in Oklahoma between 2001 and 2009. Hence, the obtained data can be safely assumed to represent dryland production, which is more susceptible to drought. Wister station (see Figure 2.1) was not included in the analysis due to gaps in wheat production data. Tian et al. (2018) conducted a similar study in the same region under limitation of data availability and found the combined dataset of winter wheat yield (irrigated plus non-irrigated) suitable for such analysis based on the low percentage of irrigated area.

2.2.3. Soil moisture based drought indices

Three previously developed SM based drought indices and a new index were calculated for each site during the study period. The existing indices included Soil Water Deficit Index (SWDI), Water Deficit Index (d), and Normalized Soil Moisture (NSM), and the new index was called Soil Moisture Evapotranspiration Index (SMEI).

2.2.3.1. Soil Water Deficit Index

The SWDI was developed by Martínez-Fernández et al. (2015) and was estimated as:

$$\mathrm{SWDI} = \left(\frac{\theta - \theta_{\mathrm{FC}}}{\theta_{\mathrm{AWC}}}\right) \times 10 \quad (1)$$

where θ is the aggregated VWC of soil profile, θ_{FC} is the VWC at FC, and θ_{AWC} is the available water content estimated as the difference between VWC at FC and WP (all in $m^3\ m^{-3}$). The weighted average of θ was estimated using the following approach as suggested by (Martínez-Fernández et al., 2015):

$$\theta = \frac{(\theta_5 \times 1)}{5} + \frac{(\theta_{25} \times 2)}{5} + \frac{(\theta_{60} \times 2)}{5} \quad (2)$$

where θ_5, θ_{25}, and θ_{60} are VWC at 5, 25, and 60 cm soil layers.

2.2.3.2. Water Deficit Index

This index was suggested by Cammalleri et al. (2016):

$$\mathrm{d} = \frac{1}{1 + \left(\frac{\theta}{\theta_{50}}\right)^{\mathrm{n}}} \quad (3)$$

where n is an empirical exponent (unitless) and θ_{50} is estimated by averaging VWC between soil moisture thresholds as described by Cammalleri et al (2016); θ was aggregated for the soil profile based on Equation (2).

2.2.3.3. Normalized Soil Moisture

The NSM was proposed by Dutra et al. (2008) as:

$$\mathrm{NSM}_{\mathrm{m,y}} = \frac{\theta_{\mathrm{m,y}} - \bar{\theta}_{\mathrm{m}}}{\sigma_{\mathrm{m}}} \quad (4)$$

where $\theta_{m,y}$ is the VWC for the month m and the year y ($m^3\ m^{-3}$), $\bar{\theta}_m$ is the mean monthly VWC ($m^3\ m^{-3}$), and σ_m is the standard deviation for all study years. This index is a mathematical imitation of the standardized precipitation anomaly used by Jones and Hulme (1996). Modeled

soil moisture estimates of the top 289 cm of soil were used by Dutra et al. (2008). In the present study, however, in-situ measurements of soil moisture were aggregated based on Equation (2) and used in calculating NSM at two different time scales—one month (NSM-1) and three months (NSM-3). For NSM-3, the average $\theta_{m,y}$ over three consecutive months was used in Equation (4) along with corresponding $\bar{\theta}_m$ and σ_m.

2.2.3.4. Soil Moisture Evapotranspiration Index

The SMEI is proposed in this study based on soil moisture and reference evapotranspiration (ET_r) estimates. The SMEI estimation follows a three-step approach. At the first step, the aggregated daily root zone water storage (in units of water depth, such as mm) is calculated using a zone-weighted approach:

$$RZWS_i = (\theta_5 \times L1) + (\theta_{25} \times L2) + (\theta_{60} \times L3) \quad (5)$$

where $RZWS_i$ is the root zone water storage on day i and L1, L2, and L3 are the layers in the crop root zone represented by each soil moisture sensor. In this study, values of 10, 30, and 40 cm were used for L1, L2, and L3, respectively, assuming a root zone depth of 80 cm (Miller et al., 2007). This aggregation of RZWS was in agreement with soil moisture sensor depths of Oklahoma Mesonet as discussed by Ochsner et al. (2013). The values of the L parameters can be modified in other applications based on the number and the depth of soil moisture sensors as well as the root zone.

In the second step, the difference between monthly average RZWS and monthly cumulative ET_r (both in units of water depth) is estimated for each month during the study period:

$$D_{m,y} = \left[\frac{1}{n}\sum_{i=1}^{n} RZWS_i\right] - \left[\sum_{i=1}^{n} ET_{ri}\right] \quad (6)$$

where $D_{m,y}$ is the difference between monthly average of $RZWS_i$ and monthly sum of ET_{ri} for month m and year y, n is the number of days in each month, and ET_{ri} is the reference ET on day i. The standardized approach of the American Society of Civil Engineers (ASCE) described by Allen et al. (2005) was adopted in estimating ET_{ri} using the REF-ET program (Allen, 2015), and Mesonet weather data were used as input. The ASCE standardized approach is based on the simplified ASCE Penman-Monteith equation for a tall agricultural crop as the reference surface. Detailed information on the required parameters and their units can be found in (Allen et al., 2005). The final step involves standardizing $D_{m,y}$ using the average and standard deviation to estimate the drought index:

$$SMEI_{m,y} = \frac{D_{m,y} - \overline{D_m}}{\sigma_m} \quad (7)$$

where $\overline{D_m}$ is the monthly average, and σ_m is the monthly standard deviation of $D_{m,y}$ for the same month among all study years.

In essence, SMEI is similar to Palmer's Z-Index where ET is subtracted from precipitation at a monthly time-step to model soil water deficit (explained later). In SMEI, however, precipitation is replaced with soil moisture since the latter parameter better represents the source of water available to agricultural crops (Tigkas et al., 2018). This is because smaller amounts of precipitation evaporate from soil and plant surfaces before reaching the root zone, and larger amounts can generate runoff or deep percolation below the root zone. In either case, the precipitated water will not be available for crop consumption. The inclusion of a water consumption/demand parameter (ET) along with a water source parameter (soil moisture) in the same index can also augment the drought signal (Tsakiris and Vangelis, 2005).

In estimating SMEI, the common approach of presenting drought indices as anomalies (Anderson et al., 2011) was followed, and z-scores were calculated by normalizing $D_{m,y}$ to a mean of zero

and a standard deviation of one. Therefore, the SMEI values can be interpreted similar to the values of Standardized Precipitation Index (SPI) and Standardized Precipitation Evapotranspiration Index (SPEI, explained later), where negative values represent drought condition. In addition to monthly SMEI (SMEI-1), 3 month SMEI (SMEI-3) was calculated in order to understand the characteristics of drought events as drought recurrence decreases and its duration increases at longer time scales (Mckee et al., 1993). The 3 month SMEI was estimated by using the corresponding parameters over three consecutive months in Equations (7) and (8) (similar to NSM-3). Longer time scales (9 and 12 month) were not included, since the focus of this study was exclusively on agricultural drought, and the 3 month time scale was considered sufficient for this purpose (Rhee et al., 2010).

One of the main merits of SMEI is the use of estimated soil moisture, which has been assigned with the highest ranking in terms of transparency of a drought index by Keyantash and Dracup (2002). In addition, the computational approach of SMEI is relatively simple. The tractability of this index may seem lower because soil moisture sensors have not been widely used by agricultural producers in the past. However, soil moisture sensing devices are becoming increasingly affordable (Paul et al., 2018), and their inclusion in public weather networks provides a valuable resource to all end-users.

2.2.4. Meteorological drought indices

Seven widely used meteorological drought indices were estimated in this study, including Atmospheric Water Deficit (AWD), Standardized Precipitation Index (SPI), Palmer's Z-Index, Palmer Drought Severity Index (PDSI), Self-Calibrated PDSI (scPDSI), Standardized Precipitation Evapotranspiration Index (SPEI), and U.S. Drought Monitor (USDM). The calculation of SPI, Z-Index, PDSI, scPDSI, and SPEI requires time series data for a minimum of 30 years for a thorough drought analysis (Ahmadalipour et al., 2017). As mentioned before, the

present study focused on the 17-year period of 2000–2016. Therefore, PRISM (Parameter-elevation Regressions on Independent Slopes Model) (Daly et al., 1994) and COOP (The National Weather Service Cooperative Observer Network) 4 × 4 km grid monthly datasets for precipitation and temperature were used for constructing the timeline before the year 2000. The PRISM data are available at https://wrcc.dri.edu/wwdt/time/. Schneider and Ford (2013) found that the PRISM database was useful in developing "climate informed decision support" in case of non-availability of long-term precipitation data. The root mean square error (RMSE) for precipitation and temperature data collected from Mesnoet (as observed data) and PRISM-COOP (as predicted data) for 2000–2016 was estimated as 18.33 mm and 0.70 °C, respectively.

2.2.4.1. Atmospheric Water Deficit

The AWD constitutes a simple calculation where weekly sums of precipitation are subtracted from weekly sums of ET (Torres et al., 2013). In this study, the AWD was calculated reversely (precipitation – ET) similar to Martínez-Fernández et al. (2015), and monthly sums were used as opposed to weekly. The ASCE standardized reference ET (ET_r) was used in AWD estimations.

2.2.4.2. Standardized Precipitation Index

The SPI is based on long-term monthly precipitation data and is calculated by fitting the time series to a probability distribution (Mckee et al., 1993). This distribution is eventually converted into normal distribution to translate the anomalies of precipitation into a score range. In this study, SPI was calculated for one and three month periods using the SPI_SL_6 program (downloaded from http://drought.unl.edu/archive/Programs/SPI/spi_sl_6.exe). The purpose of the calculations that were based on different time scales was to compare the drought indices in regard to short- and long-term drought events (Sehgal et al., 2017).

2.2.4.3. Palmer's Z-Index

Palmer's Z-Index (hereinafter Z-Index) requires monthly precipitation and temperature along with the latitude and the available water capacity of the soil as input data. A two-layer soil model

approach is used to calculate the water balance (Palmer, 1965). Hydrologic accounting is performed to compute the parameters including ET, recharge, run-off, and loss of moisture from soil along with their potential values. The potential values are further transformed using climate dependent weighting factors. These transformed values are then summed as an equivalent of precipitation required for maintaining the normal soil moisture, which is further subtracted from the actual precipitation in order to estimate the monthly moisture departure (Wells et al., 2004). Subsequently, the moisture departure is multiplied with empirically derived climatic characteristic, and the monthly moisture anomaly index known as Z-Index is estimated. Z-Index is sensitive to abrupt variation in soil moisture and thus is considered an appropriate index for monitoring agricultural droughts (Karl, 1986).

2.2.4.4. Palmer Drought Severity Index

The PDSI relies heavily on Z-Index. With the purpose of integrating the drought magnitude with time, the empirically obtained duration factor was combined with Z-Index, and PDSI values were calculated. These values represented the drought severity and were suitable for quantifying long-term droughts.

2.2.4.5. Self-Calibrated PDSI

This index makes PDSI more consistent for spatial comparisons of drought through replacing the empirical constants of PDSI with location-specific values (Sehgal et al., 2017). Z-Index, PDSI, and scPDSI were all calculated using the sc-PDSI program downloaded from the website of the GreenLeaf project at University of Nebraska–Lincoln (http://greenleaf.unl.edu/).

2.2.4.6. Standardized Precipitation Evapotranspiration Index

The SPEI works on the same principle as SPI. However, it includes the long-term variations in air temperature and follows the water balance approach by subtracting potential ET (based on the Thornthwaite method) from precipitation (Vicente-Serrano et al., 2010). One and three month

SPEI (SPEI-1 and SPEI-3) were obtained in this study using the SPEI calculator (Beguería et al., 2009).

2.2.4.7. U.S. Drought Monitor

The USDM data were obtained by downloading weekly GIS layers from the web portal of the U.S. Drought Monitor (http://droughtmonitor.unl.edu/Data/GISData.aspx). The USDM reports drought severity in one of the following categories: abnormally dry (D0), moderate drought (D1), severe drought (D2), extreme drought (D3), and exceptional drought (D4). The drought category for each study sites was extracted from USDM layers. The categories were converted to numerical values of 0, 1, 2, 3, and 4 for D0, D1, D2, D3, and D4 categories, respectively. Finally, the median numerical value in each month was used as the monthly value.

2.2.5. Performance analysis

In order to evaluate the performance of the newly developed index, its relationship with the existing SM and the meteorological indices was investigated. Correlation analysis is a widely used method for measuring the degree of association among two variables (Zhao et al., 1993). Pearson correlation analysis was employed, and the following categories of correlation coefficients (r) suggested by Mavromatis (2010) were adopted in the present study: very high (>0.9), high (0.7–0.9), moderate (0.5–0.7), weak (0.3–0.5), and very weak (<0.3). The performance of the new index was also assessed by studying its ability to track temporal and spatial variations in drought as compared with several existing indices.

The last step of the performance analysis of the new drought index included investigating its potential for assessing the impact of agricultural drought on winter wheat production between 2000 and 2016. Winter wheat is Oklahoma's largest crop with an average planted area of 2 to 2.4 million hectares every year (Marburger, 2018). This crop is usually planted in October and harvested in June of the next year, followed by a fallow period or a short-season summer cover

crop. The spring period is considered critical due to the occurrence of jointing, heading, and flowering in winter wheat (Zhang et al., 2017), and any water stress in these growth stages can cause significant fluctuations in crop yield (Hane et al., 1984). Hence, the correlation between annual winter wheat production and the averaged drought indices was estimated both for the growing season (October to June) and for the critical period related to drought stress (March and April) similar to previous drought studies comparing the magnitude of drought and crop production (Carrão et al., 2016; Narasimhan and Srinivasan, 2005; Rhee at al., 2010; Xu et al., 2018).

2.3. Results and discussion

2.3.1. Comparison with SM indices

Correlation coefficients of the new and the existing SM based indices for each study site are shown in Figure 2.2 The new index SMEI-1 had high to very high correlations with NSM-1, represented by r values ranging from 0.70 to 0.92. Moderate to high correlations were noted with SWDI and d, with r ranges of 0.62–0.75 and 0.60–0.75, respectively. In comparison to SMEI-1, SMEI-3 had similar or weaker correlations with existing SM indices, except NSM-3, where better correlations were found (most likely due to similarity in time scales).

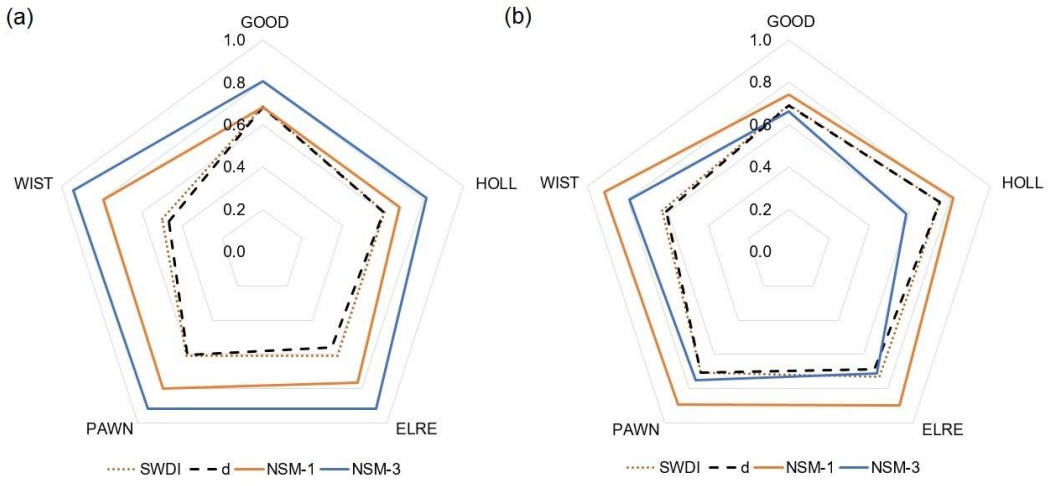

Figure 2.2. Radar plots of correlation coefficients for a) SMEI-1 and existing soil moisture-based indices (b) SMEI-3 and existing soil moisture-based indices.

2.3.2. Comparison with meteorological indices

The correlation coefficients among all studied SM and meteorological indices are graphed in Figure 2.3. Compared to existing SM indices, SMEI-1 had similar or stronger correlations with meteorological indices. Weak to moderate correlations for SMEI-1 were found with SPI-1 (0.41–0.59) and SPEI-1 (0.45–0.69) at all sites. Increasing the time scale of these meteorological indices from one to three months (SPI-3 and SPEI-3) improved correlations (0.61–0.71 and 0.64–0.77, respectively). A similar trend was noted for SMEI-3 and other SM indices, where longer time scale SPI and SPEI had stronger correlations. In case of PDSI, the correlations were improved for SMEI-3 (0.61–0.78) compared to SMEI-1 (0.56–0.72), potentially because the PDSI represents medium to long-term drought conditions.

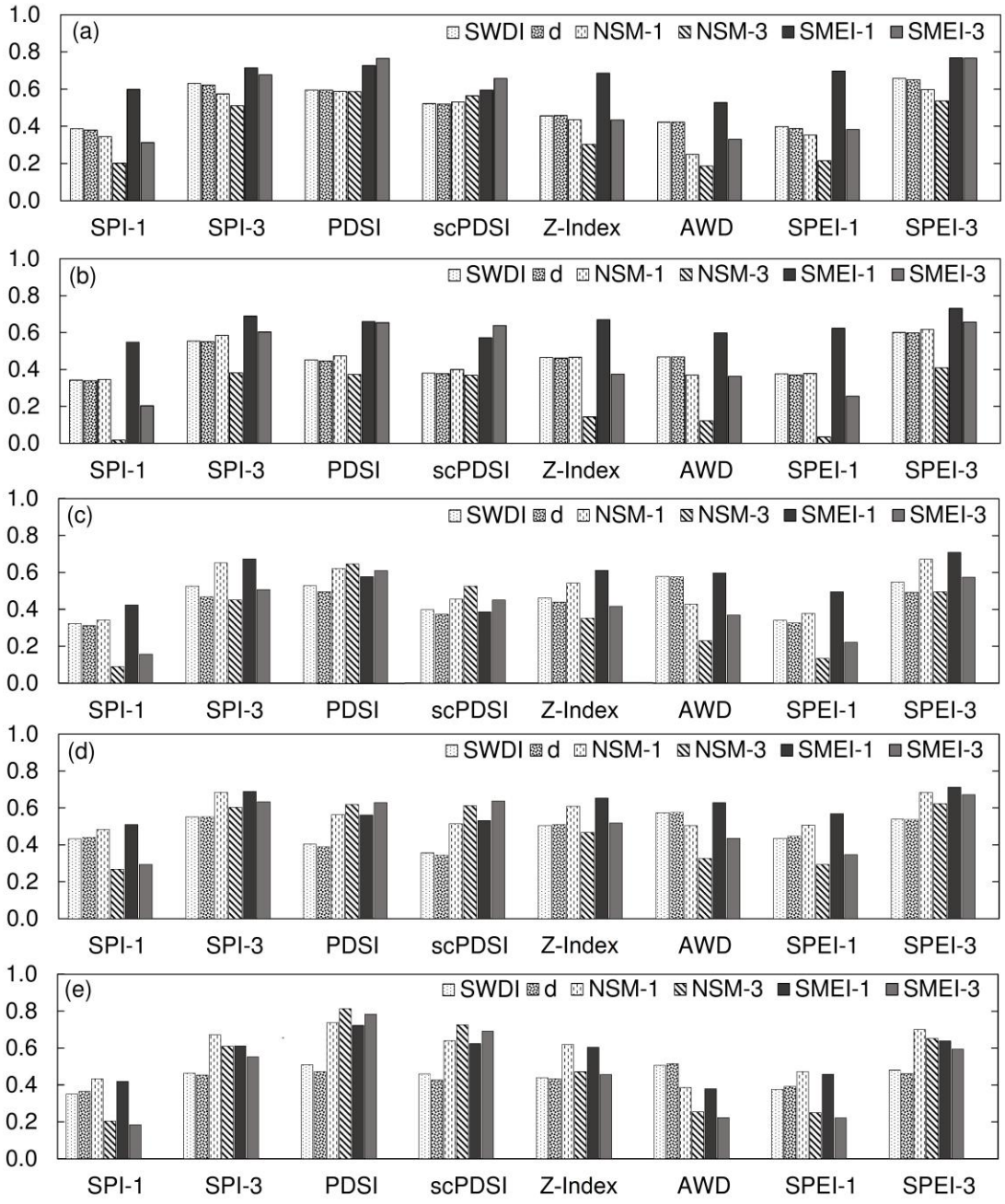

Figure 2.3. Correlation coefficients among soil moisture based and meteorological drought indices at Goodwell (a); Hollis (b); El Reno (c); Pawnee (d); and Wister (e).

Weak to moderate correlations were found between SMEI-1 and AWD (0.37–0.62), but the values were comparable or stronger than those with existing SM indices. Moderate correlations

between SMEI-1 and Z-Index (0.60–0.68) were found at all study sites. These results were expected, as Z-Index accounts for moisture departure from normal on a monthly basis, mainly in terms of ET and soil moisture losses (Quiring et al., 2003). As a result, Z-Index is more suitable for detecting variation in soil moisture over a short period of time (Karl,1986; Moorhead et al., 2015), and the same applies to SMEI-1.

To help facilitate a better comparison between new and previously developed SM indices, box and whisker plots of their correlation coefficients with all meteorological indices at all sites are shown in Figure 2.4. The average correlation between SMEI and meteorological drought indices was 1.3 times higher in comparison to existing SM indices. The SMEI-1 had the largest mean r (0.60) among all SM indices followed by NSM-1 with 0.52. The SMEI-1 also had one of the smallest ranges (0.37–0.76), indicating relatively better performance under variable climatic conditions. In general, the r values had a larger range for longer time scales such as NSM-3 and SMEI-3. This was expected, since indices estimated on a scale of three months are likely to be more strongly correlated with medium to long-term meteorological drought indices but not with short-term indices.

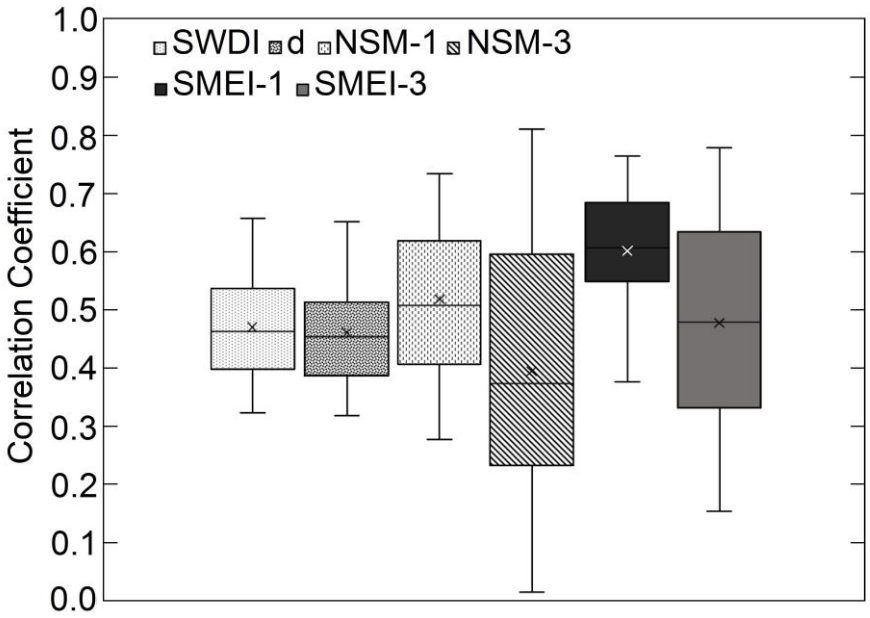

Figure 2.4. Box and whisker plots of correlation coefficients between SM and meteorological indices at all sites. Whiskers indicate the full range of estimated coefficients and crosses represent the mean.

The correlations between meteorological and existing SM drought indices found in this study were similar to those reported in previous studies. For example, the range of SWDI-AWD correlation coefficients was 0.42–0.58 in the present study. Martínez-Fernández et al. (2015) found weak to moderate correlations (0.40–0.57) between weekly SWDI and AWD in a semi-arid region with heterogeneous soils. Mishra et al. (2017) reported a correlation coefficient of 0.56 for the same indices under humid subtropical climate. In addition, moderate to high correlation coefficients (0.60–0.80) were reported for NSM-PDSI by Dutra et al. (2008) for a Mediterranean region, and this study found similar r values ranging between 0.47 and 0.74.

Spatial variations in correlation strength between SMEI-1 and meteorological drought indices at different sites were in accordance with the available literature. The strongest correlations of SMEI-1 and PDSI were found at Goodwell and Wister ($r > 0.72$), whereas Hollis, El Reno, and Pawnee had r values of 0.66, 0.58, and 0.56, respectively. Greater correlations with PDSI at arid and humid sites were most likely due to the inherent calibration of PDSI in extreme climates

(Sehgal et al., 20117). The SMEI-1 showed the strongest correlation with SPEI-3 (r = 0.76) at Goodwell and comparatively weaker correlation at Wister (r = 0.63). This may have been due to overestimation of potential evapotranspiration (PET) by the Thornthwaite equation for SPEI in humid regions (Van der Schrier et al., 2011). The SMEI correlations with SPEI would probably have been higher if the Penman-Monteith equation was used to estimate the reference ET in SPEI calculations, as recommended by Beguería et al. (2014).

2.3.3. Temporal tracking of drought

Due to the occurrence of multiple droughts of varying magnitudes between 2010 and 2015, this period was selected to further evaluate the performance of newly developed SMEI in tracking temporal variations in drought. Changes in SMEI-1 during the selected period were compared against fluctuations in USDM, two SM drought indices, and one meteorological drought index. The two SM indices were NSM-1 and SWDI. The d index was excluded from the comparison because it had the smallest average r (Figure 2.4). The single meteorological index used in comparison was the Z-Index, since it incorporates the soil–water balance in its calculations. The USDM timeline was included for comparison with the overall drought conditions. It should be noted that USDM estimates are based on a combination of meteorological drought indices, field observations, and stakeholder feedback (Zargar et al., 2011).

According to USDM, the drought condition gradually started progressing between October 2010 and June 2011 at Goodwell, starting from D0 and reaching D4 (Figure 2.5a). The drought continued for almost five years and eventually ended by June 2015. All drought indices showed multiple episodes of severe droughts during this period. The SMEI-1 and the Z-Index compared well with each other, and both indices captured the months of June and July 2011 as the worst drought-stricken months. The Z-Index values had a more rapid fluctuation, mainly due to the sensitivity of this index to unusually dry or wet months (Wells et al., 2004). The NSM-1 had a

relatively slow response, indicating wet conditions during peak drought months and gradually transforming into drought conditions. This shows the advantage of amplifying drought response by including ET in drought indices (Tsakiris and Vangelis, 2005). The SWDI trended similar to NSM-1 and signaled decreases in drought magnitude; however, it never confirmed a non-drought period. Almost all indices clearly indicated a significant wet period in May 2015, which marked the end of the drought.

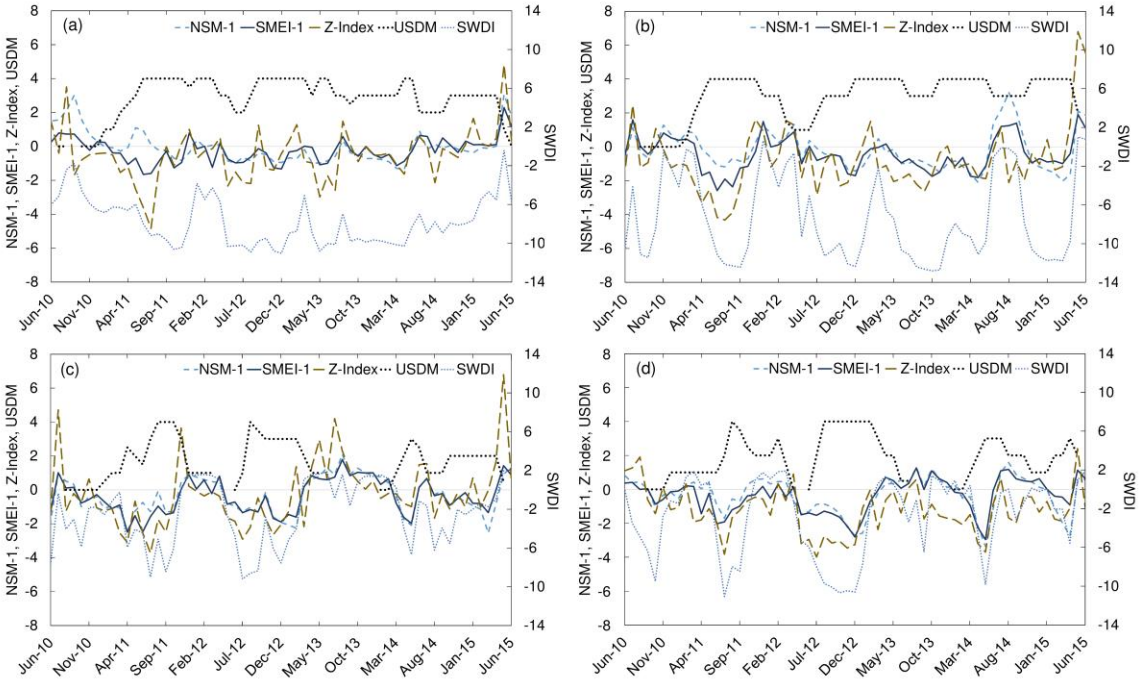

Figure 2.5. Time series of drought indices at Goodwell (a); Hollis (b); El Reno (c); and Pawnee (d).

During all major drought episodes at Hollis, El Reno, and Pawnee sites, the SMEI-1 values declined in correspondence with other drought indices (Figure 2.5b, c, and d). In general, both SMEI-1 and Z-Index had similar trends in tracking drought intensification and reliefs during the 2010–2015 period, whereas NSM-1 and SWDI showed damped response towards short-term variations in drought condition. Since SMEI-1 is based on measured daily soil moisture and ET, its capability to identify the drought is more rigorous in comparison to Z-Index. In addition,

SMEI relies on the ASCE Standardized Penman-Monteith method for estimating ETr, while Z-Index uses the less sophisticated but also less accurate Thornthwaite method (Chen et al., 2005).

2.3.4. Spatial tracking of drought

Two drought episodes in February 2006 and July 2011 were selected to investigate spatial variability in drought indices. The corresponding USDM maps were used in the analysis. According to Oklahoma Water Resources Board (2006), the period of September 2005 to March 2006 was the driest cool growing season in Oklahoma since 1921. The departure from the normal precipitation during this season ranged from −366 mm for the Southeast division (Wister) to −105 mm for the Panhandle region (Goodwell), and the severity of drought gradually reduced from east to west. In February 2006, Wister and Pawnee were under D4 and D3 categories, respectively. The remaining sites were facing D2 category. The spatial variability of SMEI-1 was in agreement with USDM (Figure 2.6), ranging from −3.34 at Wister to −1.14 at Goodwell. NSM and Z-Index also showed a similar pattern. However, SWDI had a nearly opposite trend, showing an increase in drought severity from east to west. This was most probably because this index is solely based on soil moisture availability in the root zone and does not include other parameters. In addition, it is not normalized based on the past data at each site. Despite having smaller departures of soil moisture from average, the magnitude of soil moisture was smaller in western sites compared to eastern ones due to their natural aridity. Hence, SWDI signaled a more severe drought. Keyantash and Dracup (2002) mentioned that indices that are normalized are more appropriate for comparing across locations.

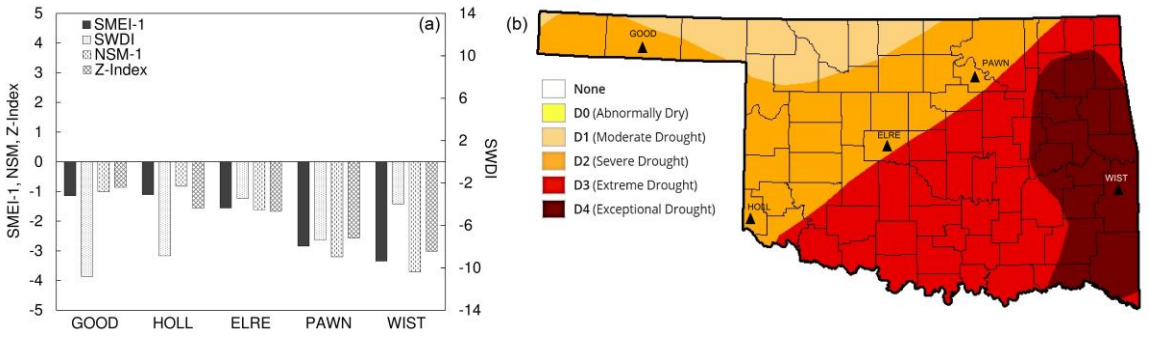

Figure 2.6. Magnitudes of selected drought indices for February 2006 at study sites (a) and the corresponding U.S. Drought Monitor (USDM) map (b).

An opposite spatial trend occurred in July 2011, and drought severity gradually decreased from Panhandle and Northwest regions towards the southeast. Based on USDM, Goodwell and Hollis experienced D4, El Reno was near the transition zone between D3 and D4, Pawnee was under D3, and Wister was under D1. The spatial pattern of SMEI-1 was in general compliance with the USDM, with the largest values of −0.41 estimated at Wister (Figure 2.7). The Z-Index followed a similar trend. However, the Z-Index had a value of −3.0 at Wister, indicating extreme drought conditions (Karl, 1986). SWDI reflected an intensification of drought moving from Wister to Hollis but a less severe drought for Goodwell. The NSM showed non-drought condition at Goodwell, mainly due to the fact that aggregated soil moisture for July 2011 merely deviated from the long-term mean. Therefore, it was not able to detect the drought.

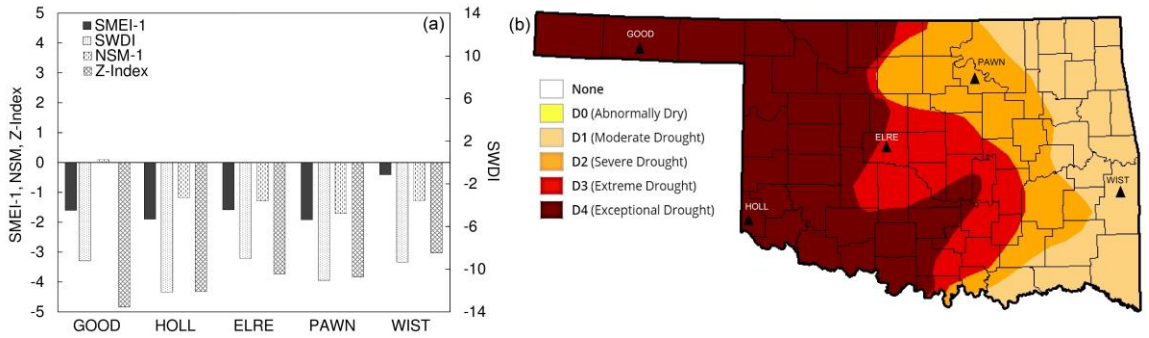

Figure 2.7. Magnitudes of selected drought indices for July 2011 at five individual study sites (a) and the corresponding USDM map (b).

2.3.5. Comparison with crop production

When considering the entire winter wheat growing season, SMEI had the strongest correlations with crop production in comparison to existing drought indices at all sites (Figure 2.8). The ranges of r were 0.41–0.79, 0.20–0.73, 0.37–0.69, and 0.35–0.64 for SMEI-1, Z-Index, SWDI, and NSM-1, respectively. These results were in agreement with previous studies. For example, Z-Index had r values as high as 0.65 when compared with the wheat yield in varying climates using modeled data embedded in the 0.5° grid (Vicente-Serrano et al., 2012). In addition, Carrão et al. (2016) compared the remote sensing-based SM drought index with non-irrigated wheat yield from a humid region in South America for a complete growing season and found an r value of 0.82. Also, a general spatial trend was noted in examining correlation coefficients among drought indices and winter wheat yields, indicating a weakening of the correlation moving from the semi-arid Panhandle to more humid regions (Figure 2.8). This spatial variation was most probably due to the fact that winter wheat production is more sensitive to drought conditions in water limited environments, as root zone water availability is the major limiting factor for crop growth in rain-fed agriculture (Aggarwal, 2009). The spatial trend was in accordance with the findings of Tian et al. (2018) who compared the winter wheat yield from Texas and Oklahoma with multiple drought indices (including Z-Index) and found stronger correlations ($r > 0.5$) in the western parts of the study area and weaker correlations towards the east.

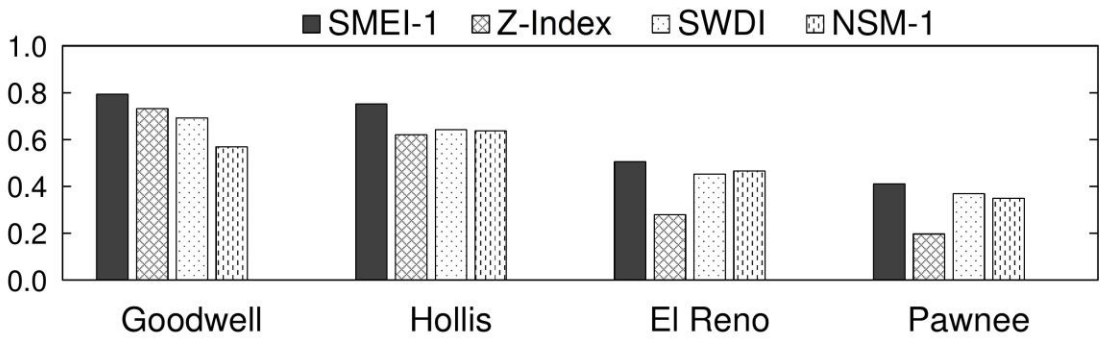

Figure 2.8. Correlation coefficients of existing indices and Soil Moisture Evapotranspiration Index (SMEI) with winter wheat production during the growing season at Goodwell (a), Hollis (b), El Reno (c), and Pawnee (d).

Comparatively larger correlations of SMEI-1 showed that the newly developed index is a useful tool for decision makers and growers to monitor drought variability and its effect on the production of winter wheat. However, the winter wheat farmers in Oklahoma would also be interested to know if they possibly could predict the anticipated yield in case of occurrence of droughts in those months that are critical for the crop growth, as they have to make important decisions by the spring period regarding grain production or utilizing the crop for grazing (Doye et al, 2018). The correlation analysis conducted between winter wheat production and the spring period's (March and April) drought indices values showed that the SMEI-1 had the largest correlations (Figure 2.9). For example, very high correlation was found at Goodwell with an r value of 0.92, whereas high (0.72) to moderate (0.61) correlations were noted for Hollis and El Reno, respectively, and weaker correlations (0.35) were noted for Pawnee. Narasimhan and Srinivasan (2005) also analyzed the impact of drought on the winter wheat yield for the same crop growth period in Texas by using SM and ET deficit based indices and found high correlations ($r > 0.75$). These findings suggest that SMEI-1 could be suitable for predicting winter wheat production in drought-prone areas of Oklahoma.

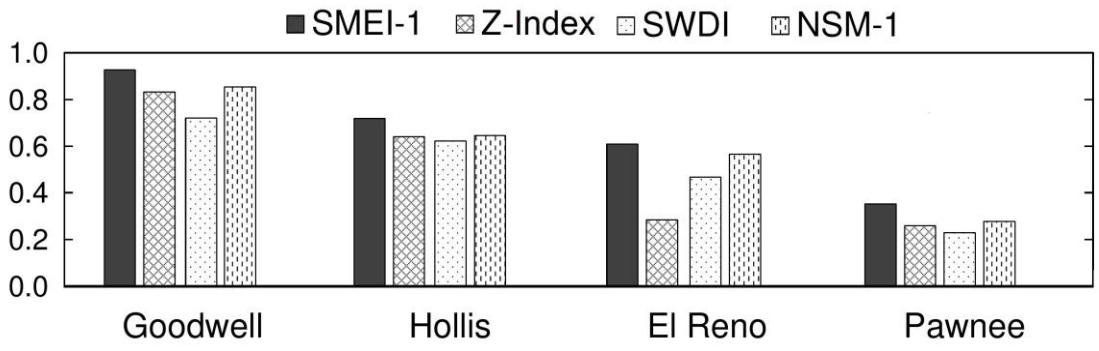

Figure 2.9. Correlation coefficients of existing indices and SMEI with winter wheat production during the spring period (months of March and April) at Goodwell (a), Hollis (b), El Reno (c), and Pawnee (d).

2.4. Conclusions

Considering the need for an improved drought monitoring tool for Oklahoma, a new agricultural drought index—the Soil Moisture Evapotranspiration Index (SMEI)—was introduced and evaluated in this study. It was estimated as the normalized difference of monthly root-zone soil moisture and reference evapotranspiration (ETr). The SMEI was estimated along with several existing soil moisture (SM) based and meteorological indices during the 2000–2016 period at five sites across Oklahoma, U.S., with variable climatic conditions. The SMEI had strong correlations with existing SM indices. The correlations between SMEI and meteorological drought indices were 33% stronger on average when compared to existing SM indices. Higher correlation coefficients of SMEI were observed at all study sites, suggesting that SMEI performs well under variable climatic conditions experienced across Oklahoma. The correlation coefficients between existing SM and meteorological indices found in the present study were similar to those reported previously.

The SMEI could capture temporal variations in drought and provided better response to the variation in drought magnitude in Oklahoma when compared to other indices. This can be

attributed to the inclusion of ET with soil moisture, which improved the drought sensitivity of the index. In addition, SMEI had a better performance capturing the spatial variations in drought when compared to other indices and the maps developed by the U.S. Drought Monitor.

In general, the correlation of drought indices with the yield of winter wheat gradually reduced when moving from the semi-arid Panhandle to more humid southeast. In comparison to other indices, however, the SMEI had the strongest correlations during the critical wheat growth stages in spring ($r > 0.9$). These results suggest that SMEI can be used more effectively to demonstrate the progress of agricultural drought under varying climates and its impacts on the crop yields. Farmers could also potentially optimize their decision making for the best use of their crops according to the predicted yield beforehand during the early crop growth stages.

The newly introduced index (SMEI) in this study was calculated using in-situ soil moisture measurements and weather data. Measured soil moisture data may not be available for all places and periods of interest. However, widely available remotely sensed and/or modeled soil moisture data can be used in calculating SMEI if measured data are not available. Future studies must analyze the effectiveness and the sensitivity of SMEI over longer periods and under different climatic conditions than those of this study.

CHAPTER III

THE EFFECTS OF PLANTING DATE AND WATER AVAILABILITY ON DRYLAND AND IRRIGATED WINTER WHEAT IN OKLAHOMA

3.1. Introduction

The Great Plains (GP) region produces more than 60% of the total wheat grown in the United States and is considered the breadbasket of the country (Paulsen and Shroyer, 2008). This region is also prone to regular droughts (Schubert et al., 2004). This makes dryland wheat production, which is dominant in the GP (Salmon et al., 2015), susceptible to precipitation deficits and heat stress (Rippey, 2012). With almost 9 million hectares (Mha) planted annually under winter wheat, the southern part of the GP is the world's largest drought-prone contiguous wheat cultivation region (Fischer et al., 2014). The main wheat farming states in the southern GP are Oklahoma, Texas, and Kansas, producing an annual amount of about 14 million metric tons of wheat.

Oklahoma holds about 40% of the total wheat planted area in the southern GP. Winter wheat, the most widely grown crop in the state (63% of total cropped area), experiences intermittent yield declines due to inconsistency in precipitation amounts and distributions during growing season (Tian et al., 2018; Mesonet, 2011). The wheat belt in Oklahoma is located across the north-south transect of central-western regions, overlaying an area of 3.9 Mha (USDA, 2018a). The average annual precipitation across this region ranges from about 300 to 600 mm and the temperatures are usually cool in the fall and spring period, with dry and cold winters and typically hot summers.

These climate characteristics provide suitable conditions for winter wheat production (McPherson et al., 2007; SIPMC, 2005). However, the recurrent drought episodes develop unfavorable environments that impinge the wheat yield, causing major financial losses. The average yield in Oklahoma is approximately 3.0 tons ha^{-1}, which is considerably smaller than the reported average potential yield of 8.0 tons ha-1 (Lollato et al., 2017). Some of the key factors governing the winter wheat production are precipitation, temperature, and soil water content at the time of sowing (GRDC, 2016). As a result, planting date plays an important role in defining winter wheat production (Epplin and Peeper, 1998). Planting too early or too late can have implications for crop yield, especially for Oklahoma, where temperature and precipitation anomalies amid drought episodes have historically impacted crop growth (Greene and Maxwell, 2007). Under such conditions, it is important to better understand the yield projections under different sowing dates and soil water content at planting. Furthermore, the occurrence of water and temperature induced stresses during different crop growth stages and their overall impact on crop yield needs to be thoroughly investigated. The decision to irrigate the wheat crop for potentially maximizing the yield and profit (Ziolkowska, 2017) also requires a comprehensive knowledge of crop yield response to irrigation.

Crop growth modeling can offer great help in understanding the dynamics of wheat yield pertinent to weather variations. Models can simulate the impact of weather anomalies on the crop and provide a basic assessment of crop damages. Policymakers and government agencies can use this information to make important monetary decisions related to subsidies and financial assistance to help farmers suffering from natural calamities (Imhoff and Badaracoo, 2019; Farhangfar et al., 2015). Drought preparedness of the farming community can be improved by using models to perform agricultural drought-risk assessment, thus mitigating the impacts of succeeding economic drought (Iglesias et al., 2009; Motha, 2011). In addition, crop modeling can

be considered as a practical tool that requires less operational cost and time in comparison to field experiments.

Several models have been previously developed to simulate wheat growth and yield, ranging from simple to complex mechanistic models (Liu et al., 2016; Silvestro et al., 2017; Lollato et al., 2017). A balance between complexity and accuracy is desirable for better adoptability of crop models (Monteith, 1996). Among the repository of complex and simple models, the AquaCrop model overlaps the domain of intermediate complexity that also provides good usability (Heng at al., 2009). Its user-friendly and practitioner-oriented interface allows for a wider utilization by experts (Steduto et al., 2009; Raes et al., 2009a). In addition, AquaCrop has been particularly designed to assess crop response towards water availability and can be potentially implemented in drought-susceptible regions like Oklahoma to investigate the impacts of water scarcity and extreme temperatures on wheat crop.

A number of previous studies have employed AquaCrop for winter wheat simulations. Iqbal et al. (2014) used AquaCrop for regional yield simulation in the North China Plain and suggested the application of the model for analyzing the constraints that limit crop production and water productivity. Xiangxiang et al. (2013) applied this model in the Loess Plateau in China to assess the water stress response of winter wheat at different growth stages under both rainfed and irrigated conditions and found that the model performed well, even with minimal input data. Impacts of sowing dates and irrigation management on winter wheat yield in central Morocco were simulated by Toumi et al. (2016). Their results showed that AquaCrop is a useful tool to improve the cultivation practices of winter wheat and to estimate the grain yield losses caused by water deficiency. Celik et al. (2018) evaluated AquaCrop in a semi-arid region of central Turkey and found the results to be highly accurate for estimating winter wheat yield and biomass.

Despite the advantages of AquaCrop compared to other models and its ability to simulate the response of winter wheat to several environmental factors, to the best of our knowledge, it has not been previously calibrated and validated for winter wheat simulation in the southern GP. Hence, there is a need to evaluate the performance of this model in the region and specifically Oklahoma, where winter wheat is the dominant crop. In addition, other models (e.g. DSSAT, SSM-Wheat, and APSIM) that have studied winter wheat in the southern GP have not investigated the combined effects of variable planting dates and soil water content at the time of planting (Greene and Maxwell, 2007; Dhakal et al., 2018; Lollato et al., 2017; Araya et al., 2019). However, these combined effects demand detailed investigation as they have a considerable influence on the yield of dryland winter wheat, particularly during drought periods (Pennington, 2017). Zhang et al. (2009) and Changhai et al. (2010) emphasized the importance of soil water storage at the time of sowing and its effects on the wheat grain production to cope with dry spells in the growing season. Moreover, Li and Shu (1991) reported more than 40% contribution of root zone soil moisture at the time of planting in governing wheat yields. Another gap in the knowledge is the role of irrigation in supporting drought-stricken wheat yields as only a few crop modeling studies have looked into this domain in the southern GP. For example, Araya et al. (2019) estimated the irrigation water productivity under various irrigation capacities for winter wheat in Kansas using the APSIM model, but the interlinkage of winter wheat yield and irrigation with respect to different sowing dates has not been studied before in this region. In the southern GP, where droughts are a recurrent feature of the climate, irrigation is pivotal to save the crop from failure (Doughty et al., 2018; Ziolkowska, 2017). Therefore, there is a need to conduct simulation studies to evaluate the effects of planting date, soil water content at planting, and irrigation on the growth and yield of winter wheat in the southern GP. Such studies must be conducted using calibrated and validated crop models over long-term periods to capture the interannual climate variabilities (Ruane et al., 2016).

The objectives of the present study were to i) calibrate and validate the AquaCrop model for simulating winter wheat production using measured data at four sites in Oklahoma; ii) use the calibrated model to assess the combined effects of variable planting dates and soil water content at planting on winter wheat yield; and, iii) compare the dryland and irrigated yields for assessing the potential of irrigation to safeguard the crop from water stress and calculate irrigation water productivity under various planting windows.

3.2. Materials and Methods

3.2.1. Study sites

The experimental data from Lollato et al. (2015) was used in the present study for AquaCrop calibration and validation. The experiments were conducted at four research fields near Stillwater (STIL), Perkins (PERK), Chickasha (CHIC), and Lahoma (LAHO) in central and northcentral Oklahoma (Figure 3.1) during 2012-2013 and 2013-2014 growing seasons. The location of these sites was within the range of Oklahoma's wheat belt. The goal of the experiment was to investigate the maximum attainable wheat yield under dryland and irrigated conditions. Soil types at study sites were loam sandy loam, and silt loam. The 30-year average total growing season (September to June) precipitation has a range of 613-743 mm among the mentioned sites and reference evapotranspiration varies between 969 and 1060 mm (McPherson et al., 2007). During the growing period of 2012-2013, no significant drought was experienced, whereas in 2013-2014 severe drought events were recorded amid wheat flowering and grain filling stages. Detailed site characteristics are available with Lollato et al. (2015).

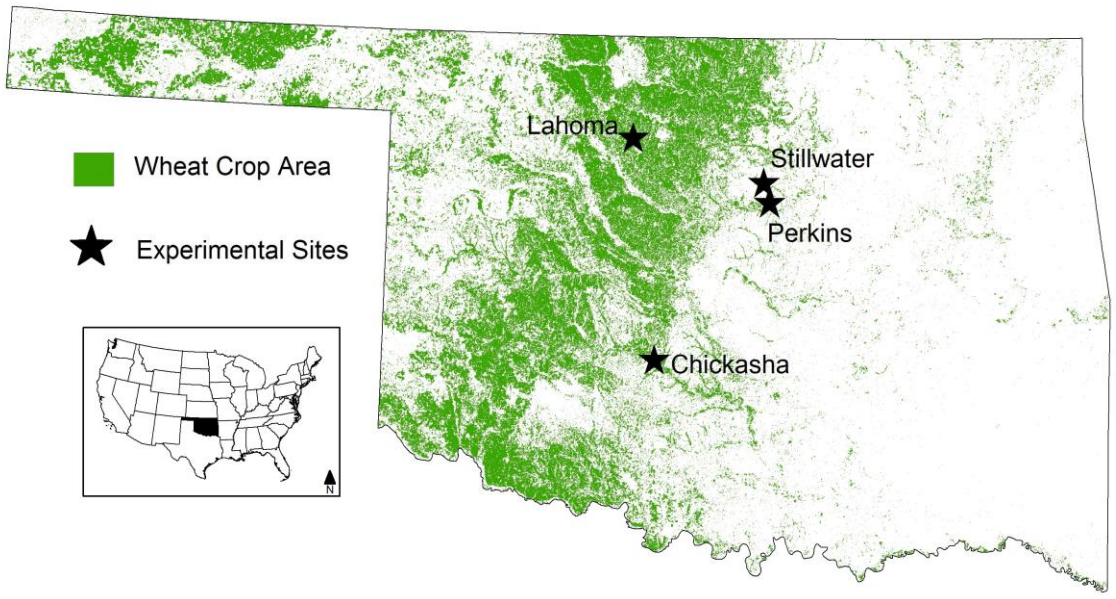

Figure 3.1. Location of four experimental sites in Oklahoma. Wheat crop area represents the cumulative crop data layers from 2008 to 2018 (USDA, 2018a)

3.2.2. Crop and Irrigation Management

Winter wheat cultivar Iba was sown at all experimental fields with row spacing of 17 cm and planting density of 67 kg ha^{-1}. The planting was done between 5 and 22 October for both 2012-2013 and 2013-2014. Fertilizer application along with weed and pest control were performed in a way that these factors could be considered non-limiting for wheat yield. At the irrigated fields of Stillwater and Perkins, irrigation was applied using overhead sprinkler to replenish soil water content (SWC) up to field capacity (FC) with a water stress threshold of 50% available water holding capacity. Four replications of neutron probes were installed in each field and SWC measurements were taken at 10, 30, 50, 70, 90, and 110 cm with 2 to 3 weeks interval during the growing season. Neutron probes were calibrated for both dry and wet soil conditions by taking soil cores, and the SWC was estimated using the gravimetric method. Crop development data collected during the experiment included leaf area index (LAI), canopy cover (CC), time of

occurrence of major development stages, and the biomass. Grain yield was estimated using three sub-samples for each experimental field with almost 20 m^2 harvested area (12 representative samples of grain yield each year). Additional details on crop and irrigation management are provided in Lollato et al. (2015).

3.2.3. AquaCrop Model

AquaCrop v6.1 was used in this study. Concepts and working mechanisms of AquaCrop model have been described in detail by Steduto et al. (2009) and Raes et al. (2009a). CC is the main governing factor in AquaCrop that translates the foliage development in crop. The AquaCrop simulates the daily water balance by differentiating between transpiration (T_r) and soil evaporation (E). When there is no crop stress related to water, fertilizer, and/or weeds, the amount of T_r is considered proportional to CC. In case of limited water availability, stress coefficients are applied to increase stomatal closure, reduce canopy development, and trigger early senescence. These stress coefficients cause reduction in T_r that directly impacts the biomass estimations of Aquacrop as the model computes the biomass production as a function of the T_r to grass-based reference ET (ET_o) (Steduto et al., 2009):

$$B = WP^* \times \sum\left(\frac{T_r}{ET_o}\right) \quad (1)$$

where WP* is water productivity normalized for climate and CO_2 and remains valid in diverse climates and locations (Steduto et al., 2007; Vanuytrecht et al., 2014). During the simulations, WP* is duly adjusted for atmospheric CO_2, type of products synthesized, and fertility level of soil. Eventually, crop yield (Y) is estimated as (Hsaio et al., 2009):

$$Y = B \times HI \quad (2)$$

where B is biomass and HI is harvest index, calculated as the ratio of grain yield to aboveground dry biomass, and it is adjusted by model with respect to environmental variables.

3.2.4. Model calibration and validation

The AquaCrop model was calibrated for winter wheat by the trial-and-error method following the guidelines and steps explained by Steduto et al. (2012). From the experimental datasets of 2012-2013 and 2013-2014 growing seasons, the calibration was performed for three dryland and one irrigated site, and validation was done for four dryland and two irrigated sites. The adjusted parameters were growing degree days (GDD), maximum canopy cover (CCx), canopy growth coefficient (CGC), canopy decline coefficient (CDC), normalized water productivity (WP*) and reference harvest index (HI_o) (Table 3.1). The tuning of GDD, CCx, CGC, and CDC was based on field observations. The WP*, a conservative parameter, was increased from 15 to 17 g m^{-2}, which was still within the range of WP* for C3 crops (15-20 g m^{-2}) in AquaCrop model. Additionally, this adjustment was in line with several previous AquaCrop winter wheat studies that increased WP* in their simulations (Xianhxiang et al., 2013; Khordadi et al., 2019; Ahmad et al., 2020; Bouras et al., 2019). HI_o was decreased from the default 48% to 40% following Lollato et al (2015), who linked the smaller harvest index of hard red winter wheat grown in the southern GP with higher protein concentration and warmer grain filling period in comparison to wheat grown in European regions. Raes et al. (2009b) categorized HI_o as cultivar specific parameter, and it varied from 36% to 51% in other AquaCrop based wheat simulation studies (e.g., Celik et al., 2018; Andarzian et al., 2011; Khordadi et al., 2019; Xiangxiang et al., 2013; Iqbal et al., 2014; Jin et al., 2014).

Table 3.1. Crop and soil parameters used in AquaCrop simulation for winter wheat

Crop parameters	**Value**	**Calibration**
Base temperature (°C) below which crop development does not progress	0	Default
Upper temperature (°C) above which crop development no longer increases with an increase in temperature	26	Default
GDD from sowing to emergence	104	Adjusted
GDD from sowing to maximum rooting depth	847	Adjusted
GDD from sowing to start senescence	1804	Adjusted
GDD from sowing to maturity (length of crop cycle)	2242	Adjusted
GDD from sowing to flowering	1493	Adjusted
GDD Length of the flowering stage (growing degree days)	78	Adjusted
GDD building-up of Harvest Index during yield formation	700	Adjusted
Maximum effective rooting depth (m)	1.5	Default
Water Productivity normalized for ET_o and CO_2 (WP*) (g/m^2)	17	Adjusted
Reference Harvest Index (HI_o) (%)	40	Adjusted
Maximum canopy cover (CCx) (fraction soil cover)	0.99	Adjusted
Canopy growth coefficient (CGC) Increase in canopy cover (fraction soil cover per day)	0.006444	Adjusted
Canopy decline coefficient (CDC) Decrease in canopy cover (fraction per day)	0.006847	Adjusted
Minimum/Maximum air temperature below/above which pollination starts to fail (cold stress/heat stress) (°C)	5/35	Default
Soil water depletion factor for canopy expansion (p-exp) - Upper threshold/ Lower threshold	0.2/0.65	Default
Shape factor for water stress coefficient for canopy expansion	5	Default
Soil water depletion fraction for stomatal control (p - sto) - Upper threshold	0.65	Default
Shape factor for water stress coefficient for stomatal control and canopy senescence	2.5	Default
Soil water depletion factor for canopy senescence (p - sen) - Upper threshold	0.7	Default
Soil water depletion factor for pollination (p - pol) - Upper threshold	0.85	Default
Maximum root water extraction (m^3 water/m^3 soil.day) in top/ bottom quarter of root zone	0.048/ 0.012	Default

Model accuracy and performance was validated based on the model's ability to simulate CC, SWC, biomass, and grain yield. Four statistical performance parameters were used to scale the level of accuracy achieved during the validation phase. These parameters include: The Root Mean Square Error (RMSE), normalized RMSE (nRMSE), the Nash-Sutcliffe Efficiency (NSE), and the index of agreement (d) and were calculated as:

$$RMSE = \sqrt{\sum_{i=1}^{n} \frac{1}{N} (M_i - S_i)^2} \quad (3)$$

$$nRMSE = \frac{RMSE}{\bar{S}} \times 100 \quad (4)$$

$$NSE = 1 - \frac{\sum_{i=1}^{n} (M_i - S_i)^2}{\sum_{i=1}^{n} (M_i - \bar{M})^2} \quad (5)$$

$$d = 1 - \frac{\sum_{i=1}^{n} (M_i - S_i)^2}{\sum_{i=1}^{n} (|S_i - \bar{S}|) + (|M_i - \bar{M}|)^2} \quad (6)$$

where M_i and S_i are the measured and simulated values, respectively, N is the number of measurements, $\bar{M}$ is the mean value of M_i, and $\bar{S}$ is the mean value of S_i.

The RMSE measures the deviation of the simulated data from the measured data with values near zero indicating good performance of the model and good agreement between the simulated and measured data. nRMSE allows comparing the model's performance between different regions and climates. NSE is a normalized statistical indicator that assesses the residual variance of simulated values in comparison to the measured data variance on a relative scale (Nash and Sutcliffe, 1970). Values of NSE range between -∞ to 1.0 (1 inclusive). Values ranging between 0.0 and 1.0 correspond to satisfactory model performance, whereas values below zero show poor performance (Marek et al., 2017). The index of agreement (d) was developed by Willmott (1981) as a "standardized measure of the degree of model prediction error" (Moriasi, 2007), ranging between 0 and 1. Zero indicates no agreement and one indicates a perfect agreement between the modeled and observed values. The AquaCrop manual suggested six categories of model performance, varying from very poor to very good, based on the ranges of estimated nRMSE, NSE, and d (Raes et al., 2018). The same categories were adopted here in interpreting model performance.

3.2.5. Model Application

The calibrated AquaCrop model was run for a 25-year period (1994-2019) to investigate the impacts of variable planting dates and SWC at sowing on winter wheat yield under dryland and irrigated conditions at STIL, CHIC, and LAHO. PERK was dropped from the application analysis because of its close proximity to STIL. The simulated scenarios included five planting dates of 15 Sep., 25 Sep., 5 Oct., 15 Oct., and 25 Oct., as winter wheat is usually planted during September and October in Oklahoma. In addition, three levels of initial SWC (the time of sowing) was considered for the dryland simulations as 40% of the total available water (TAW), 70% of TAW, and 100% of TAW, representing extreme, mild, and no water stress conditions, respectively. For irrigated simulations the initial soil moisture condition was assumed to be at FC since starting the season with SWC deficiency would have triggered an immediate irrigation event. A depletion factor of 0.55 was used for initiating irrigation by the model to maintain sufficient TAW in the root zone for wheat as suggested by Allen et al. (1998). Weather database of Oklahoma Mesonet was used for this study (McPherson et al., 2007). The irrigation water productivity (IWP) was estimated based on the yield gap between irrigated and dryland winter wheat (kg ha^{-1}) and the volume of applied irrigation water (m^3 ha^{-1}), similar to Araya et al. (2019):

$$IWP = \frac{Irrigated\ Yield - Dryland\ yield}{irrigation\ applied} \quad (7)$$

3.3. Results and discussion

The performance of the model in simulating soil water content, canopy cover, above-ground biomass, and grain yield was evaluated during model validation. The results are presented in the following sections.

3.3.1 Soil water content

The validation results showed that the performance of AquaCrop was adequate to model the soil water content (SWC). In general, the model followed the fluctuation in SWC and responded to the precipitation or irrigation events. Figure 3.2 presents the two examples of the SWC timelines for sites with the largest and smallest nRMSE. The estimated RMSE, nRMSE, NSE, and d had ranges of 15-32 mm, 5-14%, 0.34-0.75, and 0.63-0.94, respectively (Table 3.2). The ranges of nRMSE, NSE, and d indicated model's performance as good to very good, moderate poor to good, and moderate poor to very good, respectively. Also, these indicators concurred with RMSE, nRMSE, NSE, and d ranges of 6-38 mm, 8-14%, -2.62-0.98, and 0.36-0.9, respectively, reported in previous SWC simulations by AquaCrop (Zhang et al., 2013; Iqbal et al., 2014; Xiangxiang et al., 2013; Toumi et al., 2016).

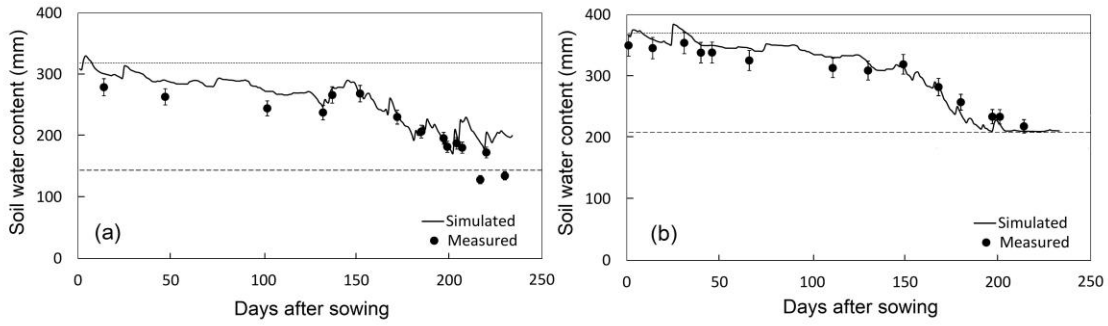

Figure 3.2. Simulated and observed soil water content at (a) the site with the largest nRMSE (PERK Irrigated 2013-2014) and (b) the site with the smallest nRMSE (STIL Dryland 2013-2014). Dotted line represents field capacity and dashed line shows the wilting point. Error bars represent 5% error.

Table 3.2. Validation results for simulated soil water content.

Site	Management	Year	RMSE (mm)	nRMSE (%)	NSE	d
STIL	Dryland	2012-2013	25	12	0.34	0.63
	Dryland	2013-2014	15	5	0.90	0.98
PERK	Irrigated	2012-2013	25	11	0.57	0.81
	Irrigated	2013-2014	32	15	0.54	0.87
	Dryland	2013-2014	25	14	0.75	0.94
LAHO	Dryland	2012-2013	26	10	0.50	0.84

Several reasons could contribute to the mismatch between measured and simulated SWC, such as soil heterogeneity among SWC measurement locations. Also, the soil water balance calculations of AquaCrop initiate drainage when the SWC is at or above the field capacity (Raes et al., 2018); nonetheless, the drainage might have already started before the drainable soil pores are completely filled (Zeleke et al., 2011). The occurrence of preferential flow could be another cause of discrepancies (Ahmadi et al., 2015).

3.3.2 Canopy cover

The modeled CC fitted the observed values well except for the overwintering period. This can be observed in Figure 3.3, which shows simulated and observed CC timelines of treatments with the largest and smallest nRMSE. The ranges of RMSE, nRMSE, NSE, and d were 7-23%, 9-59%, 0.33-0.90, and 0.83-0.97, respectively (Table 3.3). Model's performance to simulate CC can be interpreted as very poor to good, moderate poor to very good, and good to very good based on the estimated nRMSE, NSE, and d, respectively. The validation statistics for CC were comparable with previous studies that reported RMSE, nRMSE, NSE, and d ranges of 2-7%, 4-17%, 0.66-0.99, and 0.25-0.98, respectively (Zhang et al., 2013; Toumi et al., 2016; Salemi et al., 2011; Jin et al., 2014, Celik et al., 2018).

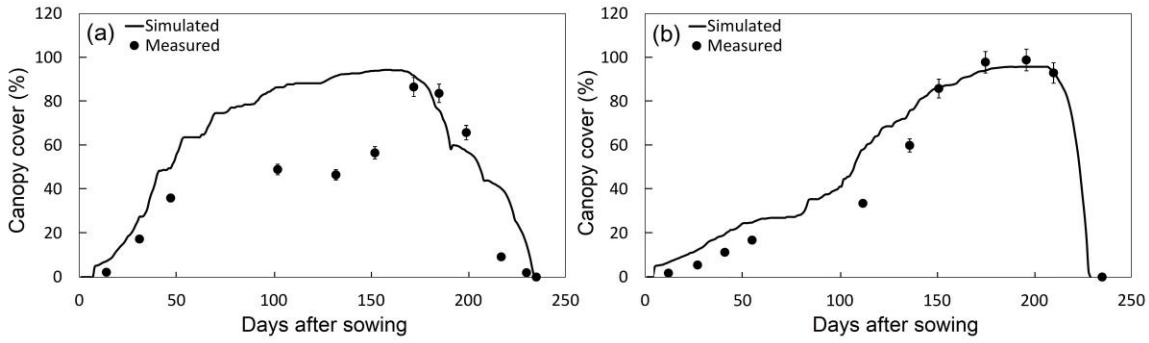

Figure 3.3. Simulated and observed canopy cover at (a) the site with the largest nRMSE (PERK Dryland 2013-2014) (b) the site with the smallest nRMSE (STILL Dryland 2012-2013). Error bars represent 5% error.

Table 3.3. Validation results for simulated canopy cover.

Site	Management	Year	RMSE (%)	nRMSE (%)	NSE	d
STIL	Dryland	2012-2013	7	9	0.95	0.99
	Dryland	2013-2014	22	43	0.57	0.91
PERK	Irrigated	2012-2013	11	15	0.90	0.97
	Irrigated	2013-2014	23	41	0.54	0.89
	Dryland	2013-2014	24	59	0.33	0.84
LAHO	Dryland	2012-2013	22	43	0.52	0.83

An overall overestimation of CC was noted between winter and early spring, which has also been reported by the Xiangxiang et al (2013) and Zhang et al (2013). A plausible explanation of this overestimation is that instead of simulating restricted growth during the overwintering period of winter wheat, AquaCrop estimates near-normal growth of CC due to lack of sophistication to simulate this physiological process. In the SGP, winter wheat acclimates to low temperature (cold tolerance) by slowing down its growth during the winter period (Lu et al., 2017), and not capturing this phenomenon causes discrepancy in CC simulations. Larger over-prediction of CC was noted for 2013-2014 in comparison to 2012-2013 treatments. This difference was most likely due to comparatively colder conditions in the former growing season as the average winter temperature was 4^{o} C less than 2012-2013 winter, causing longer-than-usual overwintering.

The simulations of SWC and CC were not precise due to previously mentioned issues and it also impacted the intermediate AGB values. The model calculation discrepancies, however, were equalled out in the final AGB and the same was noted for grain yield predictions. The validation results of AGB and grain yield are described as follows:

3.3.3 Above ground biomass

The final AGB was in compliance with the observed values, with RMSE, nRMSE, NSE, and d values of 0.80 Mg ha^{-1}, 5%, 0.95, and 0.99, respectively. As benchmarks, all indicators suggest the model performance can be interpreted as very good. Hence, the simulation results of the final AGB were satisfactory. In addition, they corresponded well with previous studies (i.e. Salemi et al., 2011; Andarzian et al., 2011; Xiangxiang et al., 2013; Zhang et al., 2013; Iqbal et al., 2014; Jin et al., 2014; Toumi et al., 2016; Celik et al., 2018) with reported RMSE, nRMSE, NSE, and d ranges of 0.16-1.84 Mg ha^{-1}, 3%-9%, 0.92-0.99, and 0.22-0.98, respectively.

3.3.4 Grain yield

The simulated and observed grain yield data were in agreement, with RMSE, nRMSE, NSE, and d estimates of 0.5 Mg ha^{-1}, 9%, 0.91, and 0.98, respectively. According to interpretations suggested by AquaCrop, these values indicate good to very good model performance. The statistical indicators also concurred with those reported in previous studies that employed AquaCrop for winter wheat yield predictions. The RMSE, nRMSE, NSE, and d values in these studies had ranges of 0.1-1.44 Mg ha^{-1}, 5-8%, 0.95-0.98, and 0.82-0.90, respectively (Salemi et al., 2011; Andarzian et al., 2011; Xiangxiang et al., 2013; Zhang et al., 2013; Iqbal et al., 2014; Jin et al., 2014; Toumi et al., 2016; Celik et al., 2018; Khordadi et al., 2019). These results show that the AquaCrop model can be effectively used for simulating the grain yield in the winter wheat belt of Oklahoma.

3.3.5. Model application

3.3.5.1. Dryland yields

The yields of dryland winter wheat simulated by AquaCrop during the 25-year (1994-2019) period of model application were generally comparable with those measured at Oklahoma Agricultural Experimental Stations at CHIC and LAHO for dryland winter wheat planted mostly in October (Marburger et al., 2018). The range of simulated yields under all planting date and initial SWC scenarios was zero to 8.35 Mg ha^{-1} in the present study, similar to the range of zero to 7.63 Mg ha^{-1} measured over the period of 2000-2008. Lollato et al. (2017) simulated the long-term (1986–2016) dryland winter wheat yield using SSM-Wheat crop model for multiple sites in Oklahoma and Kansas. Their modeled yield range (1.2-9.3 Mg ha^{-1}) was similar to this study's too.

3.3.5.2. Effects of planting date on dryland yield

Under no water stress at sowing (SWC at 100% of TAW), October planting dates provided larger dryland yields of winter wheat, especially at STILL and CHIC, where average October yields varied between 6.2 and 6.9 Mg ha^{-1} (Figure 3.4a-c). The average yields were smaller for September planting at these two sites and the ranges of simulated yields were also expanded. At LAHO, which is located farther west, the difference between September October sowing yields were smaller. However, the average yield of the best performing sowing date was also smaller than STILL and CHIC. The same pattern of improved yield with October planting was observed under two levels of SWC deficit at sowing, namely 70% and 40% of TAW. The identified favorable planting window in the present study was in accordance with the findings of field experiments conducted by Epplin and Peeper (1998) and Hossain et al. (2003), who found larger yields for winter wheat that was grown during October in Oklahoma. Furthermore, a farmers' survey demonstrated that the optimal sowing of winter wheat in Oklahoma ranged between 28-

Sep. and 16-Oct. for farmers focusing particularly on grain harvest (Epplin et al., 1998).

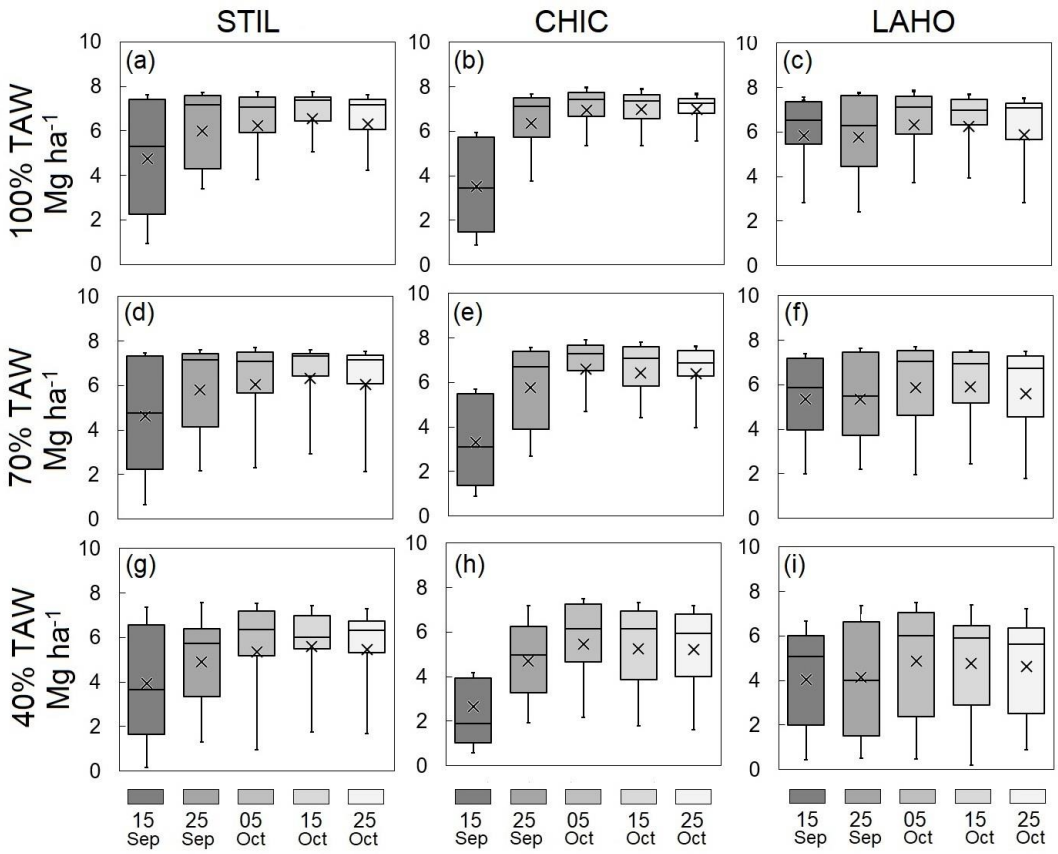

Figure 3.4. Simulated yields of dryland winter wheat at STIL, CHIC, and LAHO for five planting dates and three levels of soil water content at sowing (100%, 70%, and 40% of total available water). The whiskers show 10th and 90th percentiles.

The main reason for the smaller yield for winter wheat planted in September was the cold stress that affects the pollination. For example, the flowering period of the crop planted on 15 Sep at STIL faced near freezing temperatures in about half of the simulated seasons and consequently a reduction in harvest index. Nelly et al. (2014) discussed the reduction in wheat tolerance to freeze injury as it progresses towards flowering stage. In addition, reduction in the winter wheat grain yield because of the freeze damage at heading stage has been highlighted by Thapa et al (2020) for the southern GP, and the same has been reported from Australia for early-planted wheat crop (GRDC, 2016).

Although October planting dates outperformed September dates in terms of average dryland yield throughout the simulation period, the planting date that resulted in the largest crop yield had considerable interannual variation. This was especially the case during drought periods and could be attributed to fluctuations in temporal distribution of precipitation, a key factor that has been discussed by Edwards et al. (2006). At LAHO during the drought-stricken 2005-2006 season, for instance, senescence was triggered in early-March and before the flowering period for crop sown on 25-Sep. The sub-temporal analysis showed that the root zone SWC made available by late February precipitation events were consumed much faster in comparison to early October sowing. This caused a severe water stress and eventually early maturity was prompted. Winter wheat sown on 05-Oct, however, received 50% more precipitation by utilizing mid-March and early-April spells of rain. As a result, the crop survived and produced a larger yield compared to 25-Sep sowing, despite facing water scarcity that hindered canopy expansion. During the period of 2013-2014, considered as one of the worst seasons for winter wheat (Edwards et al., 2014), an inverse trend was noted as the 15-Sep crop received 65% more precipitation on an average compared to early-October planted wheat. This shows the uncertainty involved in decisions related to sowing time during drought years.

Figure 3.5 demonstrates the fraction of simulated seasons when each planting date resulted the largest dryland yields for each of the study sites and initial SWC scenarios. Under no-water-stress planting (100% TAW), 25-Sep and 05-Oct were the optimum planting dates at all three sites, outperforming other dates during 28 to 32% of the simulated seasons. The next best performing planting date was 15-Oct at STIL and CHIC and 15-Sep at LAHO. When the initial SWC was reduced to 70% and 40% of TAW (mild and severe water stress at sowing, respectively), 05-Oct provided the best yields most of the time at STIL and CHIC with 25-Sep ranked as second. However, at LAHO, 25-Sep was the lead planting date, generating the best yields for about 30% and 50% of the times under mild and severe initial water-stress, respectively. The second-best

planting date at LAHO was 05-Oct under mild initial water stress and 25-Oct under severe water stress. It should be noted that these results represent the ranking of planting dates based on the simulated yield. In some cases, the yield differences between the top few planting dates was small.

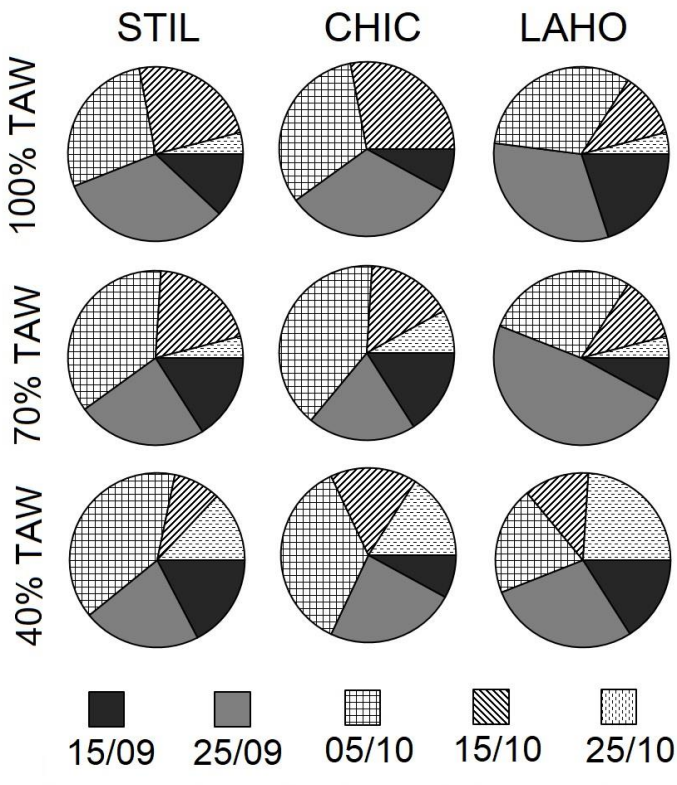

Figure 3.5. Fraction of times a planting date resulted the largest yield during the simulation period (1994-2019) at each site and under three levels of soil water content at sowing, namely 100%, 70%, and 40% of total available water (TAW).

3.3.5.3. Effects of initial soil water content on dryland yield

Simulated yields of winter wheat planted under mild water stress at sowing (70% TAW) were smaller than those planted under no water stress conditions (100% TAW). In comparison to no-water-stress planting, declines of 4%, 8%, and 7% were noted in the overall average yields at

STILL, CHIC, and LAHO, respectively (Figure 3.6). The higher sensitivity of LAHO to mild water stress at the time of sowing is mainly due to the fact that it is exposed to larger ET_o and smaller precipitation during the growing season. Therefore, mild water stress at the time of sowing had a considerable impact on the yields at this site, especially in drought seasons such as 2005-2006, 2010-2011, 2013-2014, 2017-2018. Further analysis of the root zone SWC at LAHO showed that during the aforementioned dry periods, the SWC for mild stress planting was generally 16% below no-water-stress sowing until the spring period. This limited water availability caused approximately 2.6 and 1.6 times larger canopy expansion stress and stomatal closure, respectively, in comparison to crop sown under 100% TAW.

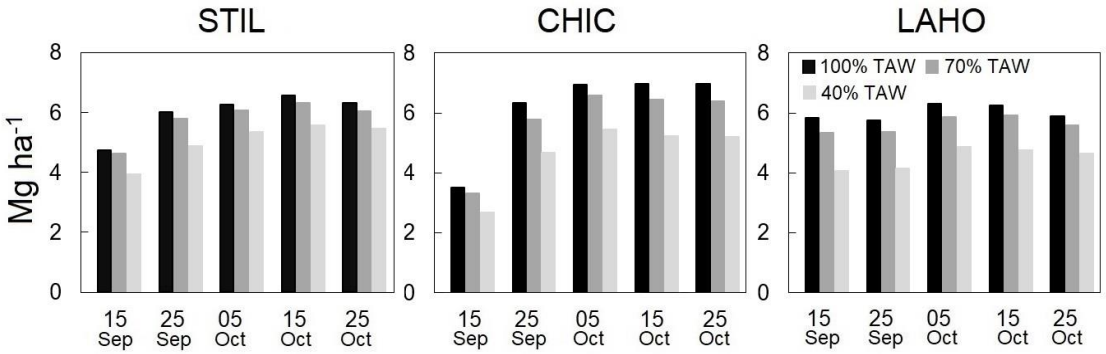

Figure 3.6. Averaged dryland winter wheat yield at STIL, CHIC, and LAHO under different soil water contents at sowing (100%, 70%, and 40% of total available water).

Reductions in yield were larger under severe water stress at sowing (40% TAW), with average declines of 19%, 32%, and 34% at STILL, CHIC, and LAHO, respectively. In general, the impact of severe moisture stress was larger for September sowing in comparison to October. The dry condition at the time of planting mainly affected the development of canopy cover, and initial growth was further curbed by negative precipitation anomalies in dry years that reduced the biomass production (Changhai et al., 2010). It is important to mention that the minimal threshold for Wheat germination is 20% TAW in AquaCrop. Therefore, the selected SWC levels at planting did not impact germination in the simulations. However, sowing in dry soil affects the emergence

rate and usually higher planting densities are recommended in dry periods to compensate the loss of seedlings (Pennington, 2017).

3.3.5.4. Irrigated yield

The average irrigated yields were 6.6, 6.4, and 7.0 Mg ha^{-1} at STIL, CHIC, and LAHO, respectively. These estimates were in agreement with the experimental irrigated yields in the region mentioned by Patrignani et al. (2014) as 6.59 Mg ha^{-1} for Oklahoma, 6.38 Mg ha^{-1} in Texas, 7.69 Mg ha^{-1} in New Mexico, 7.58 Mg ha^{-1} for Arkansas, and 7.46 Mg ha^{-1} for Kansas. Furthermore, Araya et al (2019) simulated the winter wheat yield using APSIM-Wheat model in Kansas and found yields reaching as high as 8.0 Mg ha^{-1} under sufficient nitrogen and irrigation supplies. In comparison to dryland yield with no water stress (100% TAW initial SWC) at sowing, irrigation increased the average winter wheat yields by 12%, 5%, and 16% at STIL, CHIC, and LAHO, respectively. The upper limit of irrigated yield, however, was almost the same as dryland yield. For October sowing dates, the impact of irrigation was more noticeable in comparison to the September planting dates (Figure 3.7). The increment in the yield difference between irrigated and dryland wheat sown under no water stress followed a linear trend with delay in planting dates. The average yield difference for 15-Sep planting was 0.28 Mg ha^{-1}, which increased to 0.96 Mg ha^{-1} for 25-Oct planting.

There were a few years among all planting dates when the dryland yield was slightly larger than the irrigated one. This was primarily due to the positive impact of mild water stress occurred during the yield formation period. During this phase, AquaCrop adjusted the reference harvest index upwards if the root zone depletion ranged between the lower and upper thresholds of canopy expansion stress (Raes et al., 2018). These adjustments were conducted to compensate for the remobilization of pre-anthesis assimilates for grain-filling purpose under water-stress conditions by dryland wheat (Inoue et al., 2004). It should be note that these physiological traits

are highly dependent on the drought resistance of the wheat variety (Sanjari and Yazdan, 2008) and more sophisticated crop models may be more suitable to accurately simulate such complex effects of dry spells.

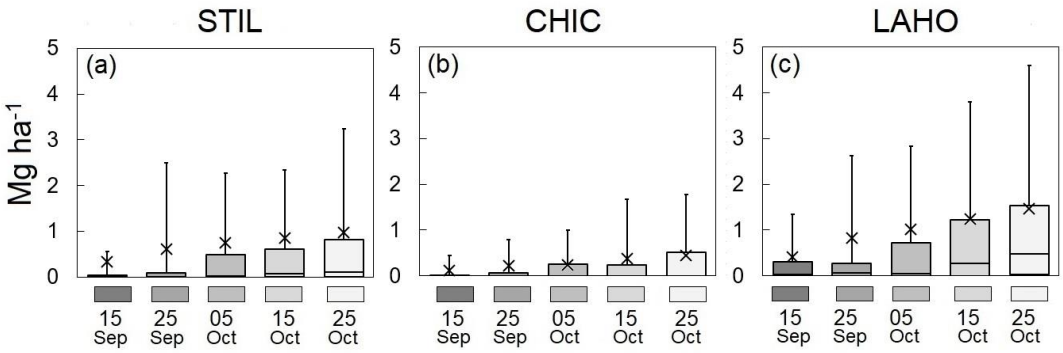

Figure 3.7. Yield difference between irrigated and dryland winter wheat yield at (a) STIL, (b) CHIC (c) LAHO.

3.3.5.5 Irrigation water productivity

The average seasonal irrigation application for STIL, CHIC, and LAHO was 104 mm, 118 mm, and 147 mm, respectively (Figure 3.8a-c). The irrigation application increased while moving from September planting dates towards October. The average increment for each two consecutive dates was 12 mm for STIL and 17 mm for both CHIC and LAHO. The average irrigation water productivity (IWP) ranged between 0.04 and 0.47 Kg m^{-3} (Figure 3.8d-e). IWP followed the same temporal trend as irrigation application and the beneficial role of irrigation was more prominent for winter wheat sown later. The IWP was also spatially variable. Among the October planting dates, the largest average IWP was 0.40 Kg m^{-3} at LAHO, followed by STIL (0.35 Kg m^{-3}) and CHIC (0.12 Kg m^{-3}). The observed differences in IWP can be attributed to higher aridity of LAHO. Moreover, soil hydraulic properties impact the IWP. For example, the soil profile at CHIC had a larger water holding capacity, which resulted in more efficient utilization of precipitation events and better dryland yields in comparison to STIL in most studied growing seasons.

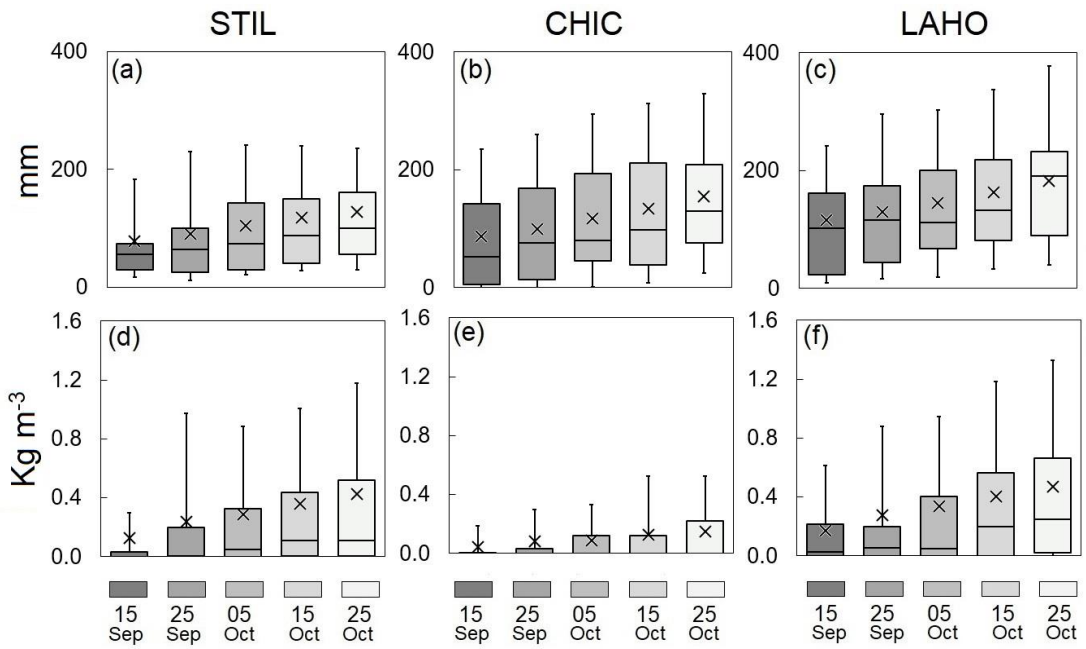

Figure 3.8. (a-c) Estimated irrigation amounts and (d-e) irrigation water productivities.

3.4. Conclusion

AquaCrop model was first calibrated and validated in this study to simulate the growth and yield of winter wheat. The model was then employed to run long-term simulations (1994-2019) at three sites across the wheat belt in Oklahoma. The AquaCrop validation results showed that this model can be used in the study area to simulate the winter wheat growth and grain yield. The overwintering phase of winter wheat was not satisfactorily simulated due to the intrinsic limitation of the crop model. However, AquaCrop accurately modeled soil water content, canopy cover, above-ground biomass, and yield at both dryland and irrigated sites.

The long-term application results revealed that grain yields were larger for October planting compared to September (about 40% on average). The early sown (mid-September) dryland wheat yield was greatly impacted by the lower temperatures during flowering stage, whereas favorable temperatures were noted for anthesis in October-planted winter wheat. 5-Oct was the most

optimum planting date in general for all study sites under all soil water contents at the time of planting, followed by 25-Sep. Soil water content deficiency at planting had a considerable impact on yield, especially at sites with higher aridity. On average, yield decreased by 25% when soil water content at planting decreased from 100% of the total available water to 40%. Irrigation improved the yields, especially in drought seasons, up to 16%. However, the upper limit of wheat yield stayed almost the same as dryland crop, indicating the limited role of irrigation in seasons that received ample precipitation. The irrigation water productivities were smaller for September-planted crop and increased with increasing delay in planting.

CHAPTER IV

SPATIAL MODELING OF WINTER WHEAT YIELD AND DROUGHT RESPONSE IN OKLAHOMA

4.1. Introduction

Drought is a recurrent climatic feature of the Southern Great Plains (SGP) of the U.S. and induces devastating impacts on regional agriculture. Historically, crop yields across the SGP have been frequently affected by drought events, and this has been especially the case for dryland crops that do not rely on irrigation to minimize adverse effects of dry spells. For instance, the recent drought of early 2018 resulted in 47% less winter wheat production Oklahoma, in comparison to the previous non-drought crop year (Marburger, 2018). Such a significant loss shows the drought susceptibility of winter wheat, a major crop in the region. The phenomenon of drought, in terms of its magnitude and duration, is highly variable both in space and time (Hansen and Jones, 2000). Similarly, the response of crops towards precipitation and temperature variation changes temporally and spatially and depends on various factors such as climate, soil properties, and topography (Basso et al., 2001).

Crop modeling is an effective tool to simulate the impacts of drought events on crops. However, modeling efforts are usually restricted to specific sites depending on the availability of data and the computational requirements. In order to have a holistic understanding of the effects of dry spells on the crop yield, it is important to apply the crop model across the drought-stricken region.

Grid-based crop modeling approaches provide a solution to this problem (Shelia et al., 2019; Motha, 2011) and can enable categorizing the region of interest into sub-areas based on the severity of simulated crop damages (Howitt et al., 2015). This not only helps in prioritizing the assistance efforts and strengthening the drought mitigation planning, but also allows farmer communities to optimize farm inputs based on the drought susceptibility of an area in relation to a specific crop. Furthermore, adaptation strategies to cope with changes in weather anomalies can be effectively developed based on the maps of crop yield response keeping in view the spatial and temporal distribution of drought (Thornton et al., 2009; Leng and Huang, 2017).

The process of developing and assimilating the gridded weather data into crop models is computationally expensive and comes with its own challenges (Abatzoglou, 2013), which could be a possible reason of fewer spatial scale crop modeling studies. However, the availability of long-term gridded weather products such as gridMET, PRISM, and NLDAS has provided great help to overcome this issue (Marambe and Milas, 2020). In addition, modifications in crop model structures are required to allow parallel runs for large-scale processes (Hansen and Jones, 2000). Efforts have been made to develop the open-source framework for running DSSAT and APSIM crop models under parallel system (Elliott et al., 2014); nevertheless, the considerable data requirement by these models for calibration and validation could be a limitation for large scale gridded crop modeling studies.

AquaCrop-Open Source (OS), a crop model with intermediate complexity, can be a good choice for crop modelers to run gridded simulations (Foster et al., 2017a). AquaCrop model has been primarily designed to study the crop yield response to water, and the OS version allows the spatial application of this model for assessing the temporal variation in crop yield and water use at regional scale. Very few studies have used the AquaCrop-OS for gridded crop modeling. For example, Nouri et al. (2019; 2020) applied this model at river basin evaluating water saving potential of drip irrigation and mulching for various crops and for mapping water footprints of

agriculture. A limited number of studies in the U.S. have focused on the impacts of drought on wheat yield at large spatial scales (e.g. Tian et al., 2018; Otkin et al., 2016; Peña-Gallardo et al., 2019). Hence, AquaCrop-OS provides a unique opportunity to assess the impacts of drought on wheat yield at regional scale.

In addition to aforementioned gap in the knowledge, many previous modeling studies that used gridded data to investigate spatial crop response to yield limiting factors have relied on coarse resolution weather and soil data (0.25^{o}~0.5^{o}) (e.g., Jang et al., 2019; Folberth et al., 2019; Franke et al., 2020). The higher resolution weather and soil datasets have been less utilized in the past and their inclusion in gridded crop modeling can substantially improve the knowledge regarding the spatial impacts of drought on crops such as winter wheat (Rezaei and Ewert, 2015; McNider et al., 2011). Another noticeable gap in the knowledge specifically related to winter wheat yield response to drought events at regional scale is that most of the previous studies have estimated correlations among winter wheat yield and drought magnitude (e.g., Mavromatis et al., 2006; Yu et al., 2018; Tian et al., 2020), whereas the regional drought sensitivity of wheat has received less attention. Drought sensitivity could be of vital importance for devising drought mitigation policies and early warning systems (Donald et al., 2000).

The specific objectives of this study were i) to simulate the long-term yield of dryland winter wheat in Oklahoma's wheat belt using the AquaCrop-OS model and high-resolution gridded weather and soil data; ii) to assess the spatial variation in wheat yield with respect to water availability in different planting windows across the study area; and iii) to calculate correlations of wheat yield with drought magnitude and to estimate drought sensitivity of winter wheat in different climate divisions of Oklahoma.

4.2. Materials and Methods

4.2.1. Study area and data collection

The study was conducted over the wheat belt in central and western Oklahoma. Crop frequency layers (CFL) developed by the U.S. Department of Agriculture (USDA, 2018) at spatial resolution (SR) of 30 m were used to select the pixels categorized as having wheat in any season during the 2008-2019 period. Gridded (SR ~ 4 km) climate data including maximum and minimum air temperature, precipitation, and grass reference evapotranspiration (ET_o) were downloaded from gridMET for the 30-year period of 1989 to 2019 (Abatzoglou, 2013), which is considered sufficient in length to accurately characterize the magnitude and duration of drought (Ahmadalipour et al., 2017) and has been previously used by several researchers (Marambe & Milas, 2020; Schwalbert et al., 2020; Khan et al., 2019). For the state of Oklahoma, gridMET data encompassed 10,406 grids/pixels, out of which, 3281 grids were selected to run the analysis based on the percentage of the 4-km gridMET grids that overlapped the 30-m CFL pixels. The gridMET pixels that had larger than 27% overlap by CFL pixels were selected. The selected 3281 pixels covered approximately 82% of the total wheat area of CFL (Figure 4.1).

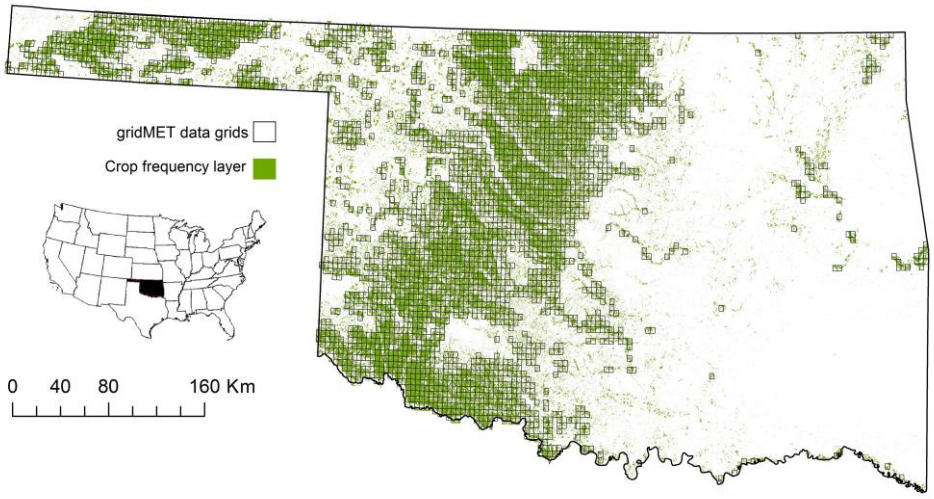

Figure 4.1. Wheat crop frequency layer and gridMET grids selected for analysis.

Soil data were collected from Gridded Soil Survey Geographic (gSSURGO) database (Soil Survey Staff, 2019). The Soil Data Development Tools for ArcGIS were used to retrieve the data. Weighted average approach was used to create soil properties maps at multiple depths and percent composition was used as the weighting factor. Soil properties maps were then aggregated by estimating means according to the resolution of gridMET grids. Since the gSSURGO does not have the data on soil moisture at saturation, the Rosetta 3.0 beta Python-SQL based tool (Zhang and Schaap, 2017) was used to estimate this parameter. Rosetta 3.0 utilizes the hierarchical pedotrasnfer functions by using artificial neural networks analysis and provides the estimations of van Genuchten water retention parameters (Ghanbarian-Alavijeh et al., 2010).

4.2.2. AquaCrop-OS

AquaCrop-OS is an open-source version of the AquaCrop water yield response model of the Food and Agriculture Organization of the United Nations (Foster et al., 2017a). The source code of AquaCrop-OS is available in Matlab for each module of the model. There are two major advantages of using AquaCrop-OS in comparison to the graphical user interface (GUI) based AquaCrop. First, the ability to run multiple parallel simulations that can be utilized to operate the model at large spatial scales. Second is the compatibility of AquaCrop-OS with the Open Modelling Interface (OpenMI) standard that enables the code to be interlinked simultaneously with other models to support studies on integrated water resource management (Foster et al., 2017b). AquaCrop-OS V6.0a (AC-OS) was used in this study. The model was run using batch run module that allows parallel simulations. There were a total of 3281 simulations, similar to the numbers of selected grids. The calibrated crop file was based on the previous chapter and the perfromance of AquaCrop-OS was also compared with the outputs of the AquaCropV6.0 for grain yield simulation at multiple locations.

4.2.3. Model Application

Aquacrop-OS was applied over the Oklahoma wheat belt to develop maps of potential yield of winter wheat under dryland conditions (Y_p). The simulated yield was considered "potential" since the model does not account for the effects of pest, disease, and/or nutrient stresses. The maps were generated for 30 cropping seasons under three different sowing dates of 25-Sep, 05-Oct, and 15-Oct, which are within the typical wheat planting window in Oklahoma. Soil moisture at the time of sowing was considered at field capacity. Pearson's correlation coefficient (r) were calculated between root zone total available water (TAW) and averaged Y_p for each of the planting dates. These correlations were calculated separately for different climate divisions (CD) in Oklahoma. These CDs correspond to the USDA's crop reporting districts (Arndt, 2012) and help visualize the overall impact of dry periods along with the interpretation of grid-wise response of crop yield to droughts.

4.2.3.1. Comparison with measured yield

Simulated Y_p estimates were compared with measured yield data of dryland, grain-only winter wheat from six experimental sites across the Oklahoma wheat belt and reported in Marburger et al. (2018). These sites (Figure 4.2) were selected based on their continuous data availability between 2000 and 2019. Though good crop management practices were implemented at the experimental sites, the measured yields cannot be considered potential due to the inevitable impacts of stresses and environmental factors. Nonetheless, the datasets were suitable to assess the performance of AquaCrop-OS in capturing temporal and spatial variations in yield in different CDs and under varying drought intensities. Several major drought incidents occurred during the 2000-2019 period in Oklahoma wheat belt, such as the 2005-2006, 2010-2011, 2013-2014, 2017-2018 events (SCC, 2017). Simulated Y_p with 05-Oct planting date was used for comparison with the measured yield because more than 90% of the experimental sites were planted in October.

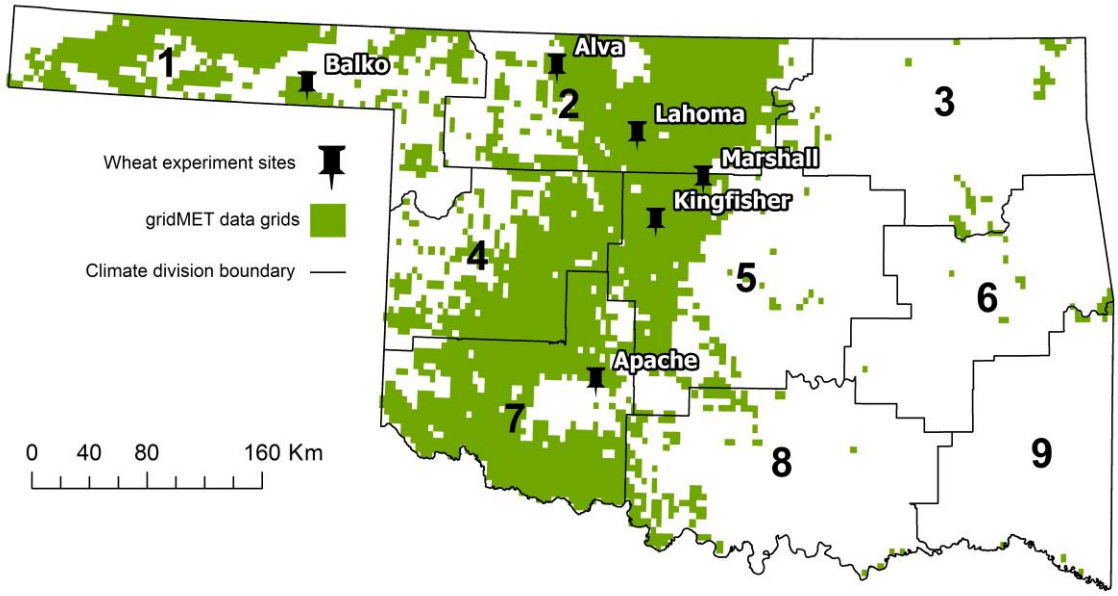

Figure 4.2. The location of winter wheat experimental sites. The Climate Divisions (CD) are 1: Panhandle, 2: North Central, 3: Northeast, 4: West Central, 5: Central, 6: East Central, 7: Southwest, 8: South Central, and 9: Southeast.

4.2.3.2. Correlations of simulated yield and drought indices

The simulated Y_p for the 05-Oct sowing date was correlated with three drought indices at each grid and distributed correlation coefficients (r) were calculated. The three drought indices included Standardized Precipitation Evapotranspiration Index (SPEI) (Vicente-Serrano et al., 2010), Palmer's Z-Index, and Palmer Drought Severity Index (PDSI) (Palmer, 1965). These indices have been widely used to monitor the magnitude of agricultural drought (Vicente-Serrano et al., 2012; Wang et al., 2016; Tian et al., 2018; Tian et al., 2020). Monthly gridded SPEI, Z-Index, and PDSI were downloaded from West Wide Drought Tracker website (https://wrcc.dri.edu/wwdt/) for the period of 1989-2019 (Abatzoglou et al., 2017). The spatial resolution of these indices was similar to the Y_p maps (~ 4 km). In this study, one-month SPEI (SPEI-1) and Z-Index were used to study the impacts of short-term droughts as they estimate the monthly drought magnitude. Three-month SPEI (SPEI-3) translated the effect of medium-term

drought events, whereas the PDSI estimated the influence of long-term droughts (~ 9 months). Monthly r values were calculated for the period between October and June, with specific focus on months of March, April, and May because of their larger correlations in comparison to other months in growing season.

4.2.3.3. Drought sensitivity of simulated yield

Linear regression models between simulated Y_p and gridded drought indices mentioned in the previous section were developed. The slopes of the linear regressions were used to investigate the spatial variation in drought sensitivity at grid and CD scales. To compare different CDs for drought sensitivity, the gridded slopes were spatially averaged. The slopes explain the sensitivity of Y_p to variation in the magnitude of drought. Smaller slopes indicate higher drought tolerance and steeper slopes point towards larger drought vulnerability (Khaki et al., 2019). The concept of using the slopes of linear regression model between yield and water stress indicators (e.g., soil water potential) has been previously implemented by studies focused on crops' drought tolerance (Kirigwi et al., 2004; Parent et al., 2017). However, very few researchers have utilized the yield-drought magnitude slopes to perform drought risk assessment at spatial or temporal scale (Kim et al., 2019).

4.3 Results and Discussion

4.3.1. Simulated yield maps

The 30-year average winter wheat Y_p, in general, followed the precipitation and temperature gradients that increase from Panhandle to southeast and northwest to southeast, respectively (Arndt, 2012) (Figure 4.3 a-c). The maps showed noticeable spatial variation across the wheat belt, and the variation was also discernible with respect to different CDs. The Panhandle region had smaller average yields because of its lower precipitation rates and heat unit availability. Overall, larger Y_p was estimated for the North Central, Central, West Central, and Southwestern

parts of the wheat belt, which benefit from improved availability of precipitation and temperature, especially on the eastern sides of these CD.

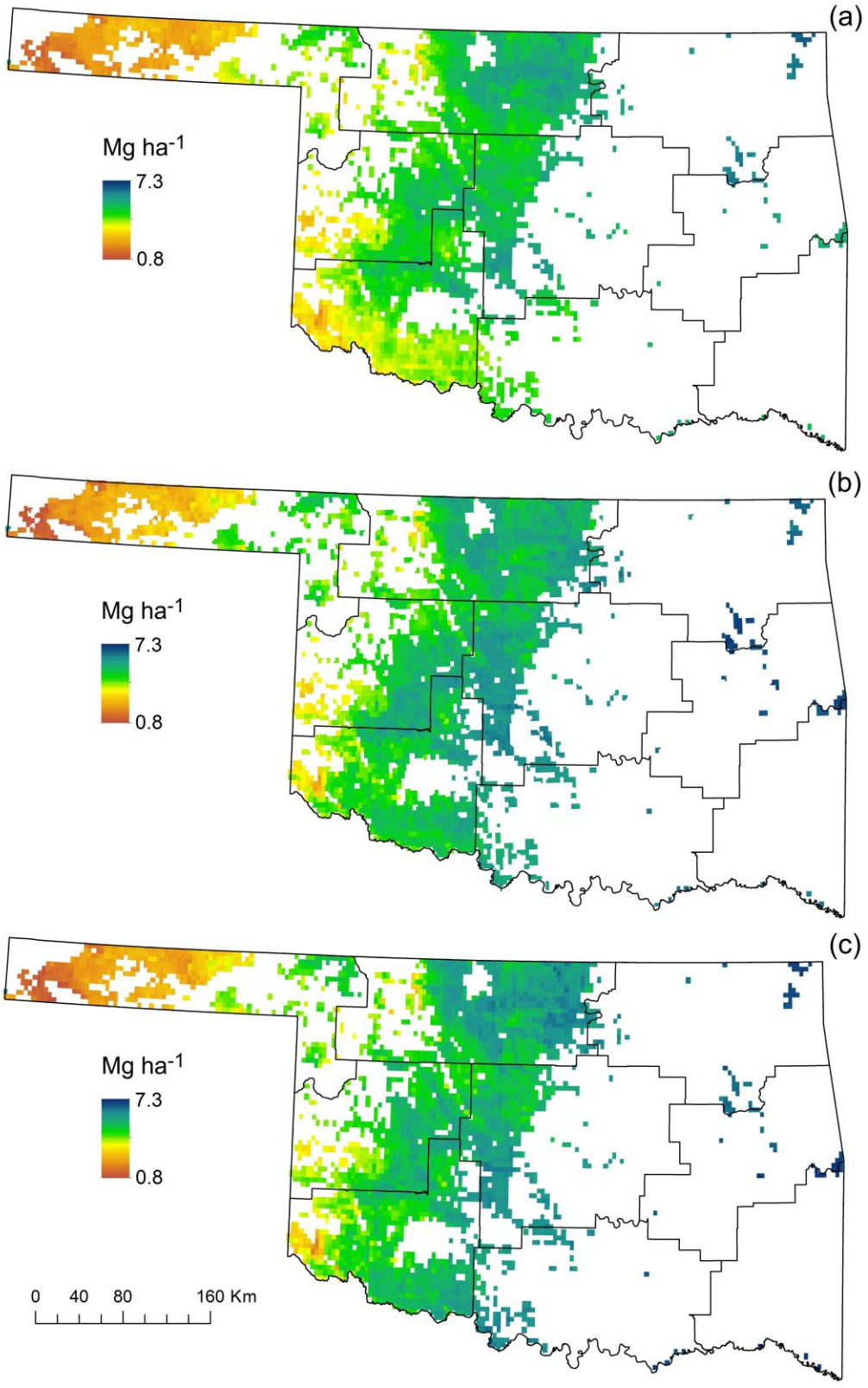

Figure 4.3. Average winter wheat Y_p for different planting dates (a) 25 Sep (b) 05 Oct (c) 15 Oct.

The Y_p simulations were generally in agreement with the simulations of standard AquaCrop model. The overall simulated Y_p for Oklahoma was 4.9 Mg ha^{-1}, which was in accordance with the average long-term water-limited potential yield of 5.2 Mg ha^{-1}, estimated for the SGP region by Lollato et al. (2017) using the SSM-Wheat model. Also, the average range of simulated Y_p in this study varied between 0.93 and 7.1 Mg ha^{-1}, and this range concurred with the county-based average potential yield ranges of 3.5 and 8.0 Mg ha^{-1}, estimated by Patrignani et al. (2014) using statistical approaches for two western and two eastern counties in Oklahoma; respectively. The average Y_p considering all simulation years and planting dates was largest in Central CD, followed by North Central, West Central, South West, and Panhanlde CDs at 5.5, 5.3, 4.8, 4.7, and 2.9 Mg ha^{-1}, respectively.

An increasing trend was noted in the maximum Y_p as the planting window moved from 25 Sep to 15 Oct, whereas the minimum Y_p followed a declining trend with delayed sowing. This trend was in agreement with the findings of Greene and Maxwell (2007), who used CERES-Wheat to simulate winter wheat yield in Oklahoma and found late planting dates allowing the crop to utilize better thermal and soil moisture conditions. By planting wheat on 25-Sep, in comparison to 05-Oct, declines in Y_p was noted in 99% of the grids in Central CD and changes in yield ranged between -1.1 and 0.1 Mg ha^{-1}. This spatial decline in Y_p was followed by Southwest, West Central, Panhandle and North Central CDs, where the decline occurred in 96%, 89%, 76%, and 72% grids, and the ranges if change in yield were -1.9 to 0.3, -0.1 to 0.3, -1.0 to 0.5, and -0.8 to 0.4, respectively. For 15-Oct planting, the increase in Y_p in comparison to 05-Oct was pronounced in North Central CD where 90% of grids had increment and the change varied between 0.7 and -0.5. The improvement in Y_p for West Central, Southwest, Panhandle, and Central was experienced at 44%, 38%, 19%, and 18% of grids and change in Y_p ranged from 0.8 to -0.6, 0.8 to -0.5, 1.0 to -0.76, and 0.3 to -0.7, respectively.

The change in the Y_p due to shift in planting date was mainly due to the variation in the precipitation amount. For example, in the lower areas of the Southwest CD, the winter wheat Y_p increased when the planting date was shifted from 25 Sep to 05 Oct, most likely due to the availability of almost 20 mm extra rain on an average for the 30-year period in that area. Similarly, for the Panhandle, moving the sowing window from 05 Oct to 15 Oct, the growing season, on an average, lost approximately 14 mm of precipitation that possibly caused decline in Y_p.

Soil properties had a considerable impact on the spatial variation of simulated winter wheat Y_p. Attenuated yields in grids having small TAW were found in the southwestern corner of the wheat belt and in the west central area (Figure 4.4). Also, in the central parts of Oklahoma, the presence of higher sand and gravel levels in the root zone along the alluvial river channels resulted in smaller TAW, and this impact was visible in the yield maps (Horton, 2017; Yang et al., 2016). The largest correlations between TAW and averaged Y_p of all three sowing dates existed in Central CD with r of 0.82. West Central CD came next with r of 0.76. The r for Southwest, North Central, and Panhandle were 0.72, 0.67, and 0.42, respectively.

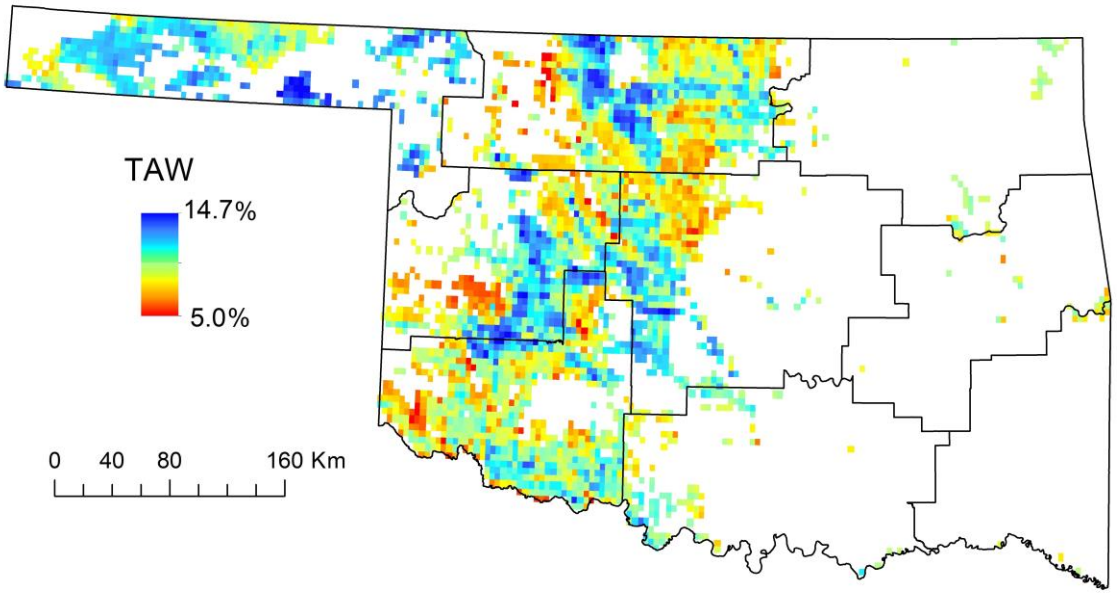

Figure 4.4. Total available water (TAW) of the top 1.5 m of the soil in volumetric percentage, estimated from gSSURGO soil properties data.

4.3.2. Comparison with measured yield

The comparison results showed that the Y_p timelines were generally in compliance with the temporal trend of measured yield at all six sites across Oklahoma (Figure 4.5). Between the period of 2000 and 2019, four major drought episodes were experienced in the winter wheat belt of Oklahoma. These drought events occurred in 2005-2006, 2010-2011, 2013-2014, and 2017-2018 (Figure S1). AquaCrop-OS duly simulated the impacts of droughts on the grain yield production in these cropping seasons. During the drought of 2005-2006, for Balko, Alva, Marshall, and Kingfisher, the simulated drought-impacted Y_p ranged from 0 to 2.25 Mg ha^{-1}, that was within the ranges of measured yield at these sites, 0 to 3.08 Mg ha^{-1}. However, for Lahoma and Apache, the model showed over-sensitivity to drought and simulated Y_p approximately 2 Mg ha^{-1} below the average measured yield. In year 2010-2011, again the yields declined due to drought. The range of Y_p at Balko, Marshall, Kingfisher, and Alva (0-2.75 Mg ha^{-1}) was within or near the ranges of measured yield (0-3.54 Mg ha^{-1}). At, Apache the model showed high sensitivity to drought, whereas for Lahoma, which was less impacted due to drought, the Y_p did not show a considerable decline and was predicted as 5.82 Mg ha^{-1}.

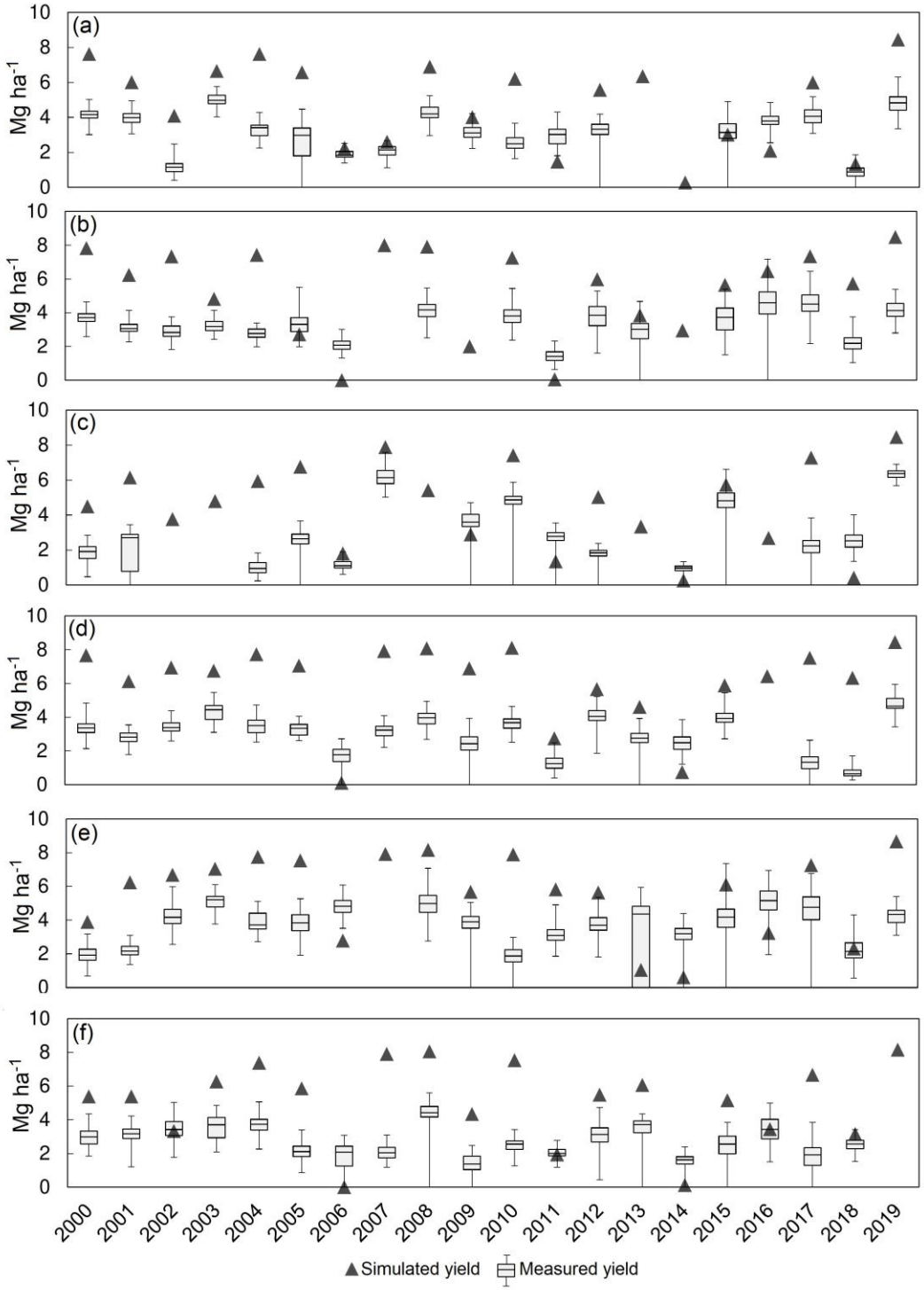

Figure 4.5. Y_p and measured yield at (a) Alva (b) Apache (c) Balko (d) Kingfisher (e) Lahoma (f) Marshall. Whiskers indicate the full range of measured yield. Year with no boxplots have missing data.

The spatial variation in yield due to different intensities of drought in the wheat belt was observed again in 2013-2014 drought episode (Oklahoma Climatological Survey, 2014). According to the site notes available with the wheat yield data from experiment stations, long-term drought at Balko, Lahoma, Marshall, and Kingfisher considerably reduced the winter wheat grain yield. A freeze event in mid-April in the region had negative impact on the grain production too. The AquaCrop-OS simulated stress response of crop towards extreme weather events and the Y_p ranged between 0.12 and 0.74 Mg ha^{-1} at the aforementioned sites, which was near the smaller ranges of measured yield (0-1.22 Mg ha^{-1}).

The more recent drought of 2017-2018 resulted in 47% loss in wheat production in Oklahoma (Marburger, 2018), the trend of Y_p was overall in agreement with the field measurements. At Alva, Lahoma, and Marshall the drought-stricken Y_p, 1.33-3.16 Mg ha^{-1}, almost overlapped the field data that ranged from 0 to 4.32 Mg ha^{-1}. At Balko, the model showed over-sensitivity to lack of water availability. At Apache, the drought impact on water-limited potential yield was not strong, most probably due to the occurrence of less severe drought during the growing season. For Kingfisher, the presence of foliar disease in the experimental field curbed the comparability of measured and simulated yield.

Examining the source of discrepancies in the spatial crop modeling could be challenging due to massive number of simulations. However, one of the major sources causing divergence between measured and simulated yield could be the gridded precipitation data. Unlike temperature, the interpolation of precipitation data at spatial scale usually face accuracy issues, which can be a significant source of uncertainty in gridded crop models simulations as described by De Wit et al (2007). Although the high density of point data collected at Oklahoma Mesonet (McPherson et al., 2007), which is an input source of GridMET (Abatzoglou, 2013; Daly, 2019), provides a unique opportunity for improved accuracy of weather data interpolation (Walsh et al., 2012; Mourtzinis et al., 2017), the spatial heterogeneity of precipitation may cause sub-grid level

variability impacting the water balance modeling (Zhao et al., 2013) that eventually effects the true water availability for crop (Ghan et al., 1997).

Another possible cause of discrepancy is the soil water balance calculation of AquaCrop-OS. The model tends to slightly underestimate soil water at high soil water contents as it does not allow the root zone to remain at saturation level for multiple days, and assumes swift drainage of the saturated soil to bring it back to field capacity within a short period of time (Mkhabela et al., 2012). Spatial aggregation of soil properties data can also have a considerable influence on the simulated yield. Hoffmann et al (2016) studied the impact of input data aggregation on regional yield simulations and found model yield bias (<15%) occurring due to aggregated soil data. Moreover, the field conditions could play an important role in governing the yield. For example, Qin (2013) used AquaCrop to study dryland winter wheat yield in Loess Plateau, China, and found that mulching and tillage practices influenced the yield. In this study, the impact of field conditions was not investigated, whereas the measured yield data varied in terms of tillage practices and presence of cover crops in non-wheat period. Furthermore, variation of the planting dates at experiment stations within the sowing window could considerably affect the yield, particularly in dry periods.

4.3.3. Coefficient of variation

The CV maps of winter wheat Y_p showed the largest deviation from the mean was in Panhandle, with an average CV of 0.85, followed by Southwest, with average CV of 0.59 (Figure 4.6). West Central, North Central, Central CDs had smaller average CVs of 0.57, 0.46, and 0.43, respectively. Grids with smaller TAW generally exhibited larger CV, which points towards the higher susceptibility of crop in these areas to droughts due to their limited ability to store water in the root zone.

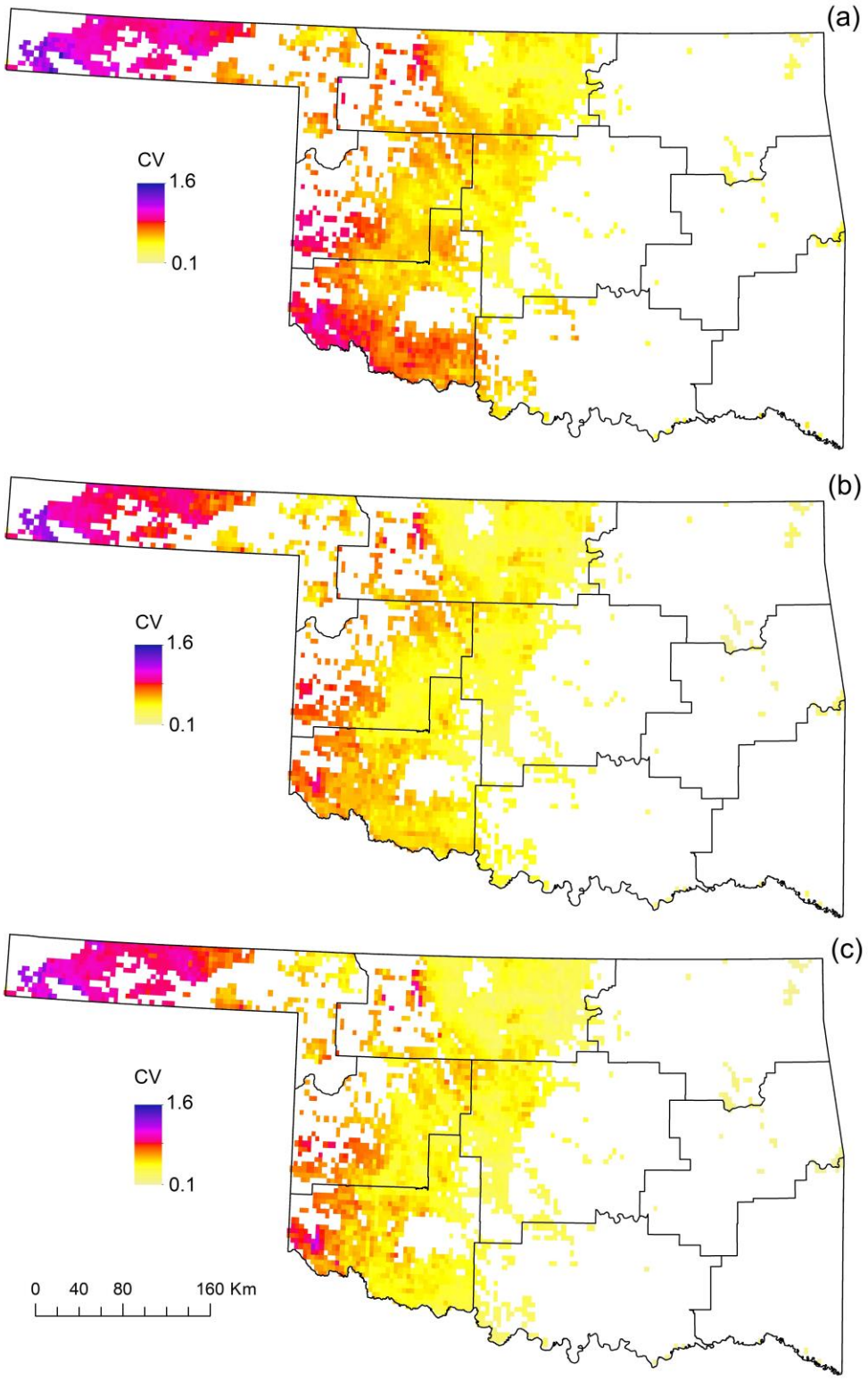

Figure 4.6. Coefficient of variation of winter wheat yield for different planting dates (a) 25 Sep (b) 05 Oct (c) 15 Oct.

The spatial variation of CV followed the precipitation gradient. Furthermore, the areas with larger yields had the lowest CV that shows their consistency in producing a better crop. These findings were in line with the results of Lollato et al (2017) who simulated the water limited wheat grain yield at more than 20 sites across Oklahoma and found CV of yield increasing from east to west. It is worth mentioning that the CV range estimated by Lollato et al (2017) was 0.13-0.52, smaller than the overall CV range of 0.1 to 1.56. This difference is most probably due to the number of sites/grids used for the analysis. For example, Lollato et al (2017) selected four sites in Panhandle in comparison to 526 grids simulated in this study.

4.3.4. Correlation of simulated yield and drought indices

The correlations between Y_p and drought indices varied during the growing season for all CDs (Figure 4.7). The average correlation coefficient for all CDs and drought indices was 0.16, 0.22, 0.34, 0.39, 0.39, 0.45, 0.49, and 0.51 for the months of Oct., Nov., Dec., Jan., Feb., Mar., Apr., and May, respectively. Overall, higher correlations existed in the months of March, April and May, and these findings were in line with the results of Hatfield and Dold (2018) who found April and May precipitation mainly governing the fluctuation in winter wheat yield in Oklahoma. The correlation trends were in accordance with the results of Tian et al (2018) who estimated county-wise correlations between winter wheat yield and SPEI, Z-Index, for South-Central U.S., and found high response during March and April. Also, the correlation values were in agreement with the correlations of wheat yield and SPEI, Z-Index, and PDSI estimated by Tian et al (2020) for multiple sites in Oklahoma during April.

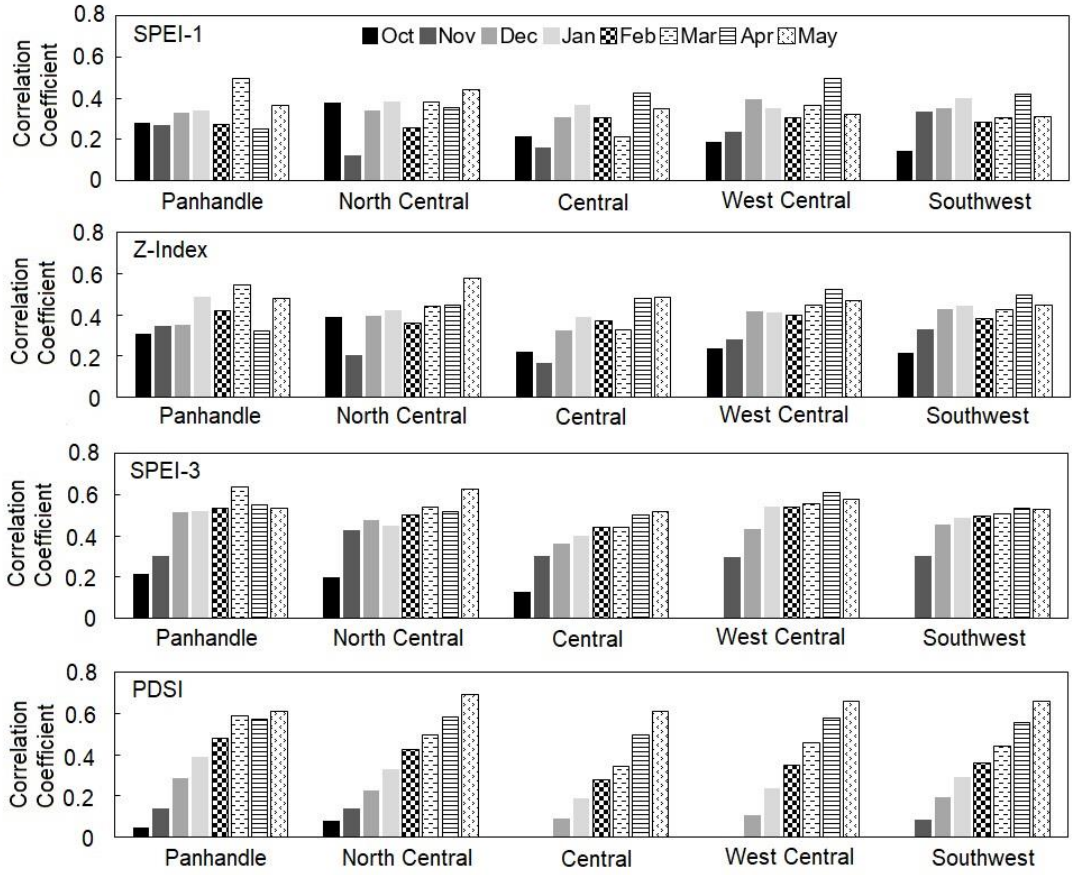

Figure 4.7. Average correlations between winter wheat Y_p and drought indices for different CD during growing season

Correlation maps (Figure 4.8) showed that the impact of short term drought (presented by SPEI-1 and Z-Index) in March was greater in North Central and western parts of the wheat belt, whereas the large correlations during April were concentrated in West Central, Central and upper parts of the South Western region. For the month of May, most of the larger correlations shifted toward north Central and upper parts of the Central and West Central regions.

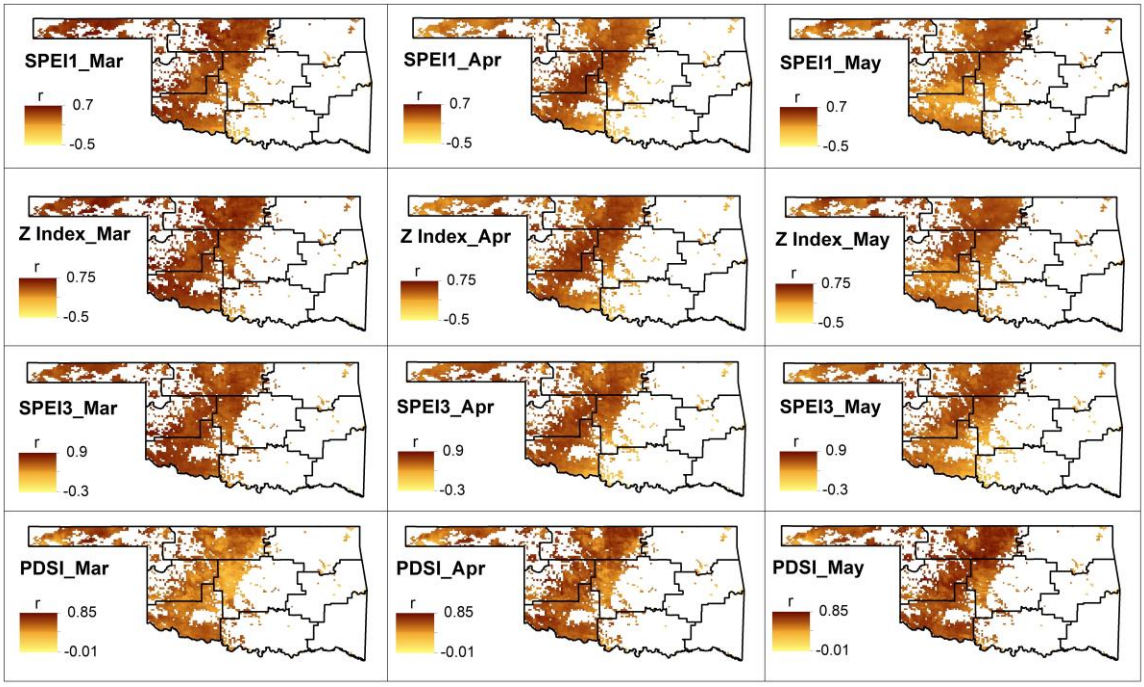

Figure 4.8. Correlations between winter wheat Y_p and drought indices for months of March, April, and May

Higher correlations of grain yield and drought indices in March for short- and medium-term droughts indicate that the availability of soil moisture in the root zone at the time when crop is entering in the greening-up phase has positive impacts on the grain development (Dhillon et al., 2019). The main reason for April being the month when strong correlations were noted in majority of the grids overlapping wheat belt is the number of growth stages occurring in this month, varying between heading and grain-filling. Since all of these stages are highly sensitive to water-stress, substantial decline in wheat yield could be expected in case of a short- to medium-term drought event.

The impact of long-term drought was more highlighted in PDSI correlations in May. Wheat crop in almost all regions in Oklahoma goes through the watery ripe and soft dough phase in May as it moves towards the maturity from late-May to early-June. A presence of long-term drought reaching till May would translate to lesser availability of wheat plant's reserves in the stem as

carbon assimilation reduces during stem elongation under stress that eventually decreases the storage in the stem (Blum, 1998). In addition, presence of heat stress during May could be another potential factor that might curb the grain yield gains especially if the high temperatures overlaps with the sensitive phases of the grain-filling period (Lollato and Knap, 2020), and lack of soil moisture would reduce the crop's ability to cope with high temperatures (Akhter and Islam, 2017).

4.3.5. Drought sensitivity of simulated yield

Winter wheat yield was most sensitive to short-term droughts in West Central CD. The slope of the Y_p vs. SPEI-1 linear model averaged for all grids in this CD and the three months of March-May, was 0.98, followed by North Central (0.94), Panhandle (0.86), Southwest (0.78), and Central (0.73) CDs (Figure 4.9). Z-Index also categorized West Central as the most sensitive and Central as the least sensitive to short-term drought, with average slopes of 0.50 and 0.40, respectively. The average slopes of Y_p vs.Z-Index ranged between 0.46-0.47 for the other CDs (Panhandle, Southwest, and North Central). The results were similar when considering mid-term (SPEI-3) and long-term (PDSI) drought indices. In case of SPEI-3, the slopes decreased from 1.5 at West Central to 1.21 at Central CD. For PDSI, slopes decreased from 0.56 at West Central to 0.44 at Central CD. This indicates that the same amount of increase in drought severity causes more declines in yield in West Central compared to other CDs.

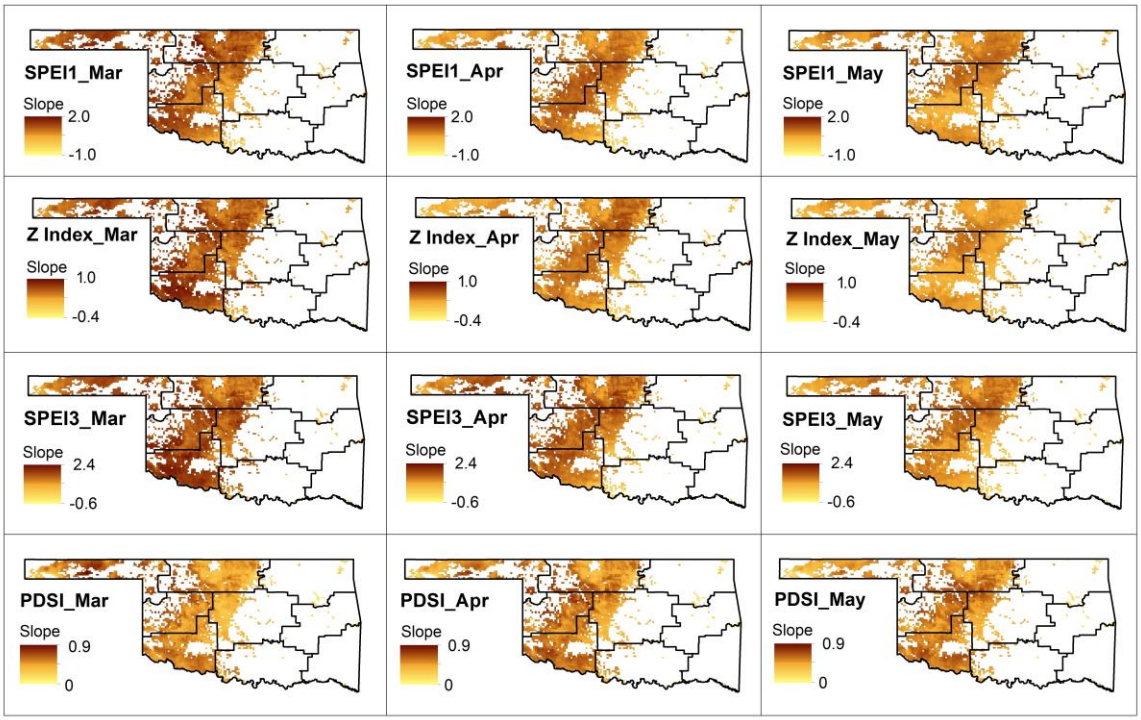

Figure 4.9. Grid-wise slopes of the linear regression models between drought indices and winter wheat Y_p for March, April, and May.

Sensitivity of wheat yield to different magnitudes of drought was broadly comparable to the findings of Kirigwi et al. (2004) who tested the wheat yield in different water regimes and found that yield was more sensitive to water availability in low moisture regimes (steeper slopes) and sensitivity decreased in high moisture regimes. The estimated slopes were generally in agreement with findings of Yu et al. (2019), who found higher sensitivity of wheat yield to drought index in semi-arid region in comparison to humid areas, and the regression slopes were approximately two times steeper in semi-arid climate. The results of the current study did not show an increase in the slope of drought magnitude vs. crop yield regression models with decrease in average annual precipitation as suggested by Kim et al. (2019).

4.4. Conclusion

Spatial crop modeling was conducted for Oklahoma using AquaCrop-OS model to investigate the potential yield of dryland winter wheat (Y_p) and its response to drought events. High resolution gridded weather and soil datasets were used for this purpose. Long-term simulations (1989-2019) were run for three different planting dates at 3281 grids overlapping Oklahoma wheat belt. The overall average Y_p varied spatially from 1.0 to 7.0 Mg ha^{-1}, comparable with previous studies and yield records from field measurements, which showed the ability of AquaCrop-OS to be used in distributed simulation of winter wheat yield and drought response.

The coefficient of variation (CV) for Y_p ranged from 0.1 to 1.6, which indicated a large interannual variability in yields across the wheat belt. Panhandle and Southwest climate divisions (CDs) had the largest CV estimates. In general, the grids with low root zone total available water (TAW) had smaller yields and exhibited larger yield CV. The long-term correlations of drought indices and winter wheat Y_p showed that the strongest correlations existed in the months of March to May, when the wheat is highly sensitive to water stress. Slopes of the linear regression models developed between Y_p and drought indices were interpreted for Y_p sensitivity to changes in drought magnitude. West Central CD was the most sensitive to dry periods in the wheat belt of Oklahoma with slopes ranging from 0.8 to 2.1 for droughts of various durations. Southwest and Panhandle came next in the sensitivity ranking where along with the water stress, Y_p was also considerably impacted by heat stress and low temperature, respectively.

CHAPTER V

CONCLUSIONS

Droughts are a recurrent feature in the climate of Oklahoma. Winter wheat holds the largest cropping area in the state and is also highly susceptible to drought. Better understanding of variation in drought magnitude and its impact on winter wheat yield can improve the drought preparedness of farming community. This research investigated the dynamics of agricultural drought in Oklahoma by using soil moisture and weather data and employing crop modeling techniques to assess the relationship of weather anomalies and winter wheat yield. The specific objectives were to: 1) develop a new drought index using soil moisture and weather data for improved drought monitoring of winter wheat; 2) calibrate and validate a crop model and employ it to study the impacts of planting date and water availability on winter wheat yield; and 3) apply the calibrated crop model across the winter wheat belt in Oklahoma to investigate the spatial variation in yield and study drought sensitivity.

In the first study (Chapter II), a new drought index named the Soil Moisture Evapotranspiration Index (SMEI) was developed using soil moisture and reference evapotranspiration data. Several existing soil moisture-based and meteorological drought indices were also calculated for assessing the performance of SMEI. The correlations between SMEI and meteorological drought indices were 33% stronger on average when compared to existing SM indices. Higher correlation coefficients of SMEI were observed at all study sites, suggesting that SMEI performs well under

variable climatic conditions experienced across Oklahoma. The SMEI captured temporal variations in drought and provided better responses to variation in drought magnitude in Oklahoma in comparison to other indices. In addition, SMEI had a better performance capturing the spatial variations in drought when compared to other indices and the maps developed by the U.S. Drought Monitor. As to existing soil moisture-based indices, SMEI had the strongest correlations with winter wheat yield during the critical growth stages in spring ($r > 0.9$). These results suggest that SMEI can be used more effectively to demonstrate the progress of agricultural drought under varying climates and its impacts on the crop yields. Farmers could also potentially optimize their decision making for the best use of their crops according to the predicted yield beforehand during the early crop growth stages.

In the second study (Chapter III), AquaCrop model was calibrated, validated, and then employed to study the impacts of variable planting dates and soil water content at the time of planting. The AquaCrop validation results showed that this model can be used in the study area to simulate the winter wheat growth and grain yield. Long-term simulations (1994-2019) at three sites across the wheat belt in Oklahoma were run. The long-term application results revealed that grain yields were larger for October planting compared to September (about 40% on average). The early sown (mid-September) dryland wheat yield was greatly impacted by the lower temperatures during flowering stage, whereas favorable temperatures were noted for anthesis in October-planted winter wheat. 5-Oct was the most optimum planting date in general for all study sites under all soil water contents at the time of planting, followed by 25-Sep. Soil water content deficiency at planting had a considerable impact on yield, especially at sites with higher aridity. On average, yield decreased by 25% when soil water content at planting decreased from 100% of the total available water to 40%. Simulations including irrigation showed improvement in yields, especially in drought seasons, by up to 17%. However, the upper limit of wheat yield stayed almost the same as under dryland conditions, indicating the limited role of irrigation in seasons

that received ample precipitation. The irrigation water productivities were smaller for September-planted crop and increased with increasing delay in planting.

In the third study (Chapter IV), gridded modeling was conducted across the wheat belt in Oklahoma using AquaCrop-OS model to investigate the potential yield of dryland winter wheat (Y_p) and its response to drought events. High resolution gridded weather and soil datasets were used for this purpose. Long-term simulations (1989-2019) were run for three different planting dates at 3281 grids overlapping Oklahoma wheat belt. The overall average Y_p varied spatially from 1.0 to 7.0 Mg ha^{-1}, comparable with previous studies and yield records from field measurements, which showed the ability of AquaCrop-OS to be used in distributed simulation of winter wheat yield and drought response. Large interannual variability in yields across the wheat belt was noted and the coefficient of variation (CV) for Y_p ranged from 0.1 to 1.6. Panhandle and Southwest climate divisions (CDs) had the largest CV estimates. In general, the grids with low root zone total available water (TAW) had smaller yields and exhibited larger yield CV. The long-term correlations of drought indices and winter wheat Y_p showed that the strongest correlations existed in the months of March to May, when the wheat is highly sensitive to water stress. Slopes of the linear regression models developed between Y_p and drought indices were interpreted for Y_p sensitivity to changes in drought magnitude. West Central CD was the most sensitive to dry periods in the wheat belt of Oklahoma, with slopes ranging from 0.8 to 2.1 for droughts of various durations. Southwest and Panhandle came next in the sensitivity ranking where along with the water stress, Y_p was also impacted by heat stress and low temperature, respectively.

REFERENCES

Ahmadalipour, A.; Moradkhani, H.; Yan, H.; Zarekarizi, M. Remote sensing of drought: Vegetation, soil moisture, and data assimilation. (2017) In Remote Sensing of Hydrological Extremes; Lakshmi, V., Ed.; Springer International Publishing: Berlin, Germany, pp. 121–149.

Abatzoglou, J. T. (2013). Development of gridded surface meteorological data for ecological applications and modelling. International Journal of Climatology, 33(1), 121-131.

Abatzoglou, J. T., McEvoy, D. J., & Redmond, K. T. (2017). The West Wide Drought Tracker: drought monitoring at fine spatial scales. Bulletin of the American Meteorological Society, 98(9), 1815-1820.

Aggarwal, P.K. (2009) Determinants of Crop Growth and Yield in a Changing Climate. In Rainfed Agriculture: Unlocking the Potential, Wani, S.P., Johan Rockström, T.O., Eds., CABI: Wallingford, UK, Available online: http://www.iwmi.cgiar.org (accessed on 17 May 2018).

AHDB – Agriculture and Horticulture Development Board (2015) Wheat Growth Guide, AHDB Cereals & Oilseeds. Retrieved from https://webdoc.agsci.colostate.edu/

Ahmad, M. J., Iqbal, M. A., & Choi, K. S. (2020). Climate-driven constraints in sustaining future wheat yield and water productivity. Supplementary Material. Agricultural Water Management, 231, 105991.

Ahmadi, S. H., Mosallaeepour, E., Kamgar-Haghighi, A. A., & Sepaskhah, A. R. (2015). Modeling maize yield and soil water content with AquaCrop under full and deficit irrigation managements. Water Resources Management, 29(8), 2837-2853.

Ajaz, A., Taghvaeian, S., Khand, K., Gowda, P. H., & Moorhead, J. E. (2019). Development and evaluation of an agricultural drought index by harnessing soil moisture and weather data. Water, 11(7), 1375.

Ajaz, A., Taghvaeian, S.,Lollato, R., Gowda, P.H. (2020) The Effects of Planting date Water Availability on Dryland and Irrigated Winter Wheat in Oklahoma

Akter, N., & Islam, M. R. (2017). Heat stress effects and management in wheat. A review. Agronomy for sustainable development, 37(5), 37.

Alderman, P. D., Quilligan, E., Asseng, S., Ewert, F., & Reynolds, M. P. (2013). Modeling wheat response to high temperature. Modeling wheat response to high temperature, 142.

Allen, R. G., Pereira, L. S., Raes, D., & Smith, M. (1998). FAO Irrigation and drainage paper No. 56. Rome: Food and Agriculture Organization of the United Nations, 56(97), e156.

Allen, R.G. (2015) REF-ET: Reference Evapotranspiration Calculator, Version 4.1, Idaho Idaho University: Moscow, ID, USA,. Available online: https://www.uidaho.edu/cals/kimberly-research-and-extension-center/research/water-resources/ref-et-software (accessed on 11 Feb 2018).

Allen, R.G.; Walter, I.A.; Elliott, R.; Howell, T.; Itenfisu, D.; Jensen, M. (2005) The ASCE Standardized Reference Evapotranspiration Equation.. Available online: https://www.kimberly.uidaho.edu/water/asceewri/ascestzdetmain2005.pdf (accessed on 11 February 2018).

Andarzian, B., Bannayan, M., Steduto, P., Mazraeh, H., Barati, M. E., Barati, M. A., & Rahnama, A. (2011). Validation and testing of the AquaCrop model under full and deficit irrigated wheat production in Iran. Agricultural Water Management, 100(1), 1-8.

Anderson, M.C.; Hain, C.; Wardlow, B.; Pimstein, A.; Mecikalski, J.R.; Kustas, W.P. (2011) Evaluation of drought indices based on thermal remote sensing of evapotranspiration over the continental United States. J. Clim. 24, 2025–2044.

Araya, A., Prasad, P. V. V., Gowda, P. H., Kisekka, I., & Foster, A. J. (2019). Yield and Water Productivity of Winter Wheat under Various Irrigation Capacities. JAWRA Journal of the American Water Resources Association, 55(1), 24-37.

Arndt, D. (2012) Oklahoma's Climate: An Overview. Oklahoma Climatological Survey. Available Online https://climate.mesonet.org/

Arndt, D.S. (2002) The Oklahoma Drought of 2001–2002 (Oklahoma Event Summary), Oklahoma Climatol Survey: Oklahoma City, OK, USA,. Available online: http://xocs.mesonet.org/summaries/event/Drought_of_2001-2002.pdf (accessed on 02 Nov 2018).

Asseng, S., Keating, B. A., Fillery, I. R. P., Gregory, P. J., Bowden, J. W., Turner, N. C., ... & Abrecht, D. G. (1998). Performance of the APSIM-wheat model in Western Australia. Field Crops Research, 57(2), 163-179.

Basara, J. B., Maybourn, J. N., Peirano, C. M., Tate, J. E., Brown, P. J., Hoey, J. D., & Smith, B. R. (2013). Drought and associated impacts in the Great Plains of the United States-a review. International Journal of Geosciences, 4(6A2 special issue), 72.

Basso, B., Ritchie, J. T., Pierce, F. J., Braga, R. P., & Jones, J. W. (2001). Spatial validation of crop models for precision agriculture. Agricultural Systems, 68(2), 97-112.

Beguería, S., Vicente-Serrano, S.M. (2009) SPEI Calculator.. Available online: http://hdl.handle.net/10261/10002 (accessed on 11 Feb 2018).

Beguería, S., Vicente-Serrano, S.M., Reig, F., Latorre, B. (2014) Standardized precipitation evapotranspiration index (SPEI) revisited: Parameter fitting, evapotranspiration models, tools, datasets and drought monitoring. Int. J. Climatol. 34, 3001–3023.

Blum, A. (1998). Improving wheat grain filling under stress by stem reserve mobilisation. Euphytica, 100(1-3), 77-83.

Bouras, E., Jarlan, L., Khabba, S., Er-Raki, S., Dezetter, A., Sghir, F., & Tramblay, Y. (2019). Assessing the impact of global climate changes on irrigated wheat yields and water requirements in a semi-arid environment of Morocco. Supplementary Information. Scientific Reports, 9(1), 1-14.

Brock, F.V., Crawford, K.C. (1995) The Oklahoma Mesonet: A technical overview. J. Atmos. Ocean. Technol., 12, 5–19.

Cammalleri, C., Micale, F., Vogt, J. (2016) A novel soil moisture-based drought severity index (DSI) combining water deficit magnitude and frequency. Hydrol. Process., 30, 289–301.

Carrão, H., Russo, S., Sepulcre-canto, G., Barbosa, P. (2016) An empirical standardized soil moisture index for agricultural drought assessment from remotely sensed data. Int. J. Appl. Earth Obs. Geoinf., 48, 74–84.

Celik, S. K., Madenoglu, S., & Sonmez, B. (2018) Evaluating AquaCrop Model for Winter Wheat under Various Irrigation Conditions in Turkey.

Changhai, S., Baodi, D., Yunzhou, Q., Yuxin, L., Lei, S., Mengyu, L., & Haipei, L. (2010). Physiological regulation of high transpiration efficiency in winter wheat under drought conditions. Plant, Soil and Environment, 56(7), 340-347.

Chen, D., Gao, G., Xu, C.Y., Guo, J., Ren, G. (2005) Comparison of the Thornthwaite method and pan data with the standard Penman-Monteith estimates of reference evapotranspiration in China. Clim. Res. 28, 123–132.

Daly, C. (2019). Descriptions of PRISM spatial climate datasets for the conterminous United States. PRISM doc.

Daly, C., Neilson, R.P., Phillips, D.L. (1994) A statistical-topographic model for mapping climatological precipitation over mountainous terrain. J. Clim., 33, 140–158.

De Wit, A. D., & Van Diepen, C. A. (2007). Crop model data assimilation with the Ensemble Kalman filter for improving regional crop yield forecasts. Agricultural and Forest Meteorology, 146(1-2), 38-56.

Dhakal, K., Kakani, V. G., & Linde, E. (2018). Climate Change Impact on Wheat Production in the Southern Great Plains of the US Using Downscaled Climate Data. Atmospheric and Climate Sciences, 8(02), 143.

Dhillon, J., Dhital, S., Lynch, T., Figueiredo, B., Omara, P., & Raun, W. R. (2019). In-Season Application of Nitrogen and Sulfur in Winter Wheat. Agrosystems, Geosciences & Environment, 2(1).

Donald A. Wilhite, M.V.K. Sivakumar and Deborah A. Wood (Eds.) (2000) Early Warning Systems for Drought Preparedness and Drought Management. Proceedings of an Expert Group Meeting held in Lisbon, Portugal, 5-7 September 2000. Geneva, Switzerland: World Meteorological Organization.

Doughty, R., Xiao, X., Wu, X., Zhang, Y., Bajgain, R., Zhou, Y., ... & Wagle, P. (2018). Responses of gross primary production of grasslands and croplands under drought, pluvial, and irrigation conditions during 2010–2016, Oklahoma, USA. Agricultural Water Management, 204, 47-59.

Douglas-Mankin, K. R. (2018). Current Research in Land, Water, and Agroecosystems: ASABE Journals 2017 Year in Review.

Doye, D., Sahs, R. (2018) Wheat Grazeout Versus Harvest for Grain. Oklahoma Coop Ext Serv., Oklahome State Universty: Stillwater, OK, USA,. AFEC-241:1–4. Available online: http://pods.dasnr.okstate.edu/docushare/dsweb/Get/Rendition-17868/ (accessed on 17 Jan 2019).

Dutra, E., Viterbo, P., Miranda, P.M.A. (2008) ERA-40 reanalysis hydrological applications in the characterization of regional drought. Geophys. Res. Lett., 35, 2–6.

Edwards, J. T., Carver, B. F., Horn, G. W., & Payton, M. E. (2011). Impact of dual-purpose management on wheat grain yield. Crop Science, 51(5), 2181-2185.

Edwards, J. T., Kochenower, R. D., Calhoun, S. R., Knori, M. W., Lollato, R. P., Cruppe, G., ... & Hunger, R. M. (2014). Oklahoma small grains variety performance tests 2013-2014. Okla. State Univer. Coop. Ext.

Edwards, J.T., Kochenower, R.D., Austin, R.E., Inda, M.K., Carver, B.F., Hunger, R.M. (2006) Oklahoma Small Grains Variety Performance Tests 2005-2006, Okla. State Univer. Coop. Ext.

Elliott, J., Kelly, D., Chryssanthacopoulos, J., Glotter, M., Jhunjhnuwala, K., Best, N., ... & Foster, I. (2014). The parallel system for integrating impact models and sectors (pSIMS). Environmental Modelling & Software, 62, 509-516.

EPA – U.S. Environmental Protection Agency (2016) What Climate Change Means for Oklahoma. EPA 430-F-16-038, August.

Epplin, F. M., & Peeper, T. F. (1998). Influence of planting date and environment on Oklahoma wheat grain yield trend from 1963 to 1995. Canadian journal of plant science, 78(1), 71-77.

Epplin, F. M., True, R. R., & Krenzer, E. G. (1998). Practices used by Oklahoma wheat growers by region. Okla. Curr. Farm Econ, 71(1), 14-24.

FAO – Food and Agriculture Organization of the United Nations (2000) Crops and Drops: Making the Best Use of Water for Argiculture. Viale delle Terme di Caracalla, 00100 Rome, Italy

Farhangfar, S., Bannayan, M., Khazaei, H. R., & Baygi, M. M. (2015). Vulnerability assessment of wheat and maize production affected by drought and climate change. International Journal of Disaster Risk Reduction, 13, 37-51.

Fischer, R. A., Byerlee, D., & Edmeades, G. (2014). Crop yields and global food security. ACIAR: Canberra, ACT, 8-11.

Folberth, C., Baklanov, A., Balkovič, J., Skalský, R., Khabarov, N., & Obersteiner, M. (2019). Spatio-temporal downscaling of gridded crop model yield estimates based on machine learning. Agricultural and forest meteorology, 264, 1-15.

Foster, T., Brozović, N., & Butler, A. P. (2017b). Effects of initial aquifer conditions on economic benefits from groundwater conservation. Water Resources Research, 53(1), 744-762.

Foster, T., Brozović, N., Butler, A. P., Neale, C. M. U., Raes, D., Steduto, P., ... & Hsiao, T. C. (2017a). AquaCrop-OS: An open source version of FAO's crop water productivity model. Agricultural water management, 181, 18-22.

Franke, J. A., Müller, C., Elliott, J., Ruane, A. C., Jägermeyr, J., Balkovic, J., ... & François, L. (2020). The GGCMI Phase 2 experiment: global gridded crop model simulations under uniform changes in CO 2, temperature, water, and nitrogen levels (protocol version 1.0). Geoscientific Model Development, 13(5), 2315-2336.

Ghan, S. J., Liljegren, J. C., Shaw, W. J., Hubbe, J. H., & Doran, J. C. (1997). Influence of subgrid variability on surface hydrology. Journal of climate, 10(12), 3157-3166.

Ghanbarian-Alavijeh, B., Liaghat, A., Huang, G. H., & Van Genuchten, M. T. (2010). Estimation of the van Genuchten soil water retention properties from soil textural data. Pedosphere, 20(4), 456-465.

GRDC – Grain Rsearch & Development Corporation. GROWNOTES. Wheat. Section 3. Planting

Greene, J. S., & Maxwell, E. (2007). Climatic impacts on winter wheat in Oklahoma and potential applications to climatic and crop yield prediction. International journal of biometeorology, 52(2), 117-126.

Greene, J. S., & Maxwell, E. (2007). Climatic impacts on winter wheat in Oklahoma and potential applications to climatic and crop yield prediction. International journal of biometeorology, 52(2), 117-126.

Hane, D.C.; Pumphrey, F.V.; Floyd, V. (1984) Crop Water Use Curves for Irrigation Scheduling. Available online: http://ir.library.oregonstate.edu/xmlui/handle/1957/4991 (accessed on 7 January 2018).

Hansen, J. W., & Jones, J. W. (2000). Scaling-up crop models for climate variability applications. Agricultural Systems, 65(1), 43-72.

Hatfield, J. L., & Dold, C. (2018). Agroclimatology and wheat production: coping with climate change. Frontiers in plant science, 9, 224.

Hayes, M.; Svoboda, M.; Wall, N.; Widhalm, M. (2011) The lincoln declaration on drought indices: Universal meteorological drought index recommended. Bull. Am. Meteorol. Soc. 92, 485–488.

Heng, L. K., Hsiao, T., Evett, S., Howell, T., & Steduto, P. (2009). Validating the FAO AquaCrop model for irrigated and water deficient field maize. Agronomy Journal, 101(3), 488-498.

Hoffmann, H., Zhao, G., Asseng, S., Bindi, M., Biernath, C., Constantin, J., ... & Gaiser, T. (2016). Impact of spatial soil and climate input data aggregation on regional yield simulations. PLoS One, 11(4), e0151782.

Horton, J. D. (2017). The State Geologic Map Compilation (SGMC) geodatabase of the conterminous United States.

Hossain, I., Epplin, F. M., & Krenzer, E. G. (2003). Planting date influence on dual-purpose winter wheat forage yield, grain yield, and test weight. Agronomy Journal, 95(5), 1179-1188.

Howell, T. A. (2003). Irrigation efficiency. Encyclopedia of water science, 467-472.

Howitt, R., MacEwan, D., Medellín-Azuara, J., Lund, J., & Sumner, D. (2015). Economic analysis of the 2015 drought for California agriculture.

Howitt, R., MacEwan, D., Medellín-Azuara, J., Lund, J., & Sumner, D. (2017). Economic analysis of the 2015 drought for California agriculture.

Hsiao, T. C., Heng, L., Steduto, P., Rojas-Lara, B., Raes, D., & Fereres, E. (2009). AquaCrop—The FAO crop model to simulate yield response to water: III. Parameterization and testing for maize. Agronomy Journal, 101(3), 448-459.

Hunt, E.D., Hubbard, K.G., Wilhite, D.A., Arkebauer, T.J., Dutcher, A.L. (2008) The development and evaluation of a soil moisture index. Int. J. Climatol., 29, 747–759.

Hwang, Y., Clark, M., Rajagopalan, B., & Leavesley, G. (2012). Spatial interpolation schemes of daily precipitation for hydrologic modeling. Stochastic environmental research and risk assessment, 26(2), 295-320.

Iglesias, A., Garrote, L., Cancelliere, A., Cubillo, F., & Wilhite, D. A. (Eds.). (2009). Coping with drought risk in agriculture and water supply systems: Drought management and policy development in the Mediterranean (Vol. 26). Springer Science & Business Media.

Illston, B.G., Basara, J.B., Fiebrich, C.A., Crawford, K.C., Hunt, E., Fisher, D.K., Humes, K. (2008) Mesoscale monitoring of soil moisture across a statewide network. J. Atmos. Ocean. Technol., 25, 167–182.

Imhoff, D., & Badaracoo, C. (2019). Crop Subsidies. In The Farm Bill (pp. 61-68). Island Press, Washington, DC.

Inoue, T., Inanaga, S., Sugimoto, Y., & El Siddig, K. (2004). Contribution of pre-anthesis assimilates and current photosynthesis to grain yield, and their relationships to drought resistance in wheat cultivars grown under different soil moisture. Photosynthetica, 42(1), 99-104.

Iqbal, M. A., Shen, Y., Stricevic, R., Pei, H., Sun, H., Amiri, E., ... & del Rio, S. (2014). Evaluation of the FAO AquaCrop model for winter wheat on the North China Plain under deficit irrigation from field experiment to regional yield simulation. Agricultural Water Management, 135, 61-72.

Jin, X. L., Feng, H. K., Zhu, X. K., Li, Z. H., Song, S. N., Song, X. Y., ... & Guo, W. S. (2014). Assessment of the AquaCrop model for use in simulation of irrigated winter wheat canopy cover, biomass, and grain yield in the North China Plain. PloS one, 9(1), e86938.

Jones, P.D., Hulme, M. (1996) Calculating regional climatic time series for temperature and precipitation: Methods and illustrations. Int. J. Climatol., 16, 361–377.

Kale, S., & Madenoğlu, S. (2018) Evaluating AquaCrop Model for Winter Wheat under Various Irrigation Conditions in Turkey. Journal of Agricultural Sciences, 24(2), 205-217.

Karl, T.R. (1986) The sensitivity of the Palmer Drought Severity Index and Palmer's Z-Index to their calibration coefficients including potential evapotranspiration. J. Clim. Appl. Meteorol. 25, 77–86.

Keyantash, J., & Dracup, J. A. (2002). The quantification of drought: an evaluation of drought indices. Bulletin of the American Meteorological Society, 83(8), 1167-1180.

Khaki, S., Khalilzadeh, Z., & Wang, L. (2019). Classification of Crop Tolerance to Heat and Drought—A Deep Convolutional Neural Networks Approach. Agronomy, 9(12), 833.

Khan, A., Stöckle, C. O., Nelson, R. L., Peters, T., Adam, J. C., Lamb, B., ... & Waldo, S. (2019). Estimating biomass and yield using METRIC evapotranspiration and simple growth algorithms. Agronomy Journal, 111(2), 536-544.

Khand, K.; Taghvaeian, S.; Ajaz, A. (2017) Drought and Its Impact on Agricultural Water Resources in Oklahoma. Oklahoma Coop Ext Ser.; Oklahoma State University: Stillwater, OK, USA; Available online: http://pods.dasnr.okstate.edu/docushare/dsweb/Get/Document-10705/BAE-1533web.pdf (accessed on 5 January 2018).

Khordadi, M. J., Olesen, J. E., Alizadeh, A., Nassiri Mahallati, M., Ansari, H., & Sanaeinejad, H. (2019). Climate Change Impacts and Adaptation for Crop Management Of Winter Wheat And Maize In The Semi-Arid Region Of Iran. Irrigation and Drainage, 68(5), 841-856.

Kim, W., Iizumi, T., & Nishimori, M. (2019). Global patterns of crop production losses associated with droughts from 1983 to 2009. Journal of Applied Meteorology and Climatology, 58(6), 1233-1244.

Kirigwi, F. M., Van Ginkel, M., Trethowan, R., Sears, R. G., Rajaram, S., & Paulsen, G. M. (2004). Evaluation of selection strategies for wheat adaptation across water regimes. Euphytica, 135(3), 361-371.

Klemm, T., & McPherson, R. A. (2017). The development of seasonal climate forecasting for agricultural producers. Agricultural and forest meteorology, 232, 384-399.

Krueger, E. S., Ochsner, T. E., & Quiring, S. M. (2019). Development and Evaluation of Soil Moisture-Based Indices for Agricultural Drought Monitoring. Agronomy Journal, 111(3), 1392-1406.

Leng, G., & Hall, J. (2019). Crop yield sensitivity of global major agricultural countries to droughts and the projected changes in the future. Science of the Total Environment, 654, 811-821.

Leng, G., & Huang, M. (2017). Crop yield response to climate change varies with crop spatial distribution pattern. Scientific Reports, 7(1), 1-10.

Li, B., Zhou, W., Zhao, Y., Ju, Q., Yu, Z., Liang, Z., & Acharya, K. (2015). Using the SPEI to assess recent climate change in the Yarlung Zangbo River Basin, South Tibet. Water, 7(10), 5474-5486.

Li, Y., & Shu, S. (1991). A comprehensive research on high efficient eco-economic system in Wangdonggou watershed of Changwu county. Sci-Tech Document Press, Beijing, China, 503-520.

Li, Z., Hao, Z., Shi, X., Déry, S.J., Li, J., Chen, S., Li, Y. (2016) An agricultural drought index to incorporate the irrigation process and reservoir operations: A case study in the Tarim River Basin. Glob. Planet. Change, 143, 10–20.

Liu, B., Asseng, S., Liu, L., Tang, L., Cao, W., & Zhu, Y. (2016). Testing the responses of four wheat crop models to heat stress at anthesis and grain filling. Global change biology, 22(5), 1890-1903.

Livingston III, D. P., Tuong, T. D., Isleib, T. G., & Murphy, J. P. (2016). Differences between wheat genotypes in damage from freezing temperatures during reproductive growth. European Journal of Agronomy, 74, 164-172.

Lollato, R. P., & Edwards, J. T. (2015). Maximum attainable wheat yield and resource-use efficiency in the southern Great Plains. Crop Science, 55(6), 2863-2876.

Lollato, R. P., Edwards, J. T., & Ochsner, T. E. (2017). Meteorological limits to winter wheat productivity in the US southern Great Plains. Field crops research, 203, 212-226.

Lollato, R. P., Edwards, J. T., & Ochsner, T. E. (2017). Meteorological limits to winter wheat productivity in the US southern Great Plains. Field Crops Research, 203, 212-226.

Lollato, R. P., Knapp, M. (2020) Effects of recent high temperatures on wheat. Agronomy eUpdates. Kansas State University. Retrieved from https://webapp.agron.ksu.edu/

Lu, Y., Williams, I. N., Bagley, J. E., Torn, M. S., & Kueppers, L. M. (2017). Representing winter wheat in the Community Land Model (version 4.5).

Mannocchi, F.; Todisco, F.; Vergni, L. (2004) Agricultural Drought: Indices, Definition and Analysis. Basis Civ. Water Sci. 286, 246–254. Available online: http://hydrologie.org/redbooks/a286/iahs_286_0246.pdf (accessed on 12 September 2018).

Marambe, Y., & Milas, A. S. (2020). Modeling Evapotranspiration for c4 and c3 Crops in the Western Lake Erie Basin Using Remote Sensing Data. The International Archives of Photogrammetry, Remote Sensing and Spatial Information Sciences, 42, 73-77.

Marburger, D. (2018a) Wheat, Department of Plant and Soil Sciences. Available online: http://wheat.okstate.edu/ (accessed on 19 October 2018).

Marburger, D. (2018b) 2017-2018 Oklahoma Wheat Crop Overview, World of Wheat

Marburger, D., Calhoun, R., Carver, B., Hunger, B., Watson, B. Gillespie, C. (2018) Oklahoma Small Grains Variety Performance Tests 2017-2018, Department of Plant and Soil Science, http://wheat.okstate.edu/

Marek, G. W., T. H. Marek, Q. Xue, P. H. Gowda, S. R. Evett and D. K. Brauer, (2017) Simulating Evapotranspiration and Yield Response of Selected Corn Varieties under Full and Limited Irrigation in the Texas High Plains Using DSSAT-CERES-Maize. Transactions of the ASABE 60:837-846.

Martínez-Fernández, J., González-Zamora, A., Sánchez, N., Gumuzzio, A. (2015) A soil water based index as a suitable agricultural drought indicator. J. Hydrol., 522, 265–273.

Mavromatis, T. (2007). Drought index evaluation for assessing future wheat production in Greece. International Journal of Climatology: A Journal of the Royal Meteorological Society, 27(7), 911-924.

Mavromatis, T. (2010) Use of drought indices in climate change impact assessment studies: An application to Greece. Int. J. Climatol., 30, 1336–1348.

Mckee, T.B.; Doesken, N.J.; Kleist, J. (1993) The Relationship of Drought Frequency and Duration to Time Scales. In Proceedings of the AMS 8th Conference on Applied Climatology, Anaheim, CA, USA, 17–22 January 1993; pp. 179–184. Available online: http://www.droughtmanagement.info/literature/AMS_Relationship_Drought_Frequency_Duration_Time_Scales_1993.pdf (accessed on 22 March 2018).

McLeman, R. A., & Hunter, L. M. (2010). Migration in the context of vulnerability and adaptation to climate change: insights from analogues. Wiley Interdisciplinary Reviews: Climate Change, 1(3), 450-461.

McNider, R. T., Christy, J. R., Moss, D., Doty, K., Handyside, C., Limaye, A., ... & Hoogenboom, G. (2011). A real-time gridded crop model for assessing spatial drought stress on crops in the Southeastern United States. Journal of Applied Meteorology and Climatology, 50(7), 1459-1475.

McPherson, R. A., Fiebrich, C. A., Crawford, K. C., Kilby, J. R., Grimsley, D. L., Martinez, J. E., ... & Melvin, A. D. (2007). Statewide monitoring of the mesoscale environment: A technical update on the Oklahoma Mesonet. Journal of Atmospheric and Oceanic Technology, 24(3), 301-321.

Meinke, H., & Stone, R. C. (2005). Seasonal and inter-annual climate forecasting: the new tool for increasing preparedness to climate variability and change in agricultural planning and operations. Climatic change, 70(1-2), 221-253.

Mesonet (2011) Drought Disasters, Mesonet Connection; Volume 2, Issue 4, May.

Miller, G.R.; Baldocchi, D.D.; Law, B.E.; Meyers, T. (2007) An analysis of soil moisture dynamics using multi-year data from a network of micrometeorological observation sites. Adv. Water Resour., 30, 1065–1081.

Mishra, A. K., & Singh, V. P. (2010). A review of drought concepts. Journal of hydrology, 391(1-2), 202-216.

Mishra, A., Vu, T., ValiyaVeettil, A., Entekhabi, D. (2017) Drought monitoring with Soil Moisture Active Passive (SMAP) Measurements. J. Hydrol., 552, 620–632.

Mishra, A.K., Singh, V.P. (2010) A review of drought concepts. J. Hydrol., 391, 202–216.

Mkhabela, M. S., & Bullock, P. R. (2012). Performance of the FAO AquaCrop model for wheat grain yield and soil moisture simulation in Western Canada. Agricultural Water Management, 110, 16-24.

Mladenova, I.E., Bolten, J.D., Crow, W.T., Anderson, M.C., Hain, C.R., Johnson, D.M., Mueller, R. (2017) Intercomparison of soil moisture, evaporative stress, and vegetation indices for estimating corn and soybean yields over the U.S. IEEE J. Sel. Top. Appl. Earth Obs. Remote Sens., 10, 1328–1343.

Monteith, J. L. (1996). The quest for balance in crop modeling. Agronomy Journal, 88(5), 695-697.

Moorhead, J.E., Gowda, P.H., Singh, V.P., Porter, D.O., Marek, T.H., Howell, T.A., Stewart, B.A. (2015) Identifying and evaluating a suitable index for agricultural drought monitoring in the Texas High Plains. J. Am. Water Resour. Assoc. 51, 807–820.

Moorhead, J.E., Marek, G.W., Gowda, P.H., Marek, T.H., Porter, D.O., Singh, V.P., Brauer, D.K. (2017) Exceedance probability of the standardized precipitation-evapotranspiration index in the Texas High Plains. Agric. Sci., 8, 783–800.

Moriasi, D. N., J. G. Arnold, M. W. Van Liew, R. L. Bingner, R. D. Harmel and T. L. Veith, (2007) Model Evaluation Guidelines for Systematic Quantification of Accuracy in Watershed Simulations. Transactions of the ASABE 50:885-900

Motha, R. P. (2011). Use of crop models for drought analysis. Agricultural Drought Indices: Proceedings of an Expert Meeting, June 2-4, 2010, Murcia, Spain, pp. 138-148

Mourtzinis, S., Edreira, J. I. R., Conley, S. P., & Grassini, P. (2017). From grid to field: Assessing quality of gridded weather data for agricultural applications. European Journal of Agronomy, 82, 163-172.

Narasimhan, B., & Srinivasan, R. (2005). Development and evaluation of Soil Moisture Deficit Index (SMDI) and Evapotranspiration Deficit Index (ETDI) for agricultural drought monitoring. Agricultural and Forest Meteorology, 133(1-4), 69-88.

Neely, C., Trostle, C., & Welch, M. (2014). Wheat Freeze Injury in Texas. Texas, A&M, Agrilife Extension: Educational programs of Texas A&M AgriLife Extension Service and the Texas A&M University: College Station, TX, USA.

Nouri, H., Stokvis, B., Borujeni, S. C., Galindo, A., Brugnach, M., Blatchford, M. L., ... & Hoekstra, A. Y. (2020). Reduce blue water scarcity and increase nutritional and

economic water productivity through changing the cropping pattern in a catchment. Journal of Hydrology, 125086.

Nouri, H., Stokvis, B., Galindo, A., Blatchford, M., & Hoekstra, A. Y. (2019). Water scarcity alleviation through water footprint reduction in agriculture: the effect of soil mulching and drip irrigation. Science of the total environment, 653, 241-252.

NRI – Nobel Research Institute (2018) Extreme Drought Affecting Great Plains and Beyond; March 1

Ochsner, T.E.; Cosh, M.H.; Cuenca, R.H.; Dorigo, W.A.; Draper, C.S.; Hagimoto, Y.; Larson, K.M. (2013) State of the art in large-scale soil moisture monitoring. Soil Sci. Soc. Am. J. 77, 1888.

OKDMT – The Oklahoma Drought Management Team (1997) Oklahoma Drought Management Plan

Oklahoma Climatological Survey (2014) Oklahoma Monthly Climate Summary

Oklahoma Water Resources Board (2006) Oklahoma Water Resources Bulletin & Summary of Current Conditions. Available online: https://www.owrb.ok.gov/supply/drought/pdf_dro/2006/195_0315_2006.pdf (accessed on 09 Mar 2018).

Otkin, J. A., Anderson, M. C., Hain, C., Svoboda, M., Johnson, D., Mueller, R., ... & Brown, J. (2016). Assessing the evolution of soil moisture and vegetation conditions during the 2012 United States flash drought. Agricultural and Forest Meteorology, 218, 230-242.

OWRB – Oklahoma Water Resources Board (2015) Report of the Oklahoma Water for 2060 Advisory Council

Palmer, W.C. (1965) Meteorological Drought. US Weather Bur. Res. Pap., 58, 45. Available online: https://www.ncdc.noaa.gov/temp-and-precip/drought/docs/palmer.pdf (accessed on 3 June 2018).

Palmer, W.C. Meteorological Drought. (1965) US Weather Bur. Res. Pap., 58, 45. Available online: https://www.ncdc.noaa.gov/temp-and-precip/drought/docs/palmer.pdf (accessed on 03 Jun 2018).

Parent, B., Bonneau, J., Maphosa, L., Kovalchuk, A., Langridge, P., & Fleury, D. (2017). Quantifying wheat sensitivities to environmental constraints to dissect Genotype× Environment interactions in the field. Plant physiology, 174(3), 1669-1682.

Patrignani, A., Lollato, R. P., Ochsner, T. E., Godsey, C. B., & Edwards, J. (2014). Yield gap and production gap of rainfed winter wheat in the southern Great Plains. Agronomy Journal, 106(4), 1329-1339.

Paul, J.D., Buytaert, W. (2018) Citizen science and low-cost sensors for integrated water resources management. In Advanced Tools for Integrated Water Resources

Management, 1st ed., Friesen, J., Rodríguez-Sinobas, L., Eds., Academic Press: London, UK, , p. 8. Available online: https://www.elsevier.com/books/advanced-tools-for-integrated-water-resources-management/friesen/978-0-12-814299-8 (accessed on 07 Jan 2019).

Paulsen, G. M., & Shroyer, J. P. (2008). The early history of wheat improvement in the Great Plains. Agronomy Journal, 100, S-70.

Peña-Gallardo, M., Vicente-Serrano, S. M., Quiring, S., Svoboda, M., Hannaford, J., Tomas-Burguera, M., ... & El Kenawy, A. (2019). Response of crop yield to different time-scales of drought in the United States: Spatio-temporal patterns and climatic and environmental drivers. Agricultural and forest meteorology, 264, 40-55.

Pennington, D. (2017) Planting wheat into dry soil. Michigan State University Extension. https://www.canr.msu.edu/news/planting_wheat_into_dry_soil Accessed on 01/25/2020

Qin, W., Chi, B., & Oenema, O. (2013). Long-term monitoring of rainfed wheat yield and soil water at the loess plateau reveals low water use efficiency. Plos one, 8(11).

Quiring, S.M., Papakryiakou, T.N. (2003) An evaluation of agricultural drought indices for the Canadian prairies. Agric. For. Meteorol. 18, 49–62.

Raes, D., P. Steduto, T.C. Hsiao and E. Fereres, (2018) Reference Manual AquaCrop (Version 6.0-6.1). AquaCrop Website http://www.fao.org/nr/water/aquacrop.html

Raes, D., Steduto, P., Hsiao, T. C., & Fereres, E. (2009a). AquaCrop—the FAO crop model to simulate yield response to water: II. Main algorithms and software description. Agronomy Journal, 101(3), 438-447.

Raes, D., Steduto, P., Hsiao, T. C., & Fereres, E. (2009b) AquaCrop Reference Manual. Annexes. Annex I. Crop Parameters. Wheat.

Rauff, K. O., & Bello, R. (2015). A review of crop growth simulation models as tools for agricultural meteorology. Agricultural Sciences, 6(09), 1098.

Reilly, J., Tubiello, F., McCarl, B., Abler, D., Darwin, R., Fuglie, K., Mearns, L. (2003) U.S. agriculture and climate change: New results. Clim. Change, 57, 43–67.

Rezaei, E. E., Siebert, S., & Ewert, F. (2015). Impact of data resolution on heat and drought stress simulated for winter wheat in Germany. European Journal of Agronomy, 65, 69-82.

Rhee, J., Im, J., Carbone, G.J. (2010) Monitoring agricultural drought for arid and humid regions using multi-sensor remote sensing data. Remote Sens. Environ., 114, 2875–2887.

Rippey, B. R. (2015). The US drought of 2012. Weather and Climate Extremes, 10, 57-64.

Rosenzweig, C., Hillel, D. (1993) The Dust Bowl of the 1930s: Analog of greenhouse effect in the Great Plains? J. Environ. Qual., 22, 9–22.

Ruane, A. C., Hudson, N. I., Asseng, S., Camarrano, D., Ewert, F., Martre, P., ... & Basso, B. (2016). Multi-wheat-model ensemble responses to interannual climate variability. Environmental Modelling & Software, 81, 86-101.

Salemi, H., Soom, M. A. M., Lee, T. S., Mousavi, S. F., Ganji, A., & Yusoff, M. K. (2011). Application of AquaCrop model in deficit irrigation management of Winter wheat in arid region. African Journal of Agricultural Research, 6(10), 2204-2215.

Salmon, J. M., Friedl, M. A., Frolking, S., Wisser, D., & Douglas, E. M. (2015). Global rain-fed, irrigated, and paddy croplands: A new high resolution map derived from remote sensing, crop inventories and climate data. International Journal of Applied Earth Observation and Geoinformation, 38, 321-334.

Sanjari, P. A., & Yazdan, S. A. (2008). Evaluation of wheat (Triticum aestivum L.) genotypes under pre-and post-anthesis drought stress conditions.

SCC – South Central Climate Science Center (2017) Drought History for Oklahoma's 9 regions. Retrieved from https://southcentralclimate.org/

Schimmelpfennig, D., & Heisey, P. (2009). US public agricultural research: Changes in funding sources and shifts in emphasis, 1980-2005. Economic Information Bulletin, (45)

Schneider, J.M., Ford, D.L. (2013) An independent assessment of the monthly prism gridded precipitation product in central Oklahoma. Atmos. Clim. Sci. 3, 249.

Schubert, S. D., Suarez, M. J., Pegion, P. J., Koster, R. D., & Bacmeister, J. T. (2004). Causes of long-term drought in the US Great Plains. Journal of Climate, 17(3), 485-503.

Schwalbert, R., Amado, T., Nieto, L., Corassa, G., Rice, C., Peralta, N., ... & Ciampitti, I. (2020). Mid-season county-level corn yield forecast for US Corn Belt integrating satellite imagery and weather variables. Crop Science.

Scott, B.L., Ochsner, T.E., Illston, B.G., Basara, J.B., Sutherland, A.J. (2013) New soil property database improves Oklahoma Mesonet soil moisture estimates. J. Atmos. Ocean. Technol., 30, 2585–2595.

Sehgal, V., Sridhar, V., Tyagi, A. (2017) Stratified drought analysis using a stochastic ensemble of simulated and in-situ soil moisture observations. J. Hydrol. 545, 226–250.

Shafer, M., Ojima, D., Antle, J. M., Kluck, D., McPherson, R. A., Petersen, S., ... & Sherman, K. (2014). Ch. 19: Great Plains. Climate change impacts in the United States: The third national climate assessment, 441-461.

Shelia, V., Hansen, J., Sharda, V., Porter, C., Aggarwal, P., Wilkerson, C. J., & Hoogenboom, G. (2019). A multi-scale and multi-model gridded framework for forecasting crop production, risk analysis, and climate change impact studies. Environmental Modelling & Software, 115, 144-154.

Shrestha, R., Thapa, S., Xue, Q., Stewart, B. A., Blaser, B. C., Ashiadey, E. K., ... & Devkota, R. N. (2020). Winter wheat response to climate change under irrigated and dryland conditions in the US southern High Plains. Journal of Soil and Water Conservation, 75(1), 112-122.

Silvestro, P. C., Pignatti, S., Yang, H., Yang, G., Pascucci, S., Castaldi, F., & Casa, R. (2017). Sensitivity analysis of the Aquacrop and SAFYE crop models for the assessment of water limited winter wheat yield in regional scale applications. PloS one, 12(11), e0187485.

SIPMC – Southern Integrated Pest Management Center (2005) Crop Profile for Wheat in Oklahoma

Sohrabi, M.M.; Ryu, J.H.; Abatzoglou, J.; Tracy, J. (2015) Development of soil moisture drought index to characterize droughts. J. Hydrol. Eng., 20, 04015025.

Soil Survey Staff. (2019) Gridded Soil Survey Geographic (gSSURGO) Database for Oklahoma. United States Department of Agriculture, Natural Resources Conservation Service. Available online at https://gdg.sc.egov.usda.gov/. March, 27, 2020

Sridhar, V.; Hubbard, K.G.; You, J.; Hunt, E. (2007) Development of the soil moisture index to quantify agricultural drought and its "user friendliness" in severity-area-duration assessment. J. Hydrometeorol., 9, 660–676.

Steduto, P., Hsiao, T. C., Fereres, E., & Raes, D. (2012). Crop yield response to water (Vol. 1028). Rome: FAO

Steduto, P., Hsiao, T. C., Raes, D., & Fereres, E. (2009). AquaCrop—The FAO crop model to simulate yield response to water: I. Concepts and underlying principles. Agronomy Journal, 101(3), 426-437.

Stewart, B. A., Thapa, S., Xue, Q., & Shrestha, R. (2018). Climate change effect on winter wheat (Triticum aestivum L.) yields in the US Great Plains. Journal of Soil and Water Conservation, 73(6), 601-609.

Stone, L. R., & Schlegel, A. J. (2006). Yield–water supply relationships of grain sorghum and winter wheat. Agronomy Journal, 98(5), 1359-1366.

Svoboda, M. D., Fuchs, B. A., Poulsen, C. C., & Nothwehr, J. R. (2015). The drought risk atlas: enhancing decision support for drought risk management in the United States. Journal of Hydrology, 526, 274-286.

Taghvaeian, S., Fox, G., Boman, R., Warren, J. (2015) Evaluating the impact of drought on surface and groundwater dependent irrigated agriculture in western Oklahoma. In Proceedings of the 2015 ASABE/IA Irrigation Symposium: Emerging Technologies for Sustainable Irrigation, Long Beach, CA, USA, 10–12 November 2015, ASABE: St. Jospeh, MI, USA, pp. 1–8.

Thornton, P. K., Jones, P. G., Alagarswamy, G., & Andresen, J. (2009). Spatial variation of crop yield response to climate change in East Africa. Global Environmental Change, 19(1), 54-65.

Tian, L., Leasor, Z. T., & Quiring, S. M. (2020). Developing a hybrid drought index: Precipitation Evapotranspiration Difference Condition Index. Climate Risk Management, 100238.

Tian, L., Yuan, S., & Quiring, S. M. (2018). Evaluation of six indices for monitoring agricultural drought in the south-central United States. Agricultural and forest meteorology, 249, 107-119.

Tian, L., Yuan, S., & Quiring, S. M. (2018). Evaluation of six indices for monitoring agricultural drought in the south-central United States. Agricultural and forest meteorology, 249, 107-119.

Tigkas, D., & Tsakiris, G. (2015). Early estimation of drought impacts on rainfed wheat yield in Mediterranean climate. Environmental Processes, 2(1), 97-114.

Tigkas, D.; Vangelis, H.; Tsakiris, G. (2018) Drought characterisation based on an agriculture-oriented standardised precipitation index. Theor. Appl. Climatol., 135, 1–13.

Torres, G.M., Lollato, R.P., Ochsner, T.E. (2013) Comparison of drought probability assessments based on atmospheric water deficit and soil water deficit. Agron. J., 105, 428–436.

Toumi, J., Er-Raki, S., Ezzahar, J., Khabba, S., Jarlan, L., & Chehbouni, A. (2016). Performance assessment of AquaCrop model for estimating evapotranspiration, soil water content and grain yield of winter wheat in Tensift Al Haouz (Morocco): Application to irrigation management. Agricultural Water Management, 163, 219-235.

Tsakiris, G.; Vangelis, H. (2005) Establishing a drought index incorporating evapotranspiration. Eur. Water, 9, 3–11.

USDA – U.S. Department of Agriculture (2016) Crop Simulation Models and GUICS. Farm Decision Aids: Graphical User Interface for Crop Simulators

USDA – U.S. Department of Agriculture (2018) National Agricultural Statistics Service Cropland Data Layer/ Crop Frequency Layer. 2018 crop-specific data layer

USDA – U.S. Department of Agriculture (2018a) National Agricultural Statistics Service Cropland Data Layer/ Crop Frequency Layer. 2000-2018 crop frequency layer

USDA – U.S. Department of Agriculture (2019) World Agricultural Production Foreign Agricultural Service Circular Series, October 2019

USDA – U.S. Department of Agriculture (2018b) National Agricultural Statistics Service. Irrigation and Water Management Survey. Table 36

USGS – U.S. Geological Survey (2012) Moderate Resolution Imaging Spectroradiometer (MODIS) Irrigated Agriculture Dataset for the United States (MIrAD-US) 250m

Van der Schrier, G., Jones, P.D., Briffa, K.R. (2011) The sensitivity of the PDSI to the Thornthwaite and Penman-Monteith parameterizations for potential evapotranspiration. J. Geophys. Res. Atmos. 116, 1–16.

van der Velde, M., Tubiello, F. N., Vrieling, A., & Bouraoui, F. (2012). Impacts of extreme weather on wheat and maize in France: evaluating regional crop simulations against observed data. Climatic change, 113(3-4), 751-765.

Van Genuchten, M.T. (1980) A closed-form equation for predicting the hydraulic conductivity of unsaturated soils. Soil Sci. Soc. Am. J., 8, 892–898.

van Keulen, H., & Asseng, S. (2019). Simulation models as tools for crop management. Crop Science, 433-452.

Vanuytrecht, E., D. Raes, P. Steduto, T. C. Hsiao, E. Fereres, L. K. Heng, M. G. Vila and P. M. Moreno. (2014) AquaCrop: FAO's Crop Water Productivity and Yield Response Model. Environmental Modelling & Software 62:351-360.

Vicente-Serrano, S.M., Beguería, S., López-Moreno, J.I. (2010) A multiscalar drought index sensitive to global warming: The standardized precipitation evapotranspiration index. J. Clim. 23, 1696–1718.

Vicente-Serrano, S.M., Beguería, S., Lorenzo-Lacruz, J., Camarero, J.J., López-Moreno, J.I., Azorin-Molina, C., Sanchez-Lorenzo, A. (2012) Performance of drought indices for ecological, agricultural, and hydrological applications. Earth Interact. 16, 1–27.

Walsh, J., Wuebbles, D., Hayhoe, K., Kossin, J., Kunkel, K., Stephens, G., ... & Anderson, D. (2014). Our changing climate. Climate change impacts in the United States: The third national climate assessment, 19-67.

Walsh, O. S., Solie, J. B., & Raun, W. R. (2013). Can Oklahoma Mesonet Cumulative Evapotranspiration Data Be Accurately Predicted Using Three Interpolation Methods? Communications in soil science and plant analysis, 44(5), 892-899.

Wang, A.; Lettenmaier, D.P.; Sheffield, J. (2011) Soil moisture drought in China, 1950–2006. J. Clim., 24, 3257–3271.

Wang, H., Vicente-Serrano, S. M., Tao, F., Zhang, X., Wang, P., Zhang, C., ... & El Kenawy, A. (2016). Monitoring winter wheat drought threat in Northern China using multiple climate-based drought indices and soil moisture during 2000–2013. Agricultural and forest meteorology, 228, 1-12.

Wells, N.; Goddard, S.; Hayes, M.J. (2004) A self-calibrating Palmer Drought Severity Index. J. Clim., 17, 2335–2351.

Willmott, C.J. (1981) On the validation of models. Phys. Geogr. 2:184–194.

WMO (World Meteorological Organization), GWP (Global Water Partnership). (2016) Handbook of Drought Indicators and Indices.. Available online: http://www.droughtmanagement.info/literature/GWP_Handbook_of_Drought_Indicators_and_Indices_2016.pdf (accessed on 14 Jan 2019).

Woli, P., Jones, J.W., Ingram, K.T. (2013) Assessing the Agricultural Reference Index for Drought (ARID) using uncertainty and sensitivity analyses. Agron. J., 105, 150.

Woli, P., Jones, J.W., Ingram, K.T., Fraisse, C.W. (2012) Agricultural reference index for drought (ARID). Agron. J., 104, 287–300.

Wu, H., & Wilhite, D. A. (2004). An operational agricultural drought risk assessment model for Nebraska, USA. Natural Hazards, 33(1), 1-21.

Xiangxiang, W., Quanjiu, W., Jun, F., & Qiuping, F. (2013). Evaluation of the AquaCrop model for simulating the impact of water deficits and different irrigation regimes on the biomass and yield of winter wheat grown on China's Loess Plateau. Agricultural Water Management, 129, 95-104.

Xu, X., Gao, P., Zhu, X., Guo, W., Ding, J., Li, C. (2018) Estimating the responses of winter wheat yields to moisture variations in the past 35 years in Jiangsu Province of China. PLoS ONE 13, e0191217.

Xue, Q., Zhu, Z., Musick, J. T., Stewart, B. A., & Dusek, D. A. (2003). Root growth and water uptake in winter wheat under deficit irrigation. Plant and Soil, 257(1), 151-161.

Yang, Y., Li Liu, D., Anwar, M. R., O'Leary, G., Macadam, I., & Yang, Y. (2016). Water use efficiency and crop water balance of rainfed wheat in a semi-arid environment: sensitivity of future changes to projected climate changes and soil type. Theoretical and applied climatology, 123(3-4), 565-579.

Yu, H., Li, L., Liu, Y., & Li, J. (2019). Construction of Comprehensive Drought Monitoring Model in Jing-Jin-Ji Region Based on Multisource Remote Sensing Data. Water, 11(5), 1077.

Yu, H., Zhang, Q., Sun, P., & Song, C. (2018). Impact of droughts on winter wheat yield in different growth stages during 2001–2016 in Eastern China. International Journal of Disaster Risk Science, 9(3), 376-391.

Zargar, A., Sadiq, R., Naser, B., & Khan, F. I. (2011). A review of drought indices. Environmental Reviews, 19(NA), 333-349.

Zargar, A.; Sadiq, R.; Naser, B.; Khan, F.I. (2011) A review of drought indices. Environ. Rev., 19, 333–349.

Zeleke, K. T., Luckett, D., & Cowley, R. (2011). Calibration and testing of the FAO AquaCrop model for canola. Agronomy Journal, 103(6), 1610-1618.

Zhang, N., Zhao, C., Quiring, S.M., Li, J. (2017) Winter wheat yield prediction using normalized difference vegetative index and agro-climatic parameters in oklahoma. Agron. J. 109, 2700–2713.

Zhang, S., Lövdahl, L., Grip, H., Tong, Y., Yang, X., & Wang, Q. (2009). Effects of mulching and catch cropping on soil temperature, soil moisture and wheat yield on the Loess Plateau of China. Soil and Tillage Research, 102(1), 78-86.

Zhang, W., Liu, W., Xue, Q., Chen, J., & Han, X. (2013). Evaluation of the AquaCrop model for simulating yield response of winter wheat to water on the southern Loess Plateau of China. Water Science and Technology, 68(4), 821-828.

Zhang, Y., & Schaap, M. G. (2017). Weighted recalibration of the Rosetta pedotransfer model with improved estimates of hydraulic parameter distributions and summary statistics (Rosetta3). Journal of Hydrology, 547, 39-53.

Zhang, Y., Yu, Q., Liu, C., Jiang, J., & Zhang, X. (2004). Estimation of winter wheat evapotranspiration under water stress with two semiempirical approaches. Agronomy Journal, 96(1), 159-168.

Zhao, F., Zhang, L., Chiew, F. H., Vaze, J., & Cheng, L. (2013). The effect of spatial rainfall variability on water balance modelling for south-eastern Australian catchments. Journal of hydrology, 493, 16-29.

Zhao, W., Khalil, M.A.K. (1993) The relationship between precipitation and temperature over the contiguous United States. J. Clim., 6, 1232–1236.

Zhu, W., Porth, L., & Tan, K. S. (2019). A credibility-based yield forecasting model for crop reinsurance pricing and weather risk management. Agricultural Finance Review, 79(1), 2-26.

Ziolkowska, J. R. (2018). Profitability of irrigation and value of water in Oklahoma and Texas agriculture. International journal of water resources development, 34(6), 944-960.

SUPPLEMENTARY MATERIAL

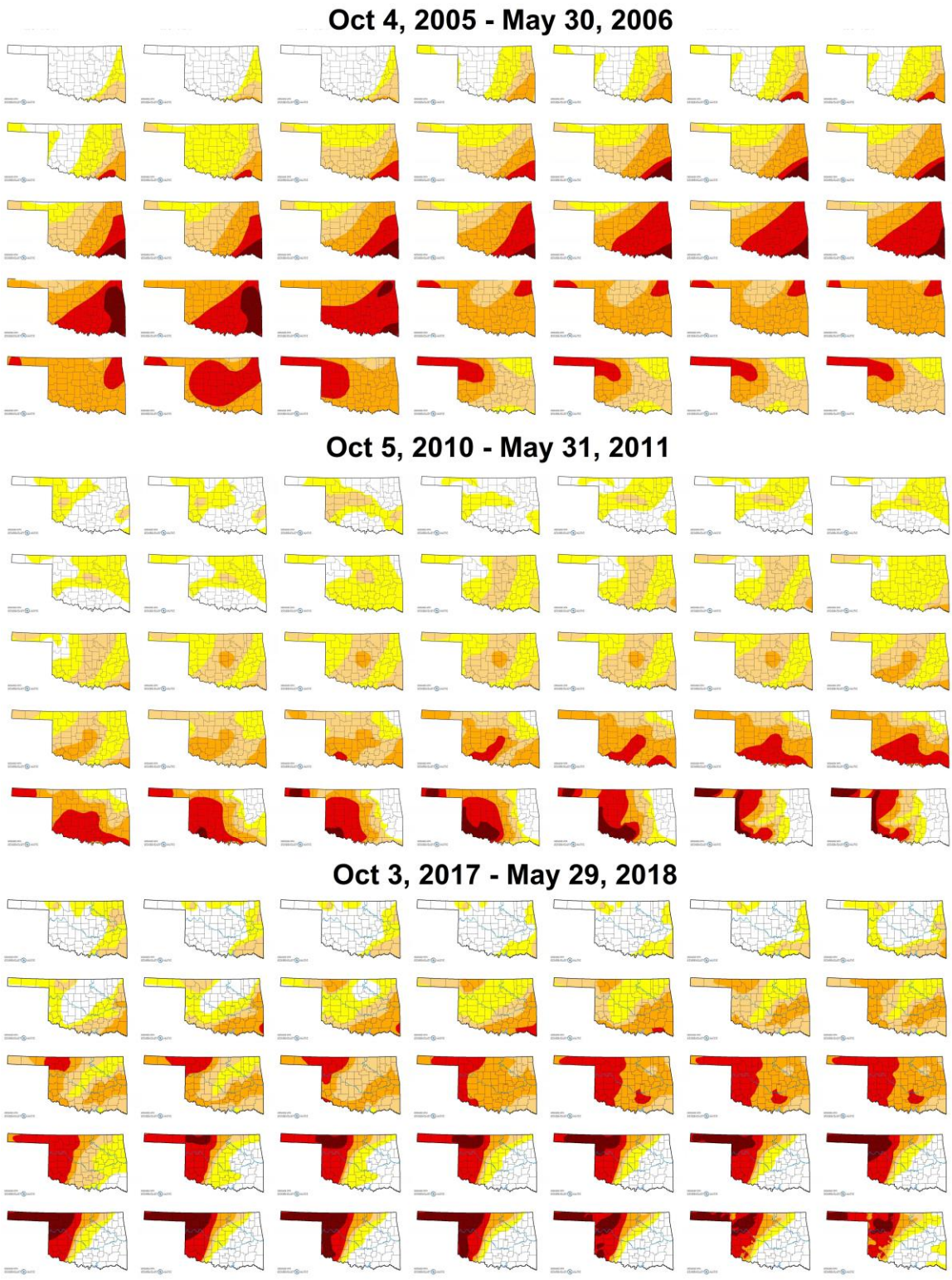

Figure S1. US Drought Monitor Weekly drought maps (moving from left-to-right) for three growing seasons affected by drought 2005-2006, 2010-2011, and 2017-2018

VITA

Ali Ajaz

Candidate for the Degree of

Doctor of Philosophy

Dissertation: IMPROVING THE DROUGHT RISK ASSESSMENT AND PREPAREDNESS FOR WINTER WHEAT FARMING IN OKLAHOMA

Major Field: Biosystems Engineering

Biographical:

Education:

Completed the requirements for the Doctor of Philosophy in Biosystems Engineering at Oklahoma State University, Stillwater, Oklahoma in July, 2020.

Completed the requirements for the Master of Science in Water Science and Engineering at UNESCO-IHE, Institute for Water Education, Delft, The Netherlands in April, 2016.

Completed the requirements for the Bachelor of Science in Agricultural Engineering at Bahauddin Zakariya University, Multan, Pakistan in 2009.

Experience:

Graduate Research Assistant, Department of Biosystems and Agricultural Engineering, Oklahoma State University, January 2017 to July 2020

Graduate Researcher–Water Resources & Remote Sensing, International Water Management Institute (IWMI), South Africa, September 2015 to June 2016

Assistant Design Engineer–Irrigation Systems, Ag Div, National Engineering Services Pakistan, Consulting Engineers, Lahore, May 2013 to October 2014

Irrigation Engineer, Contractors, August 2009 to April 2013